Development of colorimetric lateral flow assay for quantitative detection of anti-doping markers in sports

Sharma, Antareep

2020

Sharma, A. (2020). Development of colorimetric lateral flow assay for quantitative detection of anti-doping markers in sports. Doctoral thesis, Nanyang Technological University, Singapore.

https://hdl.handle.net/10356/144766

https://doi.org/10.32657/10356/144766

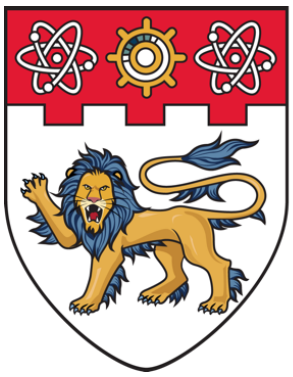

NANYANG TECHNOLOGICAL UNIVERSITY
SINGAPORE

DEVELOPMENT OF COLORIMETRIC LATERAL FLOW ASSAY FOR QUANTITATIVE DETECTION OF ANTI-DOPING MARKERS IN SPORTS

ANTAREEP SHARMA

INTERDISCIPLINARY GRADUATE SCHOOL

NTU INSTITUTE FOR HEALTH TECHNOLOGIES

2020

DEVELOPMENT OF COLORIMETRIC LATERAL FLOW ASSAY FOR QUANTITATIVE DETECTION OF ANTI-DOPING MARKERS IN SPORTS

ANTAREEP SHARMA

INTERDISCIPLINARY GRADUATE SCHOOL

NTU INSTITUTE FOR HEALTH TECHNOLOGIES

A thesis submitted to the Nanyang Technological University
in partial fulfilment of the requirement for the degree of
Doctor of Philosophy

2020

Statement of Originality

I hereby certify that the work embodied in this thesis is the result of original research, is free of plagiarised materials, and has not been submitted for a higher degree to any other University or Institution.

17/07/2020

Date

ANTAREEP SHARMA

Supervisor Declaration Statement

I have reviewed the content and presentation style of this thesis and declare it is free of plagiarism and of sufficient grammatical clarity to be examined. To the best of my knowledge, the research and writing are those of the candidate except as acknowledged in the Author Attribution Statement. I confirm that the investigations were conducted in accord with the ethics policies and integrity standards of Nanyang Technological University and that the research data are presented honestly and without prejudice.

21/07/2020

Date

ALFRED TOK LING YOONG

Authorship Attribution Statement

This thesis contains material from 2 papers published in the following peer-reviewed journals in which I am listed as an author.

Chapter 5 is published as Antareep Sharma, Alfred Iing Yoong Tok, Chleo Lee, Rajaseger Ganapathy, Alagappan Palaniappan, Bo Liedberg, "Magnetic field assisted preconcentration of biomolecules for lateral flow assaying." *Sensors and Actuators B: Chemical* 285 (2019): 431-437. DOI: 10.1016/j.snb.2019.01.073

The contributions of the co-authors are as follows:

- Prof. Alfred Tok, Dr. Ganapathy, Dr. Palaniappan and Prof. Bo Gunnar Liedberg provided the initial project direction and edited the manuscript drafts.
- I prepared the manuscript drafts along with Dr. Palaniappan. The manuscript was revised by Prof. Tok and Prof. Liedberg.
- I co-designed the study with Dr. Palaniappan and performed all the laboratory work with the help of FYP student Chleo Lee at the Centre for Biomimetic Sensor Science (CBSS), NTU. I also analyzed the data.
- Results were discussed with all the co-authors.

Chapter 6 is published as Antareep Sharma, Alfred Iing Yoong Tok, Alagappan Palaniappan, Bo Liedberg, "Gold nanoparticle conjugated magnetic beads for extraction and nucleation-based signal amplification in lateral flow assaying." *Sensors and Actuators B: Chemical* (2020): 127959. DOI: 10.1016/j.snb.2020.127959

The contributions of the co-authors are as follows:

- Prof. Alfred Tok, Dr. Palaniappan and Prof. Bo Gunnar Liedberg initiated the project and edited the manuscript.
- I prepared the manuscript drafts along with Dr. Palaniappan.

- I co-designed the study with Dr Palaniappan. The experiments were performed by me in the Centre for Biomimetic Sensor Science (CBSS), NTU. I also analyzed the data.
- Results were discussed with all the co-authors.

17/07/2020 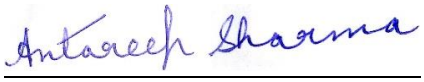

Date ANTAREEP SHARMA

Acknowledgements

This thesis was possible with the support from Ministry of Education (MOE) Tier 1 grant and the funding from Institute of Sports Research (ISR) and Centre for Biomimetic Sensor Science (CBSS).

I would like to express my sincere gratitude to my supervisor Prof. Alfred Tok for offering me the opportunity to conduct my PhD study under his guidance at Nanyang Technological University (NTU). Prof. Alfred has been instrumental in providing me with a direction throughout my PhD journey and never let me lose focus. I would also like to thank my advisor Prof. Bo Liedberg for letting me carry out my research at CBSS and for his unwavering support and guidance during my years at NTU. Both Prof. Alfred and Prof. Bo have been more than supervisors to me, and I would be indebted to them forever.

I would like to express my warmest thanks to my Thesis Advisory Committee (TAC) members, co-supervisor Prof. Zhao Yanli from the School of Physical and Mathematical Science (SPMS) and my clinical mentor Dr. Benedict Tan from Changi General Hospital (CGH) for their invaluable insights into my research and helping me improve its quality.

This thesis would not have been possible without the help and support of my mentor Dr. Alagappan Palaniappan. His insightful suggestions and candid discussions about my research, his patience while reviewing all my drafts, and his uplifting nature whenever my experiments failed, made me not just a better researcher but also a more confident person.

The uphill journey towards my PhD was enjoyable and smooth because of the perennial support from my colleagues, Ms. Garima Goyal, Dr. Gopal Ammanath, Dr. Gaurav Sinsinbar, Dr. Nevena Klisara, Dr. Iuna Tsyrulneva, Dr. Amit Kumar Khan, Dr. James Ho, Dr. Susmita Roy, Miss Mei Xia Tay, Dr. Chen Peng and everyone else from CBSS. I would also like to express my gratitude to the FYPs and interns who helped me carry out my research more efficiently.

I would like to acknowledge my school, IGS and my university, NTU for providing my scholarship and the conference funds. I would also like to thank all the admins at IGS and HealthTech who helped me with all my paperwork and documentation over the years and made my PhD journey smoother. Special thanks to Ms. Ellen Heng, Ms. Suriani Rabu, Ms. Lena Tay, Ms. Thevagi Silvarajoo, Ms. Kay Lee, Ms. Chia Huei, Ms. Charmaine and Ms. Andrea.

I would like to acknowledge my friends who have always showered me with unconditional support and love. Starting with Divya, who has tolerated me during my lows, celebrated me during my highs and has always kept me grounded. My undergraduate friends, Akshay, Gaurav Mishra, Gaurav Singh, Apurva, Shalabh, Nitish, Himanshu, Devender, Nikunj, Venky, Saurabh and Kedia, who moulded me into the person I am today. My friends from IISc, Anwesha, Rahul, Nidhi, Shruthi, Maya, Sumit, Prajakta, Aishwarya, Sachin, Jafar, Shubham, Aditi, Sai, Urvashi, Gowri, Queeny, Yudhajit, Prasanna, Sanjay and Shital, who made my Masters journey memorable. My friends in Singapore, without whom I could never have called this place home: Abhijit, Chinmayi, Sheetal, Dzeneta, Ashish, Saurabh, Garima, Vikas, Shuddho, Satnam, Ishaan and Spandan, Finally, my school buddies who have stuck with me for the last 20 years, Rupayan, Parikshit, Anupriti, Mriganka, Siddharth, Koustav, Abhigyan, Anirban, Priyanka, Navarun and Garima. Last but not the least, I extend my deepest gratitude to my parents Nalini Sharma and Ajanta Sharma, my sister Shradhanjali Sharma, and the rest of my extended family, without whom I could never have reached this far in life.

Table of Contents

Abstract

Doping in sports is defined as the use of substances, both foreign and physiological, in an unnatural manner or in abnormal quantities to enhance an athlete's performance in competitions. The current doping control mechanisms involve randomized testing of samples from athletes using laboratory techniques, which are typically cumbersome with extremely long turnaround times and are not cost effective. This reduces the efficiency of the screening process as a large number of athletes are not tested for doping. Point of care tests (POCTs) such as lateral flow assays (LFAs) can be a viable solution to increase the testing frequency and make this screening more effective by allowing large scale testing with a much smaller cost compared to laboratory tests. LFAs have several advantages over laboratory tests; they are versatile, highly mobile, require minimal sample volume, can correlate to laboratory tests without expensive instrumentation and have a rapid turnaround time, making them perfectly suited to be utilized for on-site screening tests. However, LFAs face challenges such as sensitivity, especially for visual analysis of results, which inhibits their widespread commercial usage. Thus, there is a need to develop strategies to address these challenges and improve LFA performance, especially for reliable on-site testing without involving complicated instrumentation or sophisticated testing protocols.

This thesis aims at exploring strategies to improve LFA sensitivity for analysis of complex matrices. In the first study, a novel LFA layout was developed to reduce the interference from matrix components on LFA responses. By incorporation of a magnetic bead (MB) based sample preconcentration step in the LFA, a sensitive colorimetric assay, with a visual limit of detection (LOD) of 10 ng/ml in plasma was demonstrated within a 15 min assay time. In order to improve the sensitivity, a novel nucleation-based signal amplification technique utilizing a composite signal reporter was developed in the second study. A colorimetric gold nanoparticle conjugated magnetic bead (GMB) reporter was synthesized to be used as a precursor for nucleation of gold on its surface, which enabled formation of large clusters at the test line, improving the visual sensitivity of the assay. This strategy resulted in a highly sensitive assay with a visual LOD of 0.1 ng/ml in plasma within a total assay time of 20 min. In both of these studies, a Troponin model system, involving

Troponin ICT analyte and anti-Troponin I and anti-Troponin C antibodies, was utilized to validate the results. Troponin is an important marker for skeletal and cardiac muscle regulation and is a well-studied system for LFA studies. The LFA strategies developed were then translated to detect Insulin like Growth Factor-1 (IGF-1) using anti-IGF-1 antibodies. IGF-1 is a prohibited substance in competitive sports and also a biomarker for Growth Hormone (GH) doping. IGF-1 assay, incorporating MB based sample pretreatment into the LFA, resulted in a visual LOD of 1 μg/ml in plasma, whereas the assay involving signal amplification via GMB reporters resulted in a promising visual LOD of 100 ng/ml in plasma, which was well below the allowable limit for IGF-1 in competitive sports. The third and final study is on improving the robustness of the LFA by replacing traditional antibodies with affimers, which have similar affinities towards the analytes, but a much better stability as compared to antibodies. Using an Interlukin-8 (IL-8) model system, consisting of anti-IL-8 affimer conjugated magnetic beads for colorimetric detection, a visual LOD of 1 ng/ml was obtained in PBS, which is near the physiological range of IL-8 in injured athletes.

This thesis serves as a template for future studies in LFA technologies in three main directions: development of alternative LFA layouts, innovative use of reporters and utilization of novel recognition molecules. The strategies adopted in this thesis resulted in highly sensitive assays, with LODs well within the clinically relevant ranges of the analytes in human plasma. The validation of these assays in a complex matrix such as plasma provides opportunities for on-site application of LFAs. Moreover, the generic approach of these proposed strategies allows for translation of these LFAs to detect several other biomolecules.

Table Captions

Figure Captions

enhancement. Here, "Control" corresponds to absence of cTnICT in sample matrix.

Fig 6.1: Absorption spectra of supernatant solutions upon magnetic separation of AuNPs-MB complexes for; (a) different tween 20 concentrations and (b) varying cysteamine concentrations.

Fig 6.2: (a) BCA standard plot for calculation of antibody concentration; and (b) Bar graph showing pre- incubation antibody concentration in reaction vial and post-incubation antibody concentration left in supernatant after GMB extraction, corresponding to various cysteamine concentrations.

Fig 6.3: (a) Bar graph showing luminance values corresponding to vials in (b)-(c). Lower luminance implies darker colour in the vial. Inset images: (b) GMB with varying cysteamine concentrations. (c) GMB, 5 minutes after addition of nucleation reagents. From left to right (concentration of cysteamine in μM): MB, 0, 1, 5, 15, 30, 50, 100.

Fig 6.4: DLS plots of MB, GMB and nucleated GMB

Fig 6.5: SEM images of (a) MB, (b) GMB and (c) Nucleated GMB. Inset images (red boxes) show individual construct of the particles. (d) EDX scan of GMB

Fig 6.6: Quantification of colour intensities via measurement of normalized relative luminance of test bands for assay in (a) buffer and (b) plasma. Normalized relative luminance was measured with respect to reference LFA strip. Inset images: photographs of LFA strips showing the test bands (within solid box) and the control patches (within dashed box) for assay before nucleation (left) and after nucleation (right). From left to right: 0 ng/ml, 0.01 ng/ml, 0.1 ng/ml, 1 ng/ml, 10 ng/ml, 100 ng/ml, 1000 ng/ml, reference LFA strip without GMB flow.

Fig 7.1: Quantification of colour intensities via measurement of normalized luminance of test bands for IGF-1 assay with (a) MB (Strategy 1) and (b) GMB (Strategy 2). Inset images: photographs of LFA strips showing the test bands after assay.

Abbreviations

AB	Antibody
Aff	Affimer
AMI	Acute Myocardial Infarction
AuNP	Gold Nanoparticle
BCA	Bicinchoninic Acid Protein Assay
BSA	Bovine Serum Albumin
BSE	Back Scattered Electrons
cTnICT	Cardiac Troponin I-C-T
ClIA	Chemiluminescent Immunoassay
CLIA	Clinical Laboratory Improvement Amendment
CIA	Counting Immunoassay
Cys	Cysteamine
DI	Distilled Water
DLS	Dynamic Light Scattering
EDC	1-Ethyl-3-(3-Dimethylaminopropyl) Carbodiimide
EDX	Energy Dispersive X-Ray Photospectroscopy
EIA	Enzyme Immunoassay
ELISA	Enzyme-Linked Immunosorbent Assay
EPO	Erythropoietin
FIA	Fluoroimmunoassay
FDA	Food and Drug Administration
FESEM	Field Emission Scanning Electron Microscopy
GC-MS	Gas Chromatography Mass Spectrometry
GF	Glass Fibre
GMB	Gold Nanoparticle conjugated Magnetic Bead
GH	Growth Hormone
HPLC	High Performance Liquid Chromatography
HRP	Horseradish Peroxidase
IAAF	International Association of Athletics Federation

IGF-1	Insulin like Growth Factor-1
IL-8	Interlukin-8
IOC	International Olympic Committee
ISTI	International Standard for Testing and Investigations
LC-MS	Liquid Chromatography Mass Spectrometry
LFA	Lateral Flow Assay
LLE	Liquid Liquid Extraction
LOD	Limit of Detection
LOQ	Limit of Quantification
MALDI-TOF	Matrix Assisted Laser Desorption/Ionization Time-of-Flight
MES	2-(N-morpholino) Ethanesulfonic Acid
MB	Magnetic Bead
MNP	Magnetic Nanoparticle
MRPL	Minimum Required Performance Level
NC	Nitrocellulose
NHS	N-hydroxysulfosuccinimide
OD	Optical Density
PBS	Phosphate Buffer Saline
PDI	Poly dispersity index
PDMS	Polydimethylsiloxane
PMB	Protein-A conjugated Magnetic Bead
pI	Isoelectric point
POC	Point-of-Care
POCT	Point-of-Care Test
PVDF	Polyvinylidene Difluoride
QD	Quantum Dot
RIA	Radioimmunoassay
RGB	Red Green Blue
RT	Room Temperature
RTP	Registered Testing Pool
SE	Secondary Electrons

SEM	Scanning Electron Microscopy
SELEX	Systematic Evolution of Ligands by Exponential enrichment
SPP	Selective Protein Precipitation
SPR	Surface Plasmon Resonance
T-20	Tween-20
TMB	3,3′,5,5′-Tetramethylbenzidine
TnI	Troponin I
TnC	Troponin C
TnT	Troponin T
UF	Ultrafiltration
UV/VIS	Ultraviolent- Visible Spectroscopy
VDL	Visual Detection Limit
WADA	World Anti-Doping Agency
WHO	World Health Organisation
μ-PAD	Microfluidic Paper-based Device

List of Publications

1. Antareep Sharma, Alfred Iing Yoong Tok, Chleo Lee, Rajaseger Ganapathy, Alagappan Palaniappan, Bo Liedberg, "Magnetic field assisted preconcentration of biomolecules for lateral flow assaying." *Sensors and Actuators B: Chemical* 285 (2019): 431-437. DOI: 10.1016/j.snb.2019.01.073

2. Antareep Sharma, Alfred Iing Yoong Tok, Alagappan Palaniappan, Bo Liedberg, "Gold nanoparticle conjugated magnetic beads for extraction and nucleation-based signal amplification in lateral flow assaying." *Sensors and Actuators B: Chemical* (2020): 127959. DOI: 10.1016/j.snb.2020.127959

3. Antareep Sharma, Alfred Iing Yoong Tok, Alagappan Palaniappan, Bo Liedberg, “Point of Care Testing of Sports Markers: Potential Applications, Recent Advances and Future Outlook”; *under preparation*

4. Antareep Sharma, Garima Goyal, Alfred Iing Yoong Tok, Alagappan Palaniappan, Bo Liedberg, “Lateral flow assaying of Interlukin-8 in complex matrices using small protein affimers”; *under preparation*

Chapter 1

Introduction

Even with the advancement in technology, screening of athletes for doping is performed only at a few accredited laboratories worldwide. A robust screening regimen, which includes widespread on-site testing outside competitions, is therefore required for efficient doping control. LFA, being one of the most popular point-of-care assays with several advantages over typical laboratory techniques, perfectly fits as a screening test for doping control. This thesis aims at devising strategies to improve LFA performance, especially for testing with complex samples, thereby making them suitable for on-site screening. This chapter provides a short overview of the thesis including hypotheses/problem statements, objectives and scope of this study and a brief description of each chapter of this thesis.

1.1 Background and Significance

Substance abuse or ‘doping’ has been a menacing phenomenon in the world of sports. It has plagued almost all disciplines of sports, where physical strength and endurance of athletes are of utmost importance for their performances. As athletes are rewarded almost in all levels of the competitions with lucrative deals and immeasurable fame afterwards, some of them are attracted to the folds of doping to enhance their performance.[1]

Doping can be explained as using substances, both foreign and physiological, in an unnatural manner or in abnormal quantities to enhance the performance in a competition. It is a concept that goes back centuries and is almost as old as the idea of competitive sports. There are several literatures suggesting that the ancient Greeks and Romans used plants, seeds, mushrooms and several mixtures of wine and herbs for stimulating effects in speed and endurance, and, to speed up recovery.[2-4] However, modern day substance abuse started in the late 19^{th} century.[1, 4] Since then, several sporting agencies have played a role in banning the use of performance enhancing substances. The International Association of Athletics Federation (IAAF) was the first organization that banned doping in 1928, but with little or no technology to conduct effective screening tests. This rising menace garnered widespread attention post the 1998 Tour De France doping scandal. In the following year, the International Olympic Committee (IOC) along with a few more agencies constituted the World Anti-Doping Agency (WADA).[1] The primary role of WADA is to function as an independent body to lead in monitoring doping. Its primary interest is to help nations come up with effective anti-doping programmes and help with the research in this field. Ever since its inception, WADA has maintained a list of banned substances, which is updated annually. The WADA-banned substances could be broadly classified into androgenic agents, stimulants, diuretics, narcotics, peptide hormones and glucocorticoids. These drugs have various effects like muscle growth, increasing alertness, faster recovery from injuries and easy burning of fats, and hence, are used depending on the discipline or need.[5] The detection of these substances can be either direct, through analytical testing of the substance’s presence, or indirect, through analytical testing of any of their biomarkers which correlate to the substance’s presence.

During the early days of WADA, lack of adequate resources hindered effective detection of these substances. However, with the advent of technology, detection techniques for banned substances have been substantially improved. Mass spectroscopic techniques, coupled with Gas Chromatography (GC) or High-Performance Liquid Chromatography (HPLC), are still considered the gold standard methods of detection.[6] Apart from them, other methods such as Immunoassays, Matrix-Assisted Laser Desorption Ionization–Time-Of-Flight analysis (MALDI-TOF) and Surface Plasmon Resonance (SPR) also have been deployed for detection of doping markers.[7-9] However, these methods required skilled personnel and involve sophisticated, expensive laboratory instrumentation. Currently, such tests are carried out only in about 35 WADA-accredited laboratories worldwide.[10] To complicate things further, newer drugs and the sophistication in doping process to avoid their detection, increase the challenges in doping control. In light of such a scenario, it has become extremely important to increase testing frequency by developing rapid, cost-effective and more reliable techniques for detection of substance abuse. One such viable option is a Point-of-Care Test (POCT), which could be performed on-site.[11, 12] POCTs can yield quantitative, semi-quantitative and qualitative responses, depending on the assay principle. Most of the POCTs reported yield either optical (colorimetric, luminescence, fluorescence etc.) or electrochemical responses, which are easier to be read and analyzed on-site. In the last decade, interest in these devices have increased manifolds, which has resulted in significant advanced of POCTs with improved robustness and reliability.

One of the most popular POCTs currently available is the Lateral Flow assay (LFA) strip. Pregnancy strip, a well-known LFA, constitutes a multi-billion-dollar industry, demonstrating the immense potential of LFAs. LFAs are basically pre-fabricated strips of carrier membranes, containing dried reagents that are activated by application of fluid sample containing the analyte.[13-15] As shown in Fig 1.1, a typical LFA consists of a sample pad for application of sample solution, a conjugate pad for analyte binding to recognition molecules, test pad for detection of analyte, absorbent pad to control capillary flow of fluid and a backing pad for structural support. Each pad is made of a different membrane material to suit the respective function it provides. Although, most LFAs use

antibodies for recognition of target analytes, increasing number of studies have utilized alternative recognition biomolecules such as nucleic acids and peptides.[16, 17] The detection signal provided by LFAs is due to the reporter labels, which may include enzymes such as HRP, nanoparticles such as colloidal gold (AuNP) and carbon, latex beads, fluorescent tags such as Europium and quantum dots (QDs) or even magnetic beads (MBs).[15, 18-20] Sensitivities for LFAs can vary from a few pg/ml to a few mg/ml, depending on the application and type of biomolecules to be detected. LFA devices are; easy to fabricate which makes them cost effective, portable making them perfect fit for on-site studies, need minimal or no use of instrumentation and are robust. Furthermore, LFAs yield visual response and does not require skilled personnel for performing the assay or for data analysis. Amongst the various formats of LFAs, the colorimetric LFAs are the easiest for on-site analysis because of facile and intuitive signal readability by the users. Although, traditional colorimetric LFAs yield qualitative "yes/no" responses, quantitative readout of LFAs responses has been gaining popularity.[19, 21, 22] Hence, focusing on colorimetric LFAs allows for their widespread implementation for several POC applications including doping control.

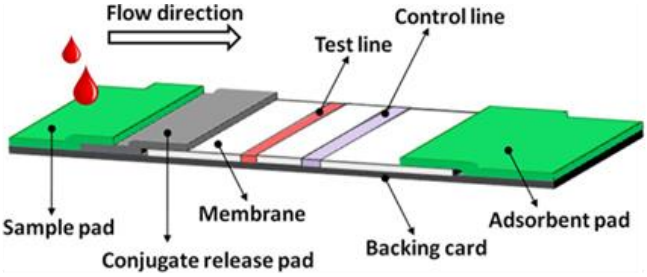

Fig 1.1: Schematic of a typical LFA strip [23]

LFAs, although useful in many ways, possess inherent challenges. The most notable amongst them being the limited sensitivity, which often hinders their commercial applications. Sensitivity may be affected by a myriad of factors, such as interferences from matrix solution that mask low analyte concentrations, low sample volumes that limit the amount of analyte available for viable detection or even environmental conditions, such as heat and humidity, which can degrade the integrity of the device.[13, 15, 24] These

challenges become even more prominent in the context of detection of doping markers because such an application would require testing complicated matrices such as blood, plasma, urine or sweat. Moreover, the samples obtained from athletes during a testing window are limited in quantity. In order to improve LFA sensitivity, sample pretreatment steps have been utilized to concentrate the analytes or reduce matrix interference before analysis.[25-27] Furthermore, use of more sensitive signal reporters is another strategy adopted for detection of trace amounts of analytes.[25, 28]

However, addition of complicated steps to the testing protocol may not be feasible in resource limited settings. Moreover, even the best colorimetric reporters, such as AuNPs, have limitations. On the other hand, use of other forms of signals such as chemiluminescence and fluorescence limits on-site usage as signal readability becomes an issue. This thesis aims to address existing LFA challenges and devise alternative strategies to improve the sensitivity and robustness of LFAs so that they can be successfully implemented for practical applications such as doping control.

1.2 Hypotheses

1. *A highly sensitive colorimetric LFA can be developed to detect biomarkers at concentrations below the physiological range, if a magnetic bead-based analyte preconcentration step to remove matrix interferents is incorporated with the LFA.*

Interferents present in complex matrices such as plasma and blood affect the sensitivity of an assay, because of which typical assays require an additional sample pretreatment step. Extraction of analyte capturing functionalized magnetic beads using an external magnetic field for analyte preconcentration is one of the most common ways of sample pretreatment.[29, 30] However, the use of external magnetic field require additional instrumentation, which increases the overall complexity of the assay for on-site analysis. Therefore, this pretreatment process should be merged with the assay in a single LFA strip. This thesis tests the hypothesis that incorporating such a magnetic field assisted analyte preconcentration with the LFA strip provides an effective sample pretreatment for a highly

sensitive colorimetric assay, utilizing magnetic beads as optical reporters.

2. *If a gold nanoparticle conjugated magnetic bead reporter is used in a colorimetric LFA, its sensitivity can be improved by a facile nucleation-based signal amplification approach.*

Magnetic beads can be easily extracted using an external magnetic field, however they have limitations when used as optical reporters. On the other hand, gold nanoparticles are the most well-known optical reporters, but not suitable for extraction.[31] Thus, a composite reporter involving a gold nanoparticle conjugated magnetic bead would serve as an ideal candidate for facile sample preconcentration and for yielding sensitive colorimetric signals. This thesis tests the hypothesis that the sensitivity of assays utilizing such a composite reporter could be improved even further by a nucleation-based signal amplification approach.

1.3 Objectives and Scope

Although the characteristics of LFAs make them a promising POCT candidate for various applications, their sensitivity limitations have often hindered widespread commercial usage. One of the main reasons for this is the interferences arising from complex matrices such as blood, urine, sweat and saliva. In such assays, sample pre-treatment involving magnetic bead-based extraction of analytes using an external magnetic field has been widely reported. The primary objective of this thesis is to devise strategies involving functionalised magnetic beads and explore their feasibility for improving LFA sensitivity in complex matrices and its robustness.

The specific objectives of this thesis are:

1. To investigate a modified LFA design, which uses magnetic beads as reporters and incorporated with a magnetic field assisted sample pretreatment step.
2. To investigate a nucleation-based signal amplification technique on an LFA using a

novel gold nanoparticle conjugated magnetic bead reporter.

3. To investigate the feasibility of an LFA layout, replacing traditional antibodies with an affimer-based system, for enhancing its robustness.

The overarching aim of this work is to make LFAs more reliable, especially for on-site testing in resource limited settings. The LFA layouts should also have a generic approach and can easily be translated for detection of other biomolecules, which also enables implementation of the proposed LFAs for detection of doping markers in athletes. The current anti-doping programme is highly expensive and tedious. It involves random testing of only a few athletes, where the samples are collected on-site and transported to specialised labs for testing. Use of the proposed LFAs as an efficient and cost effective screening method could allow organisers and officials to carry out mass testing and flag doubtful samples, both during and outside competitions, thus making the anti-doping programme much more efficient and effective in curbing out the menace of substance abuse.

1.4 Dissertation Overview

This thesis comprises of 8 chapters, brief descriptions of which are provided in the following paragraphs:

Chapter 1 is an introduction to the thesis describing the background of research. It also contains the hypothesis, objectives and scope of this work.

Chapter 2 is a literature review of the topics associated to the thesis work. It provides a review of literature on POCTs and LFAs, discussing their different aspects such as reporter signals, sensing mechanism, current status and associated challenges. This chapter also sheds light on the various doping markers and discusses the different analytical techniques currently used for detection.

Chapter 3 describes the experimental methodology and the characterisation methods used.

It also discusses the rationale behind using the various materials involved in the LFA fabrication.

Chapter 4 consists of the first set of results involving basic optimisation experiments that have been performed to fabricate the LFA layouts used in this work. It addresses various aspects of an LFA: the membranes, the reporter molecules and the sample deposition volumes.

Chapter 5 is a detailed study of a novel LFA layout, which uses magnetic bead as colorimetric reporters and incorporates a magnetic field assisted analyte preconcentration step with the LFA strip. Troponin has been used as a model system for the study and the layout has been validated in PBS buffer and plasma.

Chapter 6 describes the use of a novel gold nanoparticle conjugated magnetic bead reporter for a facile nucleation-based signal amplification. The LFA layout was tested for detection of Troponin in PBS and plasma.

Chapter 7 demonstrates proof-of-concept assays for two well-known sports markers: Insulin like Growth Factor-1 (IGF-1) and Interlukin-8 (IL-8). The IGF-1 model system was assayed in plasma using the layouts developed in chapter 5 and 6, whereas a novel affimer-based LFA layout was demonstrated for assaying IL-8 model system in PBS.

Chapter 8 presents a summary of the findings of this thesis and discusses the future outlook.

1.5 Findings and Outcomes/Originality

The work in this thesis led to several novel outcomes:

1. A novel LFA layout, which enabled a facile on-site analysis of complex sample matrices was successfully developed and validated in both buffer and plasma.

2. A facile nucleation-based signal amplification protocol utilising a novel gold

nanoparticle conjugated magnetic bead reporter was successfully demonstrated for assaying biomarkers in both buffer and plasma.

3. The feasibility of an affimer-based novel LFA layout, utilising functionalised magnetic bead reporters, was successfully demonstrated for assaying biomarkers.

References

1. Taware, G.B. and D.G. Bansode, *Doping in sports.* National Journal of Basic Medical Sciences, 2015. **6**(2): p. 89-92.

2. Holt, R.I., I. Erotokritou-Mulligan, and P.H. Sönksen, *The history of doping and growth hormone abuse in sport.* Growth Hormone & IGF Research, 2009. **19**(4): p. 320-326.

3. ES Phipson, C., *'Doping'in Athletic Contests.* The Indian Medical Gazette, 1940. **75**(8): p. 484.

4. Yesalis, C.E. and M.S. Bahrke, *History of doping in sport.* International Sports Studies, 2002. **24**(1): p. 42-76.

5. (WADA), W.A.-D.A. *The World Anti-Doping Code International Standard Prohibited List*. 2017; Available from: https://www.wada-ama.org/sites/default/files/resources/files/2016-09-29_-_wada_prohibited_list_2017_eng_final.pdf.

6. Guddat, S., et al., *Synthesis, characterization, and detection of new oxandrolone metabolites as long-term markers in sports drug testing.* Analytical and Bioanalytical Chemistry, 2013. **405**(25): p. 8285-8294.

7. Bidlingmaier, M., et al., *High-sensitivity chemiluminescence immunoassays for detection of growth hormone doping in sports.* Clinical chemistry, 2009. **55**(3): p. 445-453.

8. Beattie, J., et al., *Molecular interactions in the insulin-like growth factor (IGF) axis: a surface plasmon resonance (SPR) based biosensor study.* Molecular and Cellular Biochemistry, 2008. **307**(1-2): p. 221-236.

9. Stübiger, G., et al., *Characterization of N-and O-glycopeptides of recombinant human erythropoietins as potential biomarkers for doping analysis by means of microscale*

sample purification combined with MALDI-TOF and quadrupole IT/RTOF mass spectrometry. Journal of separation science, 2005. **28**(14): p. 1764-1778.

10. WADA. *WADA Accredited Labs*. [cited 2020 14th May]; Available from: https://www.wada-ama.org/en/resources/laboratories/list-of-wada-accredited-laboratories.

11. Drain, P.K., et al., *Diagnostic point-of-care tests in resource-limited settings.* The Lancet Infectious Diseases, 2014. **14**(3): p. 239-249.

12. Yager, P., G.J. Domingo, and J. Gerdes, *Point-of-care diagnostics for global health.* Annual Review of Biomedical Engineering, 2008. **10**.

13. Posthuma-Trumpie, G.A., J. Korf, and A. van Amerongen, *Lateral flow (immuno) assay: its strengths, weaknesses, opportunities and threats. A literature survey.* Analytical and Bioanalytical Chemistry, 2009. **393**(2): p. 569-582.

14. Ching, K.H., *Lateral flow immunoassay*, in *ELISA*. 2015, Springer. p. 127-137.

15. Sajid, M., A.-N. Kawde, and M. Daud, *Designs, formats and applications of lateral flow assay: A literature review.* Journal of Saudi Chemical Society, 2015. **19**(6): p. 689-705.

16. Blažková, M., et al., *Development of a nucleic acid lateral flow immunoassay for simultaneous detection of Listeria spp. and Listeriamonocytogenes in food.* European Food Research and Technology, 2009. **229**(6): p. 867.

17. Chen, A. and S. Yang, *Replacing antibodies with aptamers in lateral flow immunoassay.* Biosensors and Bioelectronics, 2015. **71**: p. 230-242.

18. Wang, Y., C. Fill, and S.R. Nugen, *Development of chemiluminescent lateral flow assay for the detection of nucleic acids.* Biosensors, 2012. **2**(1): p. 32-42.

19. Choi, D.H., et al., *A dual gold nanoparticle conjugate-based lateral flow assay (LFA) method for the analysis of troponin I.* Biosensors and Bioelectronics, 2010. **25**(8): p. 1999-2002.

20. Bahadır, E.B. and M.K. Sezgintürk, *Lateral flow assays: Principles, designs and labels.* TrAC Trends in Analytical Chemistry, 2016. **82**: p. 286-306.

21. Sharma, A., et al., *Magnetic field assisted preconcentration of biomolecules for lateral flow assaying.* Sensors and Actuators B: Chemical, 2019. **285**: p. 431-437.

22. Gao, Z., et al., *High-resolution colorimetric assay for rapid visual readout of phosphatase activity based on gold/silver core/shell nanorod.* ACS Applied Materials & Interfaces, 2014. **6**(20): p. 18243-18250.

23. Koczula, K.M. and A. Gallotta, *Lateral flow assays.* Essays in Biochemistry, 2016. **60**(1): p. 111-120.

24. Kasetsirikul, S., M.J. Shiddiky, and N.-T. Nguyen, *Challenges and perspectives in the development of paper-based lateral flow assays.* Microfluidics and Nanofluidics, 2020. **24**(2): p. 17.

25. Berlina, A.N., et al., *Quantum dot-based lateral flow immunoassay for detection of chloramphenicol in milk.* Analytical and Bioanalytical Chemistry, 2013. **405**(14): p. 4997-5000.

26. Molinelli, A., K. Grossalber, and R. Krska, *A rapid lateral flow test for the determination of total type B fumonisins in maize.* Analytical and Bioanalytical Chemistry, 2009. **395**(5): p. 1309.

27. Wu, W., et al., *A sensitive lateral flow biosensor for Escherichia coli O157: H7 detection based on aptamer mediated strand displacement amplification.* Analytica Chimica Acta, 2015. **861**: p. 62-68.

28. Xu, Y., et al., *Fluorescent probe-based lateral flow assay for multiplex nucleic acid detection.* Analytical Chemistry, 2014. **86**(12): p. 5611-5614.

29. Yang, Y., et al., *Magnetic nano-beads based separation combined with propidium monoazide treatment and multiplex PCR assay for simultaneous detection of viable Salmonella Typhimurium, Escherichia coli O157: H7 and Listeria monocytogenes in food products.* Food Microbiology, 2013. **34**(2): p. 418-424.

30. Bordelon, H., et al., *A magnetic bead-based method for concentrating DNA from human urine for downstream detection.* Plos One, 2013. **8**(7).

31. Jazayeri, M.H., et al., *Colorimetric detection based on gold nano particles (GNPs): An easy, fast, inexpensive, low-cost and short time method in detection of analytes (protein, DNA, and ion).* Sensing and Bio-Sensing Research, 2018. **20**: p. 1-8.

Chapter 2

Literature Review

This chapter sheds light on the background of sports doping and the current anti-doping programme. The analytical techniques used for detection of doping and the associated challenges will be elaborated with an emphasis on the significance of a POC screening device for monitoring prohibited substances. Although, various POC platforms will be briefly discussed, the focus is on LFAs because of the inherent advantages they provide. The various aspects of LFAs, including device fabrication, reaction mechanisms and signal generation will be discussed. This chapter also elaborates the importance of sample pre-treatment for any on-site assay and discusses the various methods which are currently in use. Finally, the research models utilized in this thesis are briefly discussed.

2.1 Overview of Doping

Sports have always served as the ultimate display of a person's physical abilities ever since the ancient times. The pride and resulting rewards associated with victory have intrigued sportsmen. Although sports are the ultimate test of an athlete's training and diet regimen, there are individual physical limitations on how much athletes can extract out of their body. Therefore, external substances that can aid their usual training regimen and push their physical limits have been evaluated. This moot concept eventually developed into a full-scale menace known as doping. With modern day sporting events becoming cash-rich spectacles, the stakes and rewards are higher than even before, alluring several athletes across various disciplines around the world into the folds of doping.

2.1.1 History of Doping

The concept of doping is as old as competitive sports itself. It is believed that the term "doping", which officially found its first mention in an English dictionary in 1889, has been derived from the term "dop", which was an alcoholic drink used as a stimulant in Southern Africa during the early 18^{th} century.[1] One of the earliest instances of using external substances for performance enhancement was recorded in Greece in 668 BC, where a diet of dried figs was used by athletes for racing.[1, 2] Ancient Greeks were also known for using stimulants such as concoctions of mushrooms and plant seeds, and potions containing brandy and wine during training. Such practices were prevalent in ancient Rome, where athletes drank herbal infusions to strengthen them before chariot races.[2]

Modern day substance abuse started in the early 19^{th} century, arising mainly due to advancements in medicine and pharmacology. Substances such as caffeine and alcohol were widely used by athletes during competitions. However, towards the end of the century, 'novel' recipes containing mixtures of stimulants such as strychnine and cocaine became prevalent and were frequently consumed along with caffeine or even alcoholic drinks. The first major report of doping came out in 1886 when an English cyclist, Arthur

Linton, died after overdosing on “tri-methyl”, a stimulant, during a long distance race.[1, 2]

The doping scenario in 20th century became even more rampant with several artificial substances becoming rapidly available. The IAAF banned use of stimulants in 1928, however lack of human testing implied that the doping may have persisted. By 1960s, the number of athletes overdosing on substances increased significantly, which led the International Olympic Committee (IOC) to constitute a commission to compile the first ever List of Prohibited Substances in 1967. In the following year, the first human tests were conducted in the Mexico Summer Olympics. However, awareness about the menace of doping started mainly after the 1998 Tour De France scandal, where one of the participating teams was found to possess large number of performance enhancing drugs and later admitted to regular usage.[1] This event received widespread media coverage and led to public outrage. By the end of the 20th century, use of anabolic steroids such as testosterone and several hormones such as Erythropoietin (EPO) and growth hormone (GH) had become common.[1-3]

In the recent years, athletes from several disciplines like sprinting, wrestling, boxing, tennis, etc., have been tested positive for banned substances. Marion Jones, Lance Armstrong, Martina Hingis etc. are some of the high-profile sportsmen of this century. Several reports of decades long state-sponsored doping programmes have also come to light recently. For instance, the entire Russian sporting federation was banned by WADA in late 2019 from competing in all international sporting events after the Russian Anti-Doping Agency was found to have been manipulating test results to protect their athletes.[4] Therefore, the performance enhancing substances in conjunction with modern doping techniques remains as the biggest threat to the sports community.

Knowing about the exact extent of doping today is almost impossible due to the extreme secrecy surrounding the entire phenomenon. According to WADA, around 1% of the tests conducted in their accredited laboratories are positive.[2, 5] However, the lack of frequent tests and modern masking agents indicates that 1% is only an underestimate. In a report by

the US Office of National Drug Control Policy in 2000, it was reported that doping is a widely variable practice and can affect up to 90% of the professional athletes.[2] According to a WADA commissioned study, almost 44% of the athletes admitted to using banned substances during the 2011 World Championships in Athletics, however less than 0.5% of those tested were tested positive.[6]

2.1.2 Classes of Banned Substances

WADA has been maintaining a list of banned substances since 2002 and reviews it every year.[7, 8] According to the WADA code, the banned compounds should satisfy at least two of the following three criteria:

1. The substance can potentially enhance or enhances performance of an athlete.
2. The substance can have a long-term and/or short-term health risk for the athlete.
3. The substance, when used, violates the spirit of sports.

Additionally, any substance or method that can potentially mask the use of other banned substances can also be added to the list. The list is reviewed by a committee of international experts, circulated to stakeholders for commentary, and approved by the WADA Health, Medicine, and Research Committee as well as the Foundation Board.[9]

The banned substances can be broadly divided into three main categories: substances prohibited at all times (anabolic steroids, peptide hormones, masking agents etc.), substances prohibited in-competitions (stimulants, narcotics, glucocorticoids and cannabinoids) and substances prohibited in particular sports (β-blockers). The summarized list of WADA categorized list of prohibited substances is given in Table 2.1.

Table 2.1: Summarized list of prohibited substance by WADA [2, 9-15]

Class	Name	Effect on Athletes	Risks	Selected Examples
Prohibited at all times				
S1.1a	Exogenous anabolic androgenic steroids	Increase muscle mass, muscle strength, reduce post-exercise recovery time	Skin disorders such as acne, liver abnormalities, tumour risk, high blood pressure, psychiatric disorders such as depression and rage, infertility	Bolasterone, boldenone, clostebol, fluoxy-methandienone, methyltrienolone, methyltestosterone, mibolerone, nandrolone; norbolethone, oxandrolone, oxymesterone, stanozolol, 1-testosterone, tetrahydrogestrinone
S1.1.b	Endogenous anabolic androgenic steroids			Androstenediol; androstenedione; dihydrotestosterone; testosterone;
S1.2	Other anabolic agents			Clenbuterol, selective androgen receptor modulators, tibolone, zeranol
S2	Hormones and related substances	Enhance lipolytic activity, augment muscle building, improve oxygen availability, reduce fatigue and exhaustion, speed up recovery	Joint pains, muscle weakness, risk of diabetes and vision problems, high blood pressure	Erythropoietin, growth hormone, insulin, adrenocorticotrophin; insulin-like growth factor 1, chorionic gonadotropin
S3	β2-agonists	Dilate the bronchial passages, enhance oxygen intake, aids in muscle building, lowering of body fat	Chest pain, irregular heart beat, insomnia, muscle spasms	Salbutamol, salmeterol, and terbutaline
S4	Hormone antagonists and modulators	Block oestrogen receptors and increase testosterone levels	Bloating, Abdominal pain, Headaches, Nausea	Aminoglutethimide, tamoxifen, clomiphene, myostatin inhibitors
S5	Diuretics and masking agents	Control natural balance of fluids and salts, help in rapid weight loss, help in dilution of urine which can mask prohibited substances	Dehydration, muscle cramps, salt deficiency, low blood pressure, loss of coordination and balance	Diuretics, probenecid, plasma expanders (e.g., intravenous administration of albumin, dextran, hydroxyethyl starch and mannitol)

Table 2.1: Summarized list of prohibited substance by WADA [2, 9-15]

Class	Name	Effect on Athletes	Risks	Selected Examples
Prohibited in-competition				
S6.a	Nonspecified stimulants	Effect central nervous system to increase heart rate, resuling in stimulation of oxygen supply, lowering of fatigue and exhaustion, increased alertness	Loss in focus, nervous irritability, dehydration, high blood pressure, hallucinations, elevated risk of stroke, abnormal heart rhythms and insomnia	Amphetamine, amphetaminil, benzphetamine, benzylpiperazine, bromantan, carphedon, clobenzorex, cocaine, dimethylamphetamine, ethylamphetamine, fenproporex, mesocarb, d-methamphetamine, methylenedioxyamphetamine, methylenedioxymethamphetamine, p-methylamphetamine, modafinil, prolintane
S6.b	Specified stimulants			Ephedrine, fencamfamin, levmetamphetamine, methylephedrine, methylpheniidate, parahydroxyamphetamine, pemoline, selegiline
S7	Narcotics	Not many ergogenic effects but mainly used for lowering of anxiety or tremor prior to competition, psychomotor effects or control appetite	Lowering of motor skills, headaches, hypertension, disorientation, nausea, immune dysfunction and psycological disorders such as depression. Chronic use can cause cardiac and liver disorders.	Buprenorphine, heroin, fentanyl, hydromorphone, meperidine, morphine, oxycodone, oxymorphone, pentazocine
S8	Cannabinoids			Hashish, marijuana, tetrahydrocannabinols
S9	Glucocorticosteroids	Oral, rectal, intravenous and intramuscular administration is prohibited. Faster recovery from injury, increase availability of metabolic substrates for energy production, maintain normal vascular integrity	Elevated risk of osteoporosis, insulin resistance, and hypertension	Methylprednisone, prednisone, budesonide, triamcinolone acetonide
Prohibited in particular sports				
P1	β-blockers	Block adrenaline in the body, reduce heart rate, lower anxiety	Severe blood sugar changes, weakened heart, chest pain, difficulty breathing, weight gain, extreme fatigue, nausea and weakness	Acebutolol, alprenolol, betaxolol, bunolol, carteolol, labetalol, esmolol

2.1.3 Current Anti-Doping Programme

The main governing agency for all anti-doping programmes across the world is the WADA. After the 1998 Tour De France scandal, the IOC along with several public agencies across the world commissioned WADA in 1999.[2] WADA approved and implemented the World Anti-Doping code in 2002. This served as the basis for development of anti-doping test protocols across the world. The current doping control and analysis protocol includes collection of biological samples from an athlete, identification and in some cases quantification of banned substances. Urine and blood are considered to be the ideal matrices for detection of banned substances and hence WADA has developed protocols for collection and sample preparation of same.[16] Urine assay has been very popular as it is a non-invasive approach compared to assaying blood with inherent limitations.

In a typical urine based testing protocol, an athlete's urine sample is collected and divided into two parts: A and B, with each part preserved within sealed and labelled containers.[1, 17] These samples are then transferred to a WADA accredited laboratories and stored separately. Upon testing, if the A sample is positive, the athlete is given an option of getting the B sample tested as well. If the second sample tests positive as well, violation of WADA's anti-doping rule is confirmed, and legal proceedings are initiated against the athlete. However, with an ever-increasing number of dietary supplements and sophistication of doping techniques adopted by the trainers and physicians of athletes, it has become very important to change strategies involving collection and testing of samples. A combination of 'no notice' out-of-competition tests, as well as, real-time competition tests, with proper analytical approach is performed currently to serve as a deterrent for athletes from using banned substances.[17] Nonetheless, out of competition doping control is still not very popular as the high logistical and economic issues hinder facile testing. WADA's International Standard for Testing and Investigations (ISTI) has a "Whereabouts rule" under which athletes need to be available for at least one hour every day for out of competition testing and share their locations for that hour with their national anti-doping agencies.[18] However, this rule is only limited to a few handpicked top-level athletes,

who are part of a Registered Testing Pool (RTP). The general schematic followed for testing samples is shown in Fig 2.1.

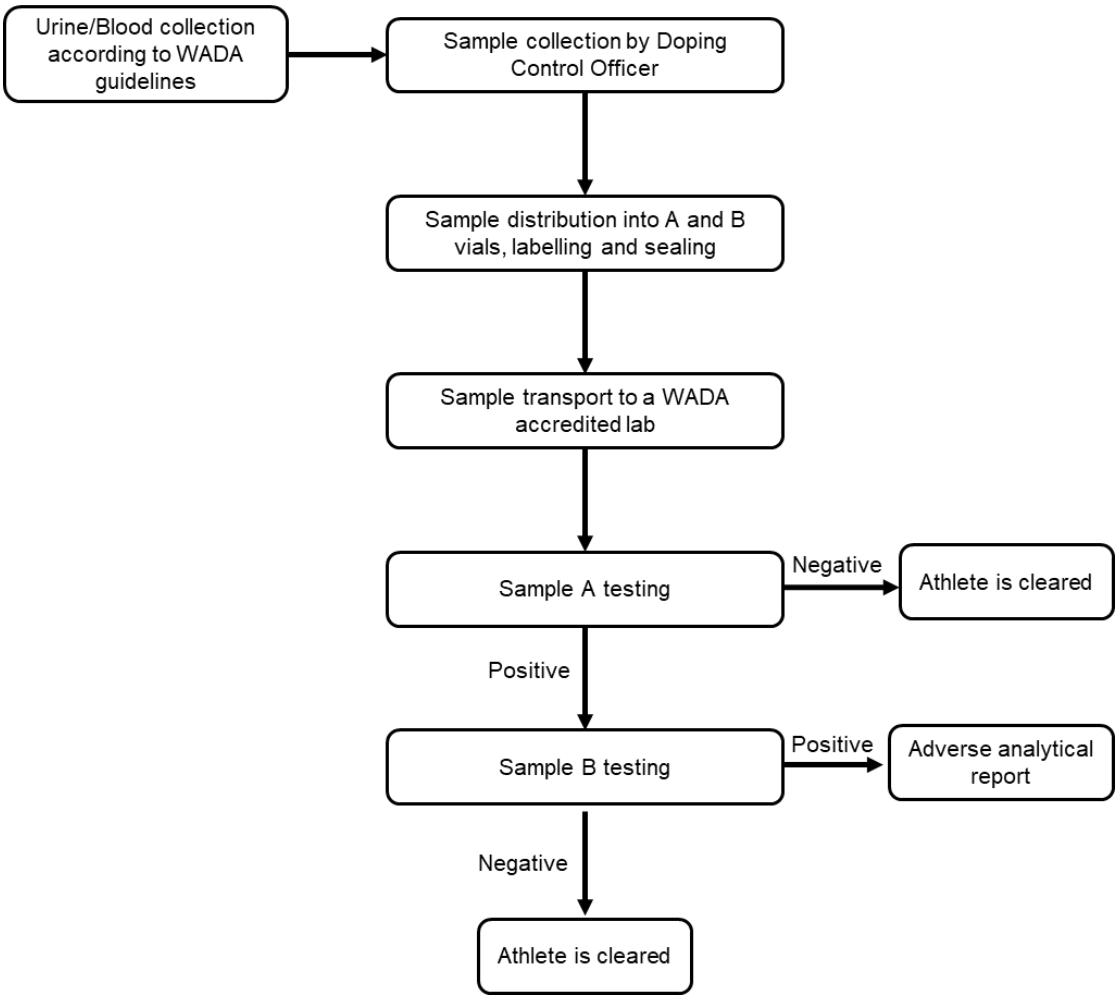

Fig 2.1: Typical workflow of anti-doping testing procedure

2.2 Current Analytical Techniques

Various laboratory analytical techniques have been reported for detection of banned substances. WADA has accredited 35 labs worldwide to carry out these tests.[19] To maintain the homogeneity in results between these laboratories, WADA has set Minimum Required Performance Levels (MRPL) for the analytical tests.[16] The technique used

depends on the class of substance to be tested. The most common techniques currently used are listed in the following section.

2.2.1 Mass Spectroscopic Techniques

1. Gas Chromatography-Mass Spectrometry: It is an instrumental technique, where a Gas Chromatograph (GC) is coupled to a Mass Spectrometer (MS). The sample is injected into the GC through an inlet, where it vaporizes and carried to a chromatographic column by a mobile phase (mostly Helium). In the chromatographic column, the molecules in the mixture of interest move at different speeds due to the varying affinity of the molecules to the stationary phase (the wall of the column and the solid constituents supported by it). This leads to separation of the mixture as it travels along the column. The separated molecules then pass through a heated transfer line and are ionized before entering the spectroscopic mass analyzer. The mass analyzer sorts the ions based on their mass-to-charge ratio and creates a mass spectrum. The separated ions then enter a detector, which collects data and translates it to readable format about the amount and concentration of the molecules. The obtained mass spectrum is compared with that of the reference spectrum of the banned substances of interest.[20, 21]

GC-MS remains the gold standard for detection of several classes of banned substances, most notably anabolic steroids.[16, 22] Anabolic steroids can have several isomers or metabolites and may widely vary in concentrations, making its detection particularly challenging. GC-MS is especially useful in such scenarios because of the wide availability of mass-spectral libraries and low instrument variability across labs. This technique has also been successfully used for detection of other prohibited substances such as β-blockers, diuretics and even xenon from urine.[16, 23, 24]

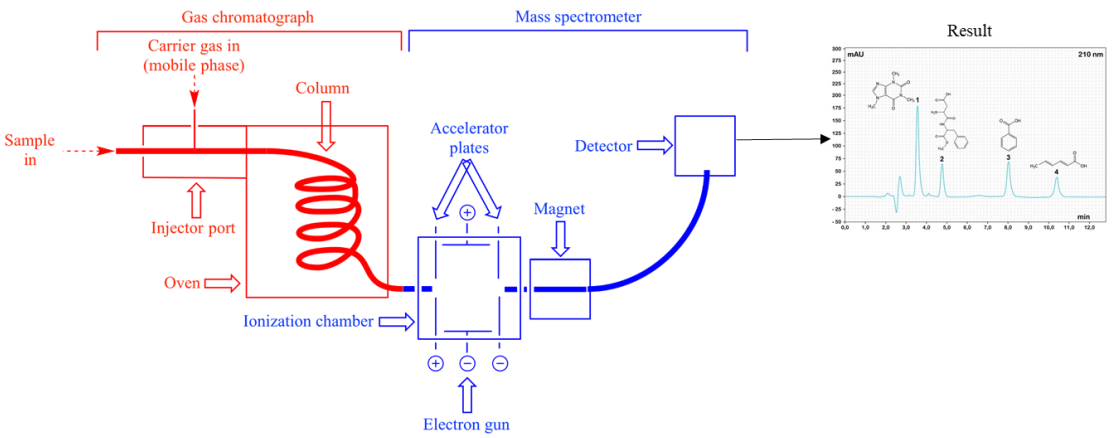

Fig 2.2: Schematic of a typical GC-MS system. [25] The red part on the left shows how a sample is injected through the inlet and the transported through a column by a carrier gas. The blue part shows the functioning of the ionizer before the sample enters the detection chamber. The spectrum obtained using the mas to charge ratio shows characteristic peaks of the compounds.

2. Liquid Chromatography-Mass Spectrometry: This technique combines the physical separation process of liquid chromatography (LC), where the moving phase is a liquid medium carrying the analyte solution, with the analytics of an MS. LC-MS became popular mainly because of its shorter turnaround time and higher sensitivity than GC-MS. Moreover, the sample preparation before LC-MS is much easier when compared to GC-MS. There are 5 types of LC-MS systems typically used in analytical laboratories for sample assessment: adsorption chromatography, partition chromatography, ion-exchange chromatography, size exclusion chromatography and affinity chromatography. Amongst them, Reverse Phase (RP) mode of partition chromatography is the most popular. In RPLC-MS, the components of a liquid mixture are distributed between two immiscible phases, i.e., stationary and mobile. The mobile phase is generally a mixture of water and other polar solvents like methanol, isopropanol and acetonitrile. On the other hand, the stationary phase is a non-polar matrix, prepared by attaching long-chain alkyl groups (e.g., n-octadecyl or C18) to the surface of irregularly or spherically shaped porous silica particles. The basis of RPLC separation is the hydrophobic interaction between the analyte and the nonpolar matrix of the stationary phase. Another approach, which is used widely to improve resolving power and throughput of RPLC is to limit the size of the porous silica particles between 2-50 µm and increase the operating pressure of liquid phase to ~400

bar.[20, 26] This is known as High Performance Liquid Chromatography (HPLC). The typical dimensions of the separation columns in HPLC-MS are 20-30 mm long with a diameter of 2.1–4.6 mm.[20, 27] For multiple analytes, often LC-MS/MS or LC-tandem mass spectroscopy, is used. It is a technique where two MS analyser instruments are used in conjunction. The first MS filters for the precursor ion followed by a fragmentation of the precursor ion with high energy. The second MS filters for the product ions, generated by the fragmentation. LC-MS is most useful for detection of small peptides such as Growth Hormone Releasing Hormone (GHRH) and is also used to detect stimulants, anabolic steroids and several hormones like GH and IGF-1.[16, 27]

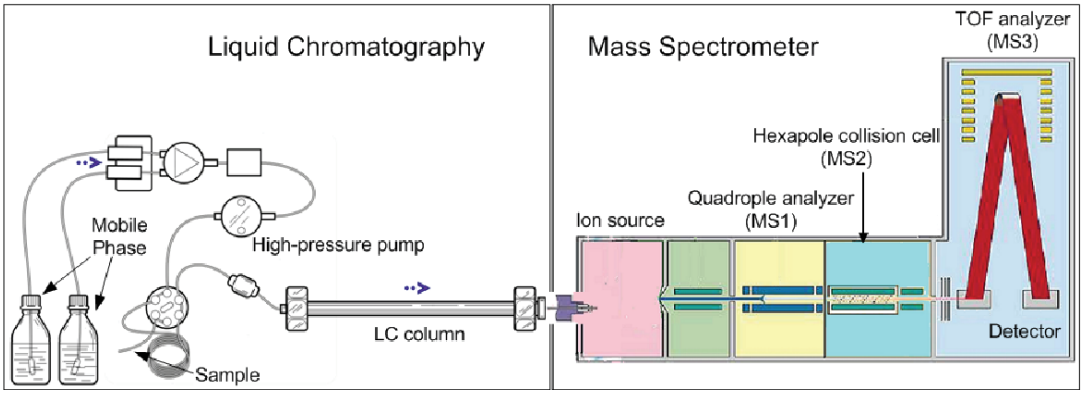

Fig 2.3: Schematic of a typical LC-MS system [28] The left part of the schematic shows the functioning of the liquid chromatograph. Here the sample is carried by a liquid phase under high pressure through a functionalized column where separation of components takes places. The right part shows the functioning of the mass spectrometer, which is same as GC-MS.

3. Isotope Radio Mass Spectrometry (IRMS): This is a technique where mass spectroscopy is used to detect and measure relative amounts of isotopes in a given sample. The basic principle behind IRMS is the acceleration of ionized gaseous molecules through a magnetic field, which causes a separation of molecules according to their mass-to-charge (*m/q*) ratio. This causes beams of isotopically lighter ions to bend more than beams of isotopically heavier ions. The ion beams are focused into Faraday collectors that continuously record the electronic current generated by each beam.[29]

It is most commonly used in detection of Testosterone and other androgenic steroids from urine samples. Testosterone contains a mixture of ^{13}C and ^{12}C, but it is known that endogenous Testosterone has higher ^{13}C than the synthetic forms. IRMS is used to measure the amounts of each isotope and thus give an indication of Testosterone abuse. In this technique, samples must be introduced as pure gases. This can be achieved by pyrolysis in a combustion chamber before the spectral analysis. The analytes are separated from urine by GC and then taken to a combustion chamber. Here, every carbon atom is converted to either $^{12}CO_2$ or $^{13}CO_2$. The IRMS measures the amount of isotopic variants of CO_2 in the sample and calculates a value known as '$\delta^{13}C$' (delta), which is expressed in percentage. This value represents the difference between $^{13}C/^{12}C$ ratio measured from the sample and that of an international standard value.[30, 31] This technique has been found to be quite accurate and hence now WADA allows anti-doping agencies to sanction athletes caught using testosterone or its derivatives solely based on IRMS results.[32]

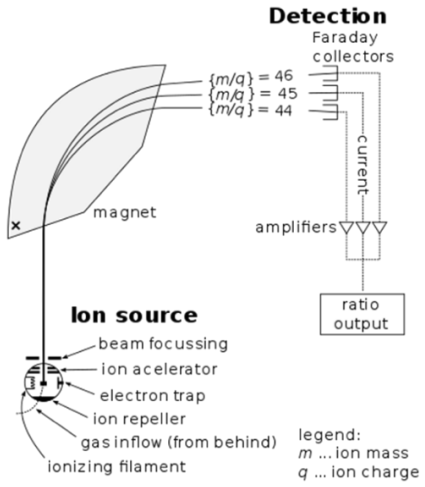

Fig 2.4: Schematic of a typical IRMS system [33] An ion source provides enough energy to separate the input gaseous sample into its ionic fragments, which are then separated by a magnetic field based on the m/q ratio.

2.2.2 Electrophoretic Techniques

1. Isoelectric Focussing (IEF): This technique is based on the principle of separating proteins according to their isoelectric point (pI), which is the pH at which net charge on the molecule is 0. It is an electrophoretic process, where proteins move through an acrylamide gel, under an electric field. This method is especially used for detection of Recombinant Erythropoietin (rEPO), a protein hormone, which can help in production of red blood cells and increase endurance of an athlete. An EPO containing sample is applied at one end of the polyacrylamide gel having a pH gradient. If the proteins are present in a pH region below their pI, they will have a net positive charge, and thus move towards the cathode, which is negatively charged. On the other hand, if the proteins are present in a pH region above their pI, they will move towards the anode, which is positively charged. As EPO moves in the pH gradient, it starts losing its charge and eventually stop migrating when the net charge is 0, which is the pI. The principle behind using this technique is that rEPO and endogenous EPO have different pI. Therefore, they form separate bands in the gel, which are eventually visualised by chemiluminescence.[34] However, IEF requires preconcentration of analytes by methods such as ultrafiltration and immunopurification prior analysis.[35-37]

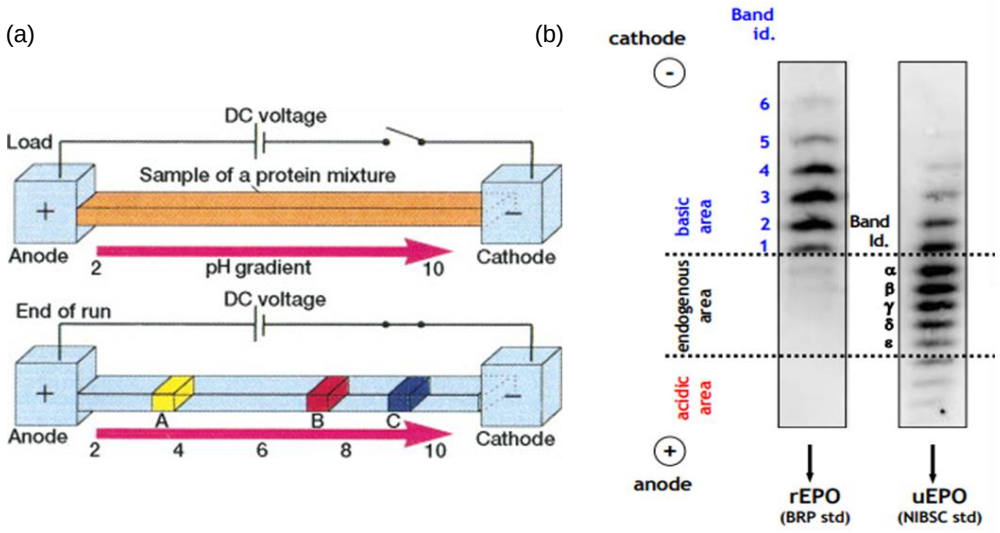

Fig 2.5: (a) Schematic of a typical IEF system (Reprinted with permission.) [38] Sample proteins A, B and C in the schematic move through a pH gradient from one electrode end to the other and eventually stop when they reach their pI. (b) Illustration of an IEF test result for EPO [34]

2. Sodium Dodecyl Sulphate-Polyacrylamide Gel Electrophoresis (SDS-PAGE): Recently WADA approved SDS PAGE as a confirmatory test for rEPO and its analogues such as Peginesatide.[34] It is an electrophoretic technique where proteins move in a polyacrylamide gel under an electric field. Here, the molecules do not separate because of charge but because of size difference. The protein mixture to be tested is first treated with SDS, an anionic surfactant, to solubilize the proteins and linearize the molecules of interest and give them a negative charge, proportional to size.[39] The mixture then moves in the sieving gel, which allows smaller molecules to move faster. In this technique, a standard endogenous EPO channel is run in parallel to the samples in the testing channels. rEPO and its analogues can be easily distinguished from endogenous EPO due to the difference in the migration behaviour between the two forms, owing to their different molecular weights. This results in a characteristic band shape and position for each type of molecule.

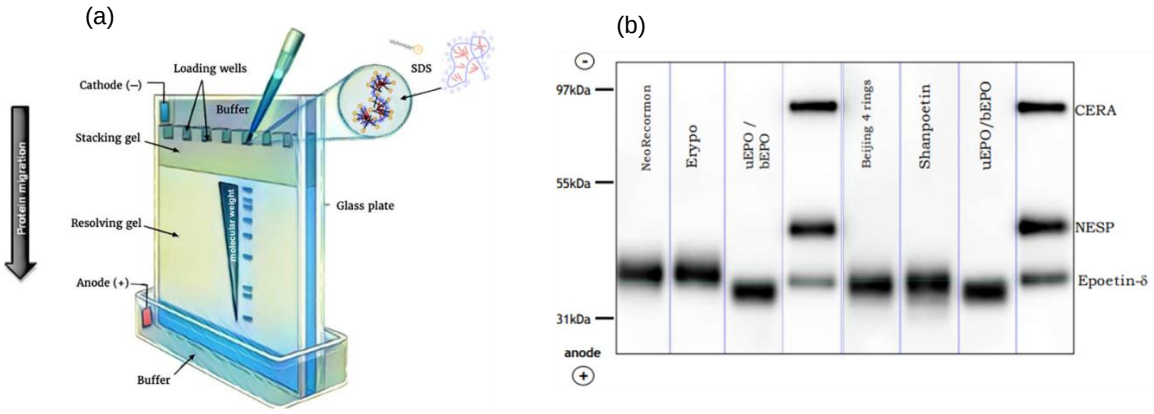

Fig 2.6: (a) Schematic of a typical SDS-PAGE system (Reprinted with permission.) [40] (b) An illustrative SDS-PAGE result showing bands corresponding to several EPO analogues. [34]

2.2.3 Immunoassays

Immunoassays are analytical tests involving the use of antibodies, which selectively bind to analyte of interest to yield a quantifiable signal that correlates to the analyte concentration. The emanated signals are a result of "labels" or reporter molecules conjugated to the antibodies such as enzymes and nanoparticles. The three main types of immunoassays used are direct (labelled antibody binds directly to analyte molecules),

indirect (primary antibody binds to analyte molecule and a labelled secondary antibody binds to the primary antibody) and sandwich (analyte is sandwiched between a primary antibody and a labelled secondary antibody). Immunoassays can also be classified into several categories depending on the type of signal they generate, the common ones being enzyme immunoassay (EIA), radioimmunoassay (RIA), fluoroimmunoassay (FIA), chemiluminescent immunoassay (CLIA) and counting immunoassay (CIA).[41] Immunoassays are useful as they provide rapid responses without requiring heavy instrumentation. Enzyme-linked immunosorbent assay (ELISA) is one of the most commonly used immunoassay technique.[42, 43] It uses Horseradish Peroxidase (HRP) labelled antibodies to bind specifically to analyte molecules in a well plate. Upon formation of antibody-antigen conjugate, substrates such as 3,3′,5,5′-Tetramethylbenzidine (*TMB)* are used to generate an optical signal, which is quantified using a UV-Visible Spectrophotometer.

Immunoassays are mostly used for testing prohibited hormones such as GH, IGF-1 and their isoforms.[44, 45] The WADA approved immunoassay for GH involves detection of the 22 kDa isoform of GH.[45] Although GH is present as a mixture of isoforms in the body, recombinant GH is known to be similar to the 22 kDa isoform. Intake of exogenous GH not only increases 22 kDa isoform concentration, but also suppresses secretion of all other isoforms. The GH test involves a sandwich immunoassay, consisting of a pair of antibodies. A GH-specific capture monoclonal antibody is pre-coated on the surface of the well plate. Subsequently, the captured GH molecules is bound in a sandwich consisting of a detection antibody, which is labelled with acridinium ester, a chemical that gives a luminescent signal when excited at a specific wavelength. Typically, a luminometer is used for quantification.

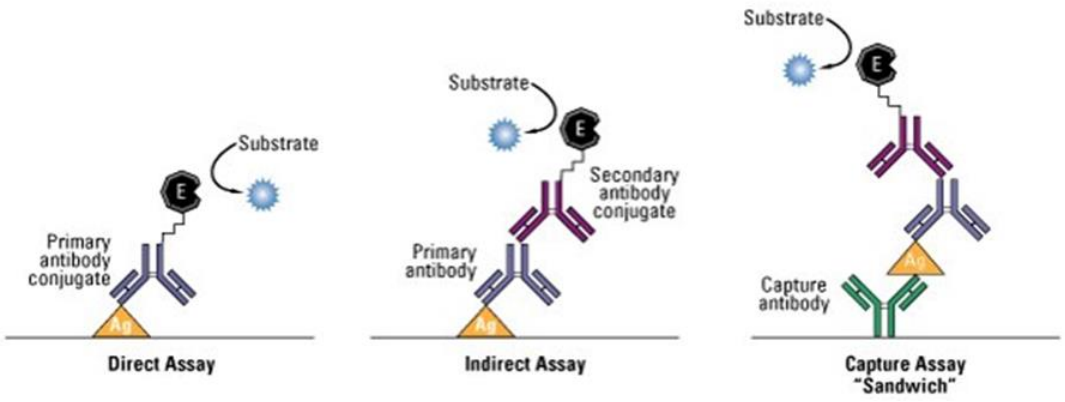

Fig 2.7: Schematic of direct, indirect and sandwich assays. [46] Primary antibodies are required in all three formats, however secondary antibodies are needed in indirect assays for signal generation. A sandwich assay would require a secondary antibody for signal generation if none of the primary antibodies are labelled.

2.2.4 Analytical Challenges

The WADA approved testing methods are governed by specific guidelines and standard operating procedures. However, there are still several analytical challenges associated to these tests.

The first challenge is the requirement of extensive sample preparation for most of these tests. For instance, most GC-MS systems would require a solid phase extraction in which sample is passed through a solid column containing sorbent materials. This helps remove the biological matrix interferents and concentrate the analyte in the injected solution, resulting in a improvement in peak resolution.[47] Similarly, sample dilution is also a common practice before MS analysis. The dilution factors can vary anywhere between 1:1 to 1:25.[16] IEF systems require preconcentration of analytes by methods such as centrifugal ultrafiltration through membranes and immunopurification prior to analysis.[36, 37] These sample pre-treatment strategies are not only time consuming and tedious but are also error prone. Furthermore, non-uniformity in the procedures across labs can be detrimental to accurate analysis and in extreme cases, may also lead to false positives.

The second challenge is the lack of standardization of equipment across the WADA accredited labs, which may lead to lot of variability in results. For example, mass spectrometer instruments often differ in a various aspects across labs. The detectors used maybe single quadrupole or triple quadrupole, which may affect the resolution of the spectrum.[16] GC-MS systems use both types of detectors, however LC-MS mostly use triple quadrupole detectors. Similarly, the luminometers used for immunoassays may use different sets of filters with varying qualities, which may cause variation in the internal calibration. Filter issues can also affect sensitivity of the assay.[48] Thus, standardization across labs in terms of instrument specification, calibration procedures and handling steps is very important.

The third challenge is the non-homogenous physiological profiles of biomarkers across athletes. For example GH levels can be affected by age, sex, stress levels and even by time of the day.[49] Similar effect is observed for several other doping markers such as EPO, testosterone etc. It is well known that several endogenous and exogenous factors influence steroid profiles.[50] Recently, there have been several high profile cases, such as that of Caster Semenya (South Africa) and Dutee Chand (India), where the athletes were banned due to presence of prohibited substances beyond permissible limits. However, it was confirmed later that the athletes were not using prohibited substances, but their biological conditions had led to excessive production of several hormones. Although, use of a “biological passport” of an athlete is gaining popularity, it’s implementation is still challenging.[51] Creating an accurate baseline for a particular marker in an athlete would require frequent testing, both during and beyond training seasons. This is difficult to achieve using the current tests approved by WADA, which are typically complicated, expensive and time consuming.

2.3 Point-of-Care Tests

The analytical techniques discussed in section 2.2 are carried out in accredited laboratories with sophisticated facilities. These tests entail high logistical costs (sample collection, transportation and storing), rely on heavy instrumentation and cannot be conducted on-site.

Moreover, operating these instruments and subsequent data analysis require highly skilled professionals. These issues also mean that such tests are always performed sporadically. Thus, the screening process for athletes, although effective up to some extent, is still not efficient and fool proof due to the lack of frequent testing. Therefore, there is a significant need for reliable and cost-effective Point-of-Care Tests (POCTs).

POCTs are portable analytical devices which can be used for testing analytes on-site.[52, 53] They have a rapid turnaround time of a few minutes, are easy to fabricate and operate and therefore cost effective, require small sample volumes and can be versatile. These devices can be multiplexed easily, thus allowing for detection of multiple analytes. POCTs can be quantitative, semi-quantitative or qualitative in nature.

Table 2.2: Assessment details of a few prohibited substances **[**54-56]

Prohibited Substance	**Analytical Technique Used**	**Matrix**	**WADA Decision Limit**
19-Norandrosterone	GC-MS	Urine	2.5 ng/mL
Carboxy-THC	LC-MS		180 ng/mL
Salbutamol	LC-MS		1.2 µg/mL
Formoterol	LC-MS		50 ng/mL
Morphine	LC-MS		1.3 µg/mL
Cathine	LC-MS		6.0 µg/mL
Ephedrine	LC-MS		11 µg/mL
Methylephedrine	LC-MS		11 µg/mL
Pseudoephedrine	LC-MS		170 µg/mL
rEPO	IEF or SDS-PAGE	Blood	Comparison with standard gel bands
Aranesp	IEF or SDS-PAGE		
Peginesatide	SDS-PAGE		
IGF-1 (GH Biomarker)	Immunoassay or LC-MS with LOQ ≤ 50ng/ml	Blood	Based on GH score*
P-III-NP (GH Biomarker)	Immunoassay with LOQ ≤ 1ng/ml		Based on GH score*
GH isoform	Immunoassay with LOQ ≤ 0.050ng/ml		Based on isoform ratio**

***** GH Score: Weighted score factoring biomarker concentrations, gender and age of athlete

****** Isoform ration: the ratio of monomeric 22k GH to pituitary GH

2.3.1 Regulations and Guidelines

There are several types of tests that can be classified as point-of-care. The World Health Organisation (WHO) defined the characteristics of an ideal POCT device in 2003. These characteristic guidelines can be summarised by the acronym 'ASSURED'.[53]

A: Affordable. Low cost.

S: Sensitive. Low false negatives.

S: Specific. Low false positives.

U: User friendly.

R: Rapid and Robust. Low turnaround time and easy handling and storage.

E: Equipment free. No complex instrumentation.

D: Delivered. Availability to end users

It has been deemed that any POCT meeting the ASSURED parameters would be an ideal choice for commercialization. Although regulatory control over most POCT platforms are minimal, the requirements vary between countries. Most developed nations have strict regulations that monitor POCTs whereas regulations in developing nations are often relaxed to keep the overall costs low.[57] In the US, diagnostic tests are governed by the Clinical Laboratory Improvement Amendment (CLIA) of 1988, which defines the complexity of any testing procedures and classifies them into three categories: highly complex, moderately complex and CLIA waived.[57-59] All POCT programmes in the US have to apply for a CLIA waiver before accreditation by any of the regulatory agencies such as FDA. However, there can also be on-site tests, which may not have CLIA waiver, but such tests have to meet other lab testing regulations. Currently there is no WADA approved POCT for doping control. However, they have recently invested in research ,which could lead to a viable "lab-on-chip" or POC technology.[60]

2.3.2 Types of POCTs

POCT devices can be categorized according to the sensing mechanism, type of signal being emanated or the application they are used for. However, generally, there are two main types of POCTs, which engulf all other classifications: small hand-held POCT devices and larger

bench top POCT devices.[61-63] Amongst the two types, small hand-held devices are the most popular forms of POCTs due to their advantages over the latter. They are easily portable, have much simpler functioning mechanisms and are far more cost effective.[61] Some of the most commonly used hand held POCTs are briefly described in this section.

1. Paper based bio-affinity sensors: Paper based sensors involve pre-fabricated strips consisting of polymeric carrier membranes, which are modified and assembled for selective capture of analyte molecules at specific sites for detection. The analyte solutions, once introduced on the sensor, are allowed to flow through homogenously by capillary forces, which are often enhanced by a wicking material such as cellulose. The analytes are captured at the test zones using recognition molecules, most commonly antibodies, which selectively bind to analyte molecules of interest.[64, 65] In the recent years, several other recognition molecules, such as nucleic acid aptamers [66-68] and small peptide affimers [69, 70], also have been extensively researched upon because of the higher stability, extended shelf life and lower cost as compared to antibodies. The various recognition molecules have been described in detail in section 2.4. The most common paper based sensors are lateral flow assays (LFAs) [64] and dipsticks [71]. These assays use different labels conjugated to recognition molecules to yield detection signals, for instance, colour, fluorescence, chemiluminescence and magnetic field. The interpretation of these signals can make the assays either qualitative where no external instrumentation is used [72] or quantitative where the assays are coupled with technologies to precisely determine signal strength and correlate it to analyte concentration.[73, 74] A few commonly used labels are gold nanoparticles (AuNP) [73], enzymes like HRP [75], latex beads [76], carbon nanoparticles [77], upconverting phosphors [78] etc. The typical testing times for such assays may vary between 5-30 minutes.[64, 74, 79, 80]

2. Electrochemical sensors: Electrochemical sensors consist of electrode transducers, which are coupled to bio-recognition elements for ultra-sensitive detection of analytes. These sensors generate electrical signals upon binding of the analytes to the recognition molecules by means of the transducer they use. The transducers are generally substrates made of either metals (like gold, platinum etc.) [81], semiconductors (like indium-tin oxide,

iridium oxide etc.) [82] or carbon based materials (like graphite, carbon paste, glassy carbon etc.) [83]. Two types of signals are generated by these sensors, depending on the type of transducer used: change in current or change in potential. Amperometric transducers apply a constant voltage and detect the change in current signal upon binding of analyte, whereas, potentiometric transducers use ion-selective electrodes (ISE) to provide a change in voltage upon analyte binding.[84] The detection mechanism may vary depending on the recognition element such as active enzymes (glycolate oxidase, glucose oxidase, etc.) [85], protein based antibodies [86], nucleic acid aptamers [87] and composites [88]. These types of sensors are ultrasensitive, highly specific and easy to miniaturize. This miniaturization allows inclusion of arrays of transducers in a single device, enabling easy multiplexing. Turnaround time for electrochemical sensors is much faster than paper-based sensors (generally a few seconds). The commonly used glucose meter is a well-known example of an electrochemical biosensor.

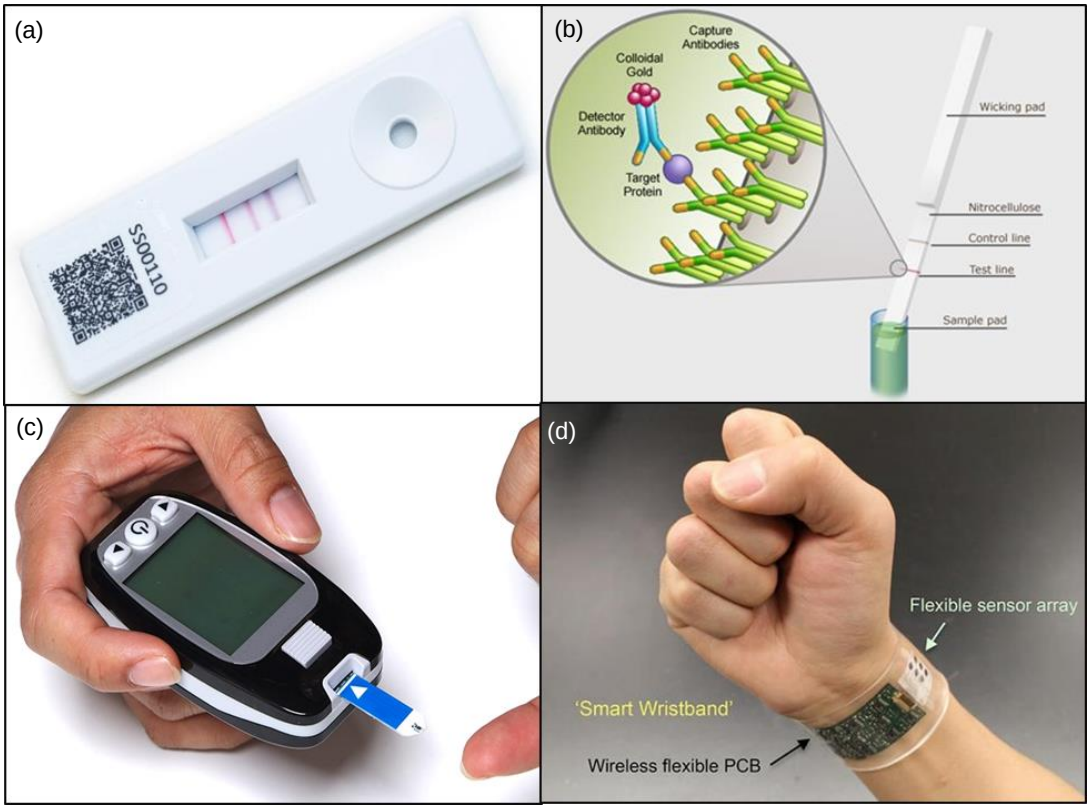

Fig 2.8: (a) A typical paper based LFA [89], (b) Schematic of a paper based dipstick immunoassay [90], (c) An electrochemical glucose meter [91], (d) A flexible substrate wearable electrochemical sensor [92]

3. Microfluidics based sensors: Microfluidics allows precise flow control of small volumes of analyte solutions through fabricated or 'printed' microchannels for controlled, sensitive and multiplexed detection. Several types of sensors use microfluidics for 'lab-on-chip' applications. Incorporating microfluidics into the sensing mechanism has helped researchers and manufacturers to miniaturize sensors for efficient POC applications. Such sensors can utilize several detection mechanisms such as electrochemical sensing [93], affinity based optical and magnetic sensing [94, 95] and even change in surface plasmon resonance (SPR) [96]. Different type of substrates are used to fabricate such sensors. Use of glass, paper, polymers (such as PDMS) and semiconductor substrates (such as silicon) are common. These sensors are fabricated by printing microchannels onto the substrates. The fabrication technique depends on the substrate being used and the application. In the early days, paraffin and wax dipping was used to create hydrophobic coatings for separating the lanes to channelize the flow.[97, 98] However, technological advancements have allowed development of much more sophisticated techniques such as photolithography [99], PDMS printing [100], laser treatment [101] and high resolution wax printing [102] for precise control of the fabrication process.

(a) (b)

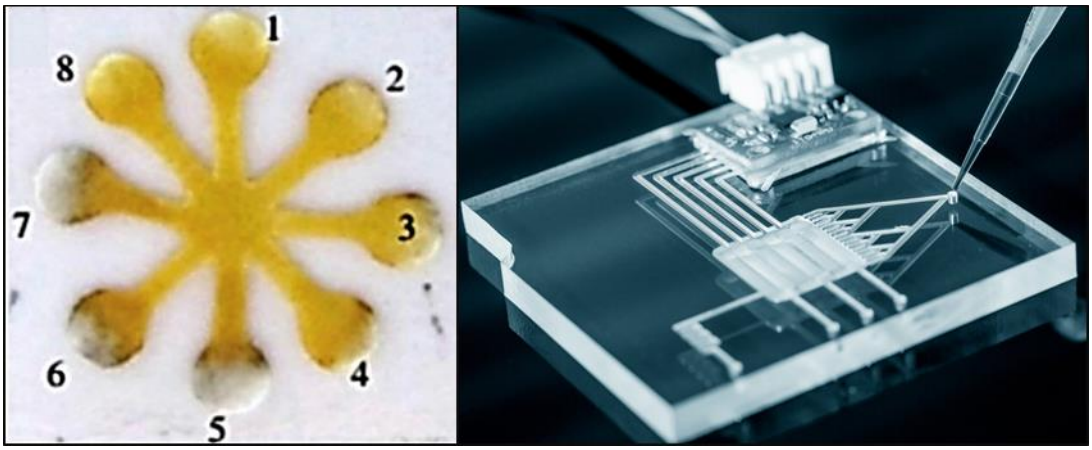

Fig 2.9: (a) A paper based µPAD for colorimetric detection of Cu^{2+}ions in water [103] (Reprinted with permission.), (b) A PDMS based microfluidic lab-on-chip system [104]

2.4 Lateral Flow Assays

An ideal choice of a POCT would be the one which not just has an intuitive simplicity on a user's end but also has a low cost, which could attract mass appeal even in low income countries. As a result, amongst the several types of POCTs listed in section 2.3, lateral flow assay (LFA) strips have become the frontrunner POCT devices for commercialisation. The versatility of such devices in terms of fabrication techniques, as well as the associated low costs and high portability, make them suitable for a myriad of applications; one of the potential application being screening of prohibited substances for doping control. However, the most prominent application of LFAs is in the form of pregnancy strips, which is a multi-billion dollar industry and a highly saturated area of research.[105, 106] LFA strips have several other advantages as well. They are easy to operate and hence require no skilled personnel, require very low sample volumes ($\leq$ 100 µl) and can yield quantitative signal readouts with ubiquitous devices such as smart phones.[107, 108]

2.4.1 LFA Layout

LFAs are basically pre-fabricated strips of some carrier membrane, containing dried reagents that are activated by application of a fluid sample containing the analyte. The sensitivity and specificity of typical LFA layouts are dependent on mainly three parameters: use of miniaturised thin-layer chromatography membranes such as nitrocellulose, capture of analytes by analyte-specific recognition molecules such as antibodies or DNA/RNA sequences, and signal generation by reporter molecules such as AuNP. A typical LFA schematic, as shown in Fig 1.1 of chapter 1, consists of a sample pad, conjugate pad, test pad consisting of a test line and control line, absorbent pad and a backing pad for supporting the assembly.[106] Each pad is made of a specific membrane to suit the respective function it provides. They are placed adjacent to each other, in such a way that a small portion of one membrane overlaps the other membranes adjacent to it. The entire assembly is placed in a plastic housing/cassette. The function, material used and problem associated with each component pad is summarised in Table 2.3. When an assay is performed, a small volume of a sample is applied onto the sample pad, which migrates

along the conjugate pad, and then carries conjugated particles to the test pad. The capillary flow is assisted by a wicking absorption pad at the end of the assay layout. Analytes in the sample interact specifically with recognition molecules (antibodies, peptides, aptamers etc.), which are immobilized at the test line and control line and release a signal.[106, 109] The signals generated in LFAs are due to reporter molecules which are conjugated to biomolecules in the conjugate pad, details of which have been explained in section 2.4.4.

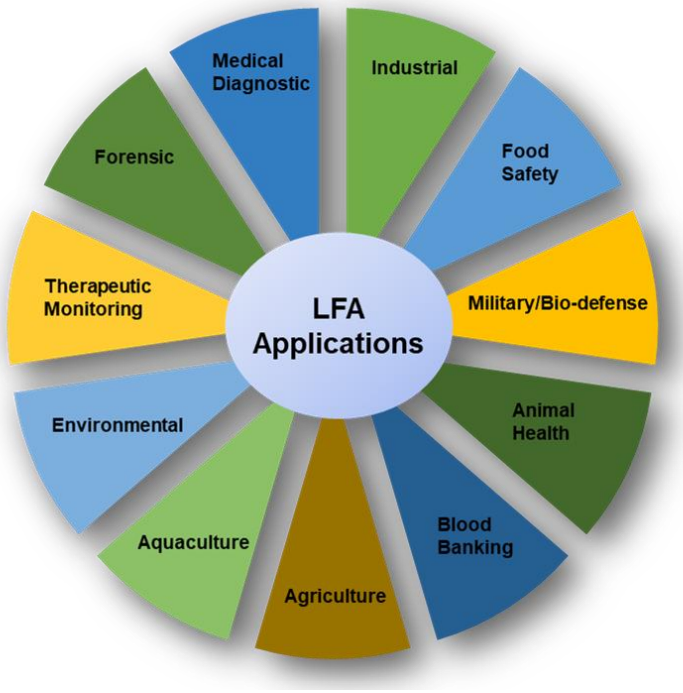

Fig 2.10: Applications of LFA devices

Table 2.3: Summary of different membranes used in LFA [61]

Component	Function	Material	Potential Problems
Sample Pad	Convert the analytical sample to one suitable for analysis	Cotton linter, glass fibre, rayon	Flooding with excess sample, cannot always filter out contaminants
Conjugate Pad	Couples the sample analyte to the measurement conjugate	Glass fibre, polyesters	Variation in uptake, inconsistent binding and release of conjugate
Reaction Membrane (test and control zone)	Acts as capturing mechanism and forms a readable test line when analyte present or absent. Capturing molecules (e.g., antibodies) can be deposited on the membrane to form a test zone and a control zone by	Nitrocellulose, nylon	Inconsistent flow characteristics, protein incompatibility to bind with nitrocellulose
Backing Layer	Provide rigidity and enable easy handling	Polystyrene	Can cause variations in run time and appearance of
Device Housing or Cassette	Protect the properties and features of the device	Plastic	Overflow of sample into cassette

2.4.2 Assay Mechanisms

Mainly two assay formats are used in LFA: sandwich and competitive.[64, 109] In the sandwich format, a labelled recognition molecule binds to the target analyte and forms a conjugate. This conjugate moves downstream to the test line, where target analyte bind specifically to immobilized recognition molecules to form a recognition molecule-analyte-capture molecule complex, which stops migrating. The excess of the labelled recognition molecules from the conjugate pad, which are unbound to the analyte, move beyond the test zone and are eventually captured at the control line by another type of capture molecule. On the other hand, in the competitive format, labelled recognition molecule reacts with capturing molecules deposited in the test zone. The analyte, which is mixed with labelled recognition molecules, competes for the binding sites with the capturing molecules on the test zone. If the analytes are already captured by recognition molecules in the solution during the mixing stage, they are not captured at the test zone, thus no signal is generated. A similar control line is used in the competitive format as well. It is to be noted that the capture molecule in the control line is specific to the recognition molecule rather than the

analyte. The main purpose of the control line is to serve an indicator that ensures that the test is working properly. The sandwich assay is preferred when there are multiple epitopes in the analyte of interest, while the competitive assay is preferred in case of small molecules or in case of single specific antigen epitope.

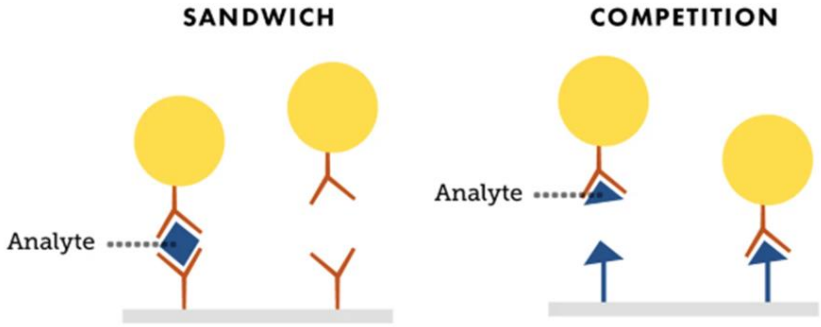

Fig 2.11: Competitive LFA vs Sandwich LFA [110]

2.4.3 Recognition Molecules

1. Antibodies: The most popular biomolecules used for detection and capture of analytes in LFAs are antibodies (Ab) or immunoglobulins (Ig). LFAs involving antibodies are also known as Lateral Flow Immunoassays (LFIA). Antibodies are "Y" shaped proteins having a molecular weight of ~150 kDa, produced by plasma cells, so-called B lymphocytes .[111] Each antibody consists of a binding site known as a paratope at the tip of the "Y". The paratope specifically identifies binding sites known as epitopes on an antigen or analyte molecule. Each analyte molecule can bind to multiple antibodies depending on the number of epitopes present. There are two types of antibodies: monoclonal antibodies, which can bind to only one type of epitope and polyclonal antibodies, which can bind to multiple epitopes on the same analyte molecule.[112, 113] The binding is similar to a lock and key mechanism, which is precise at a site and specific for a system. The interaction is non-covalent and can be a resultant of electrostatic interactions, hydrogen bonds, van der Waals forces and hydrophobic interactions. Typically, LFIA test lines are immobilized with analyte specific primary antibodies, whereas the control line consists of primary antibody specific secondary antibodies. A wide range of antibodies are commercially available

against the common analytes, making them a popular choice for LFIA studies. Moreover, specific antibodies can also be raised against relatively less common analyte molecules. However, antibody production is a tedious and expensive process involving immunizing animals with target molecules, followed by sub-cloning and purification. Several sensitive LFIAs with LODs in the range of a few pg/ml to a few ng/ml have been reported using antibodies as recognition elements.[73, 79]

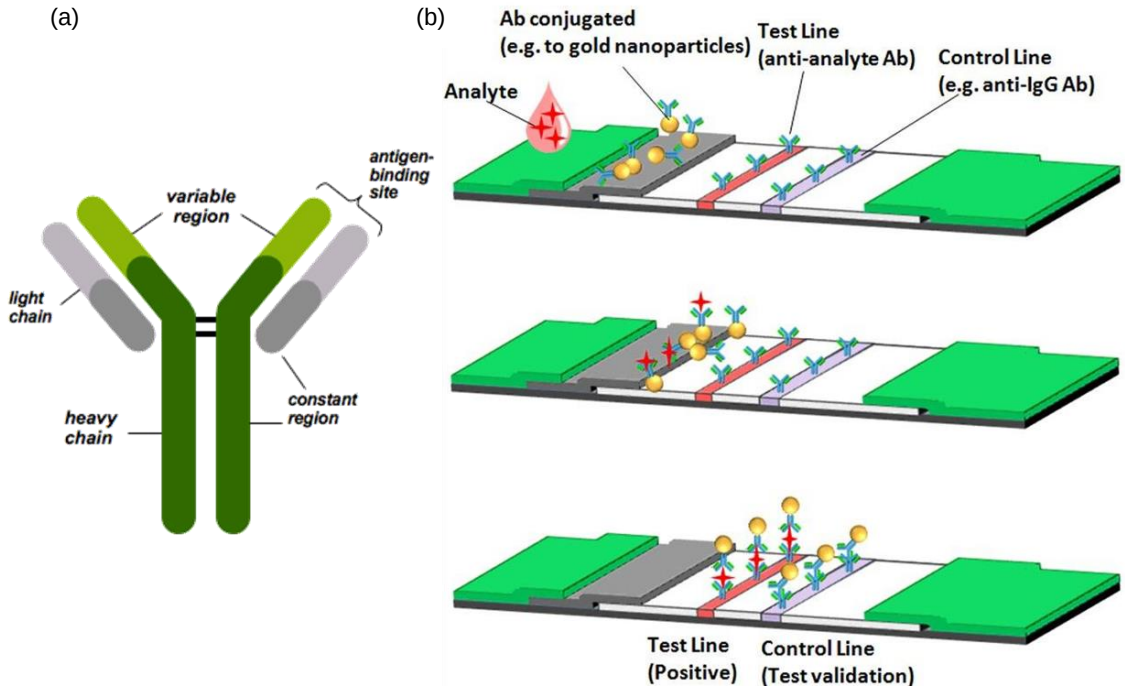

Fig 2.12: A schematic of: (a) an antibody showing the different functional regions. [114], (b) sandwich LFIA using AuNP reporter. [106] The analyte deposited on the test strip binds to Ab conjugated AuNPs and is captured by anti-analyte antibodies at the test line. The control line antibodies capture the free AuNP-Ab conjugates.

2. Aptamers: Nucleic acid aptamers are short, single-stranded oligonucleotides that can form 3-dimensional conformations upon binding specifically with target analytes. The target can be proteins, nucleic acids, cells and even tissues.[115] The analyte-aptamer bond is relatively strong and is a result of hydrogen bonds and electrostatic interactions between the aptamer and analyte. A lot of other factors such as the structure of target and aptamer, stacking interactions between aromatic compounds and the nucleobases of aptamers also

induce aptamer-analyte binding.[115, 116] These short chain oligonucleotides can be both DNA and RNA chains and typically consist of 25-75 nucleotide bases. Aptamers are produced via chemical synthesis route, by a process called 'SELEX' (Systematic Evolution of Ligands by Exponential enrichment).[117] It involves oligonucleotide library selection, attaching binding molecules to the oligonucleotides, eluting the binding DNAs, amplifying them and finally repeating these steps 7-8 times to achieve satisfactory yield. This process ensures that a homogenous batch of highly specific molecules with high binding affinity is obtained. Sensitivity and specificity of aptamers is similar to that of antibodies. However, production of aptamers is easier making them cheaper than antibodies. Using aptamers for LFAs is a relatively new concept as compared to antibodies which have been used for over six decades. Therefore, there is still a limited commercial availability of aptamers, even for the commonly studied target molecules.

3. Affimers: Affimers (Aff) constitute a class of small proteins which specifically bind to target molecules just like antibodies. Affimers are engineered proteins which are generally 12-14 kDa in size, i.e. almost 10 folds smaller than antibodies, and have similar sensitivity and specificity as them.[118] Affimer proteins have a large binding surface provided by two peptide loops and an N-terminal sequence that can be randomised to bind to desired target proteins with high affinity and specificity.[118-120] The high degree of control over their production process allows modifications to provide high stability and robustness, even at varying temperature (stable up to ~80^{o}C) and pH conditions (stable in the range of 2-13).[121] The binding mechanism of affimers is similar to that of antibodies and involve non-covalent interactions between affimer and analyte, resulting from electrostatic interactions, hydrogen bonds, van der Waals forces and hydrophobic interactions. The production cycle of affimers for a target molecule can take between 12-14 weeks, which is much faster than antibodies.[118] The production process involves high yield expression in simple bacterial expression systems, which provides homogeneity amongst batches and makes affimers cost effective. Use of affimers is a relatively new concept, first reported only in 2005.[122] However, the widespread advantages of these small proteins have gained a lot of attention amongst researchers around the world, especially in the field of sensing.

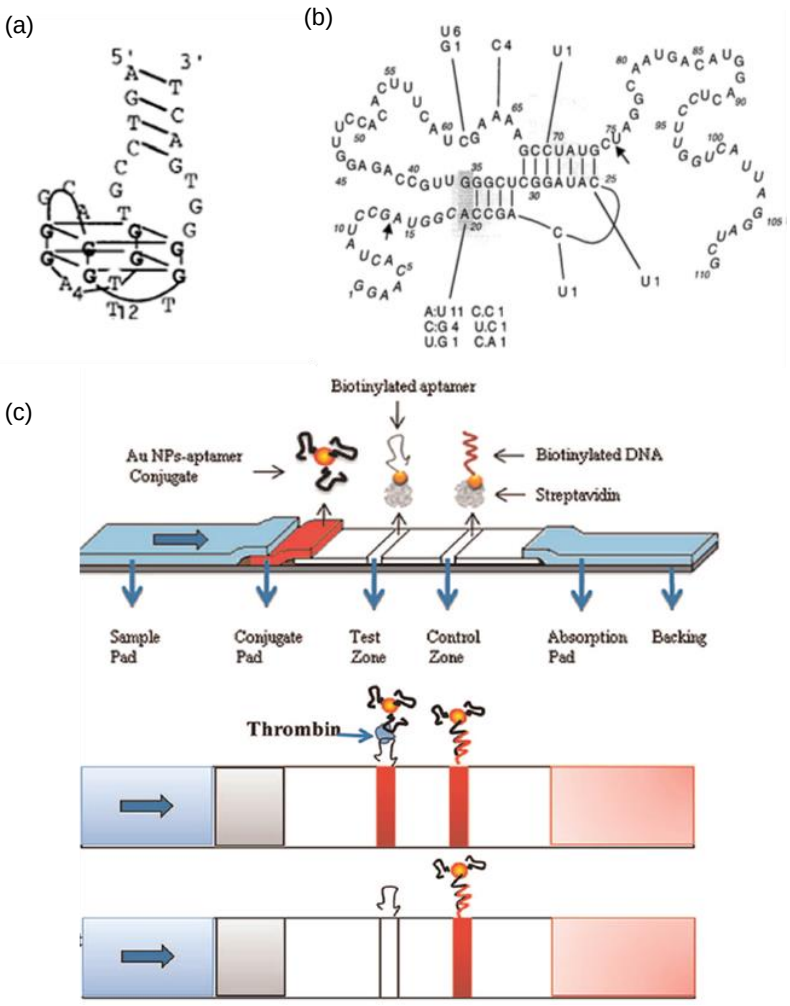

Fig 2.13: Examples of structural conformations of nucleic acid aptamers: (a) thrombin binding aptamer folded as G-quadruplex complex [123]; (b) sequence of biotin aptamer complex sequence folded as a pseudoknot [124]; (c) Aptamer based sandwich LFIA for thrombin detection [125] The analyte molecules bind to AuNP conjugated aptamers at the conjugate pad and are captured by immobilized capture aptamers at the test line. A complementary DNA sequence identifies the free AuNP-aptamer conjugate and captures them at the test line. (a-c are reprinted with permission)

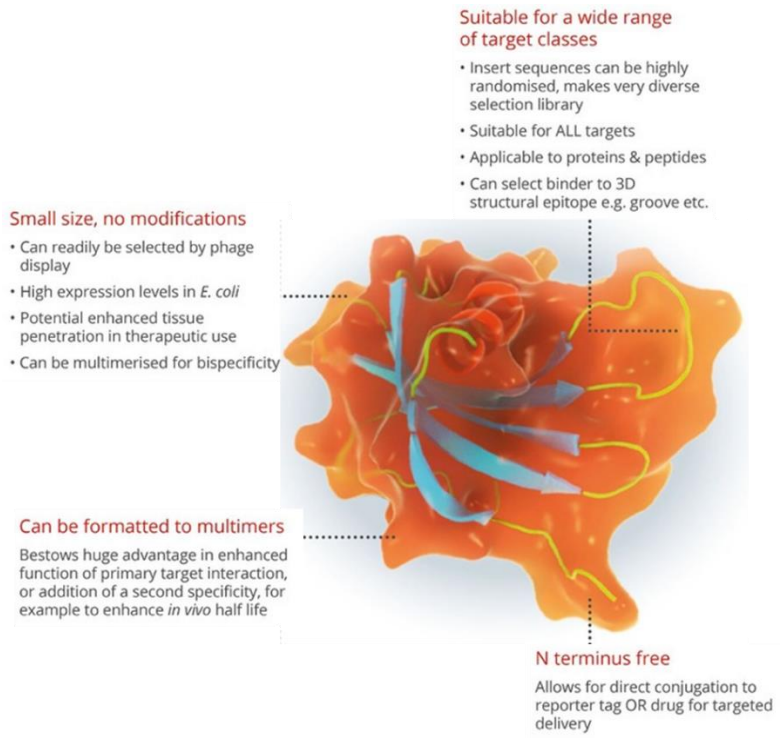

Fig 2.14: A 3D rendition of an affimer molecule, listing few of its advantages.[126]

2.4.4 Reporter Labels

The signals generated in an LFA are due to the reporter label molecules. The labels are conjugated to the recognition molecules detection biomolecules, for instance, antibodies or aptamers, via various chemical routes. They concentrate on the test/control line upon completion of an assay, which serves as an indication of presence or absence of the analyte and its concentration. An ideal label molecule would be stable under test conditions and have a wide dynamic range for detection. Moreover, it should have the ability to be conjugated easily with the detection biomolecules, without a loss in chemical property or biological integrity.[106] There are a wide range of reporter labels available commercially, ex., colloidal particles (AuNP, carbon black etc.), fluorescent materials (Europium beads, quantum dots etc.) and enzymes (HRP etc.).

Amongst the several types of reporter signals, the most intuitive and easily recognizable signal is the colorimetric signal and hence it is the most preferred option for POC

applications.[127] A few of the most popular colorimetric reporters have been listed in this section.

1. Nanoparticles: Several nanoparticles have been used as colorimetric labels. AuNP is the most widely preferred label for LFAs.[64, 106, 128] They have an intense pink/red coloration when dispersed, are easy to conjugate, have high bio-affinity, have easily tunable chemical properties, and are of low cost. AuNPs have also been used for signal amplification in LFAs.[129] The most common way of synthesizing AuNPs is via chemical reduction of chloroauric acid. AuNPs in the size range of 20-40 nm are considered best for visual applications.[130] Below 20 nm, the AuNPs do not have a bright hue and above 40 nm they become prone to flocculation. However, colloidal stability of AuNP is prone to several external factors, such as pH and salt concentration. Hence, they are usually stored in a citrate stabilized buffer. AuNPs have been used to detect a wide range of analytes, a summary of which has been provided in Table 2.4.

Magnetic nanoparticles (MNP) or magnetic beads (MB) have gained a lot of popularity in the recent years.[64, 128] MBs are superparamagnetic in nature, highly homogenous and can easily be functionalized. They release magnetic signals, which are stable over a long period of time. The use of MBs as colorimetric reporters have also gained popularity in the recent years.[131] MBs have a molar absorption coefficient comparable to AuNPs in the visible range and they can produce a dark brown band upon accumulation at the test/control line, which makes them suitable for visual detection in LFAs.[132] Another advantage of MBs is that they can be controlled using external magnetic fields, which enables facile analyte extraction from a complex sample solution.

Carbon nanoparticles in the form of colloidal carbon, carbon nanotubes, carbon nanostrings etc. are a set of inexpensive colorimetric labels, which can be easily functionalized to conjugate a wide range of biomolecules.[64, 128] The intense black coloration generated by these particles enable detection of analytes with high sensitivity. The production of carbon nanoparticles is easy and scalable, and the stability of conjugates ensure that the signals generated remain stable with respect to time.

Latex beads are spherical polymeric particles, which are usually made of amorphous polymers such as polystyrene.[76, 133, 134] They are available in a wide range of colours and are often a favoured choice for multiplex detection of analytes. The size ranges can be from 100 nm to ~2 µm, making them versatile for detecting several types of analytes. Generally, electrostatic coupling methods are preferred for attachment of latex beads to detection biomolecules as covalent conjugation process leads to aggregation of beads.

2. Enzymes: Enzyme based LFAs yield a colorimetric response upon addition of a suitable substrate.[128] The most widely used enzyme for LFAs is HRP, which can be easily labelled for detection biomolecules. In the presence of H_2O_2, TMB substrate reacts with HRP to yield a blue coloration, which is easily detectable with naked eye. Apart from HRP, other enzymes such as glucose oxidase, alkaline phosphatase etc., also have been utilized in LFA. However, the addition of an extra step in substrate addition and the long-term stability of substrates and enzymes are some of the main challenges affecting use of enzymes as reporters in LFAs.

Table 2.4: Summary of a few colorimetric LFAs

Type of Label	Enhancement Strategy	Analyte	Matrix	LOD	Assay Time
AuNP	Dual AuNP conjugation	Troponin I [73]	Serum	0.01 ng/ml	10 min
	AuNP clustering at Test Line	Cronobacter sakazakii [135]	Skim Milk	103 cfu/ml	15 min
	Ag staining of AuNP	Multiplexed fumonisin B1 and deoxynivalenol [136]	Diluted maize flour extract in methanol /water	2.0 ng/mL for fumonisin B1, 40 ng/mL for deoxynivalenol	10 min LFA + 6 min Ag staining
	Pt coating of AuNP	Prostate-specific antigen [137]	Assay diluent buffer	Naked eye detection of 2 ng/ml without substrates, 20 pg/ml with substrates	15 min LFA + 5 min enhance-ment
	None	Prostate-specific antigen [138]	Serum	1 μg/l	20 min
MB	None	Troponin ICT complex [79]	Plasma and PBS	Naked eye detection of 10 ng/ml in Plasma, 1 ng/ml in PBS	15 min
	Aggregation of Fe3O4 clusters at test line	Paraoxon Methyl [132]	PBS	69.7 ng/ml with Fe_3O_4 particles, 1.7 ng/ml with Fe_3O_4 aggregates	15 min
	Use of dual magnetic nanoparticle probes	Furazolidone metabolite of 3-amino-2-oxazolidinone [139]	PBS	0.044 ng/ml	20 min
Carbon nanotubes	None	Protein A [140]	PBS	NA	15 min
Carbon Nanoparticles	None	Circulating cathodic antigen [141]	Urine	0.3 ng/ml	30 min
	None	Human chorionic gonadotropin [142]	Urine	10 mIU/ml	5 min
Latex beads	None	Synthesized DNA [143]	Human plasma	3.75 fmol	15 min
	None	Multiplexed IgG/IgM against dengue and chikungunya [144]	Plasma	300 μg/ml	10 min
HRP Enzyme	Use of TMB substrate	Troponin I [145]	Serum	0.027 ng/ml	20 min

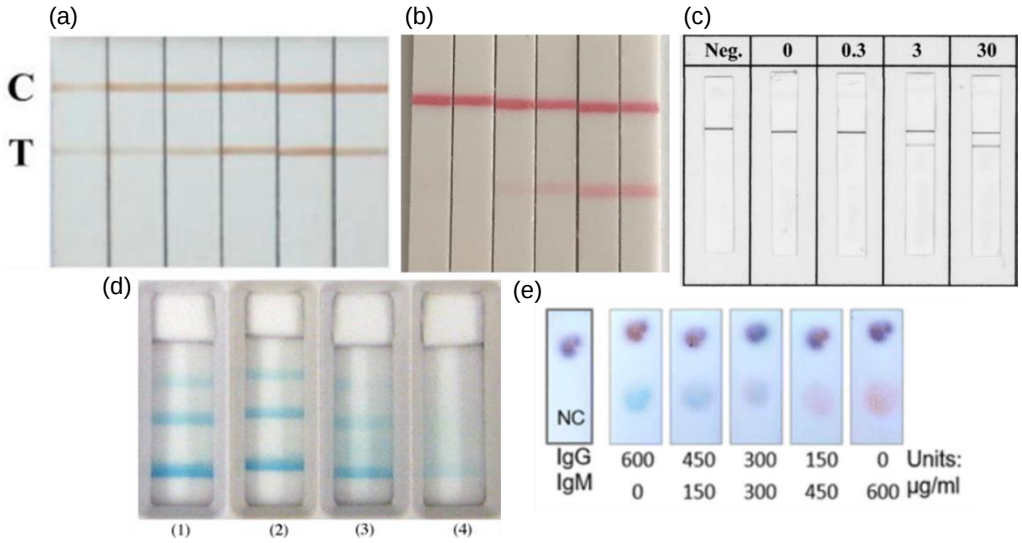

Fig 2.15: LFA for detection of (a) furazolidone in milk using MB (reprinted with permission) [139], (b) citrinin in cereals using AuNP [146], (c) antigens for diagnosis of Schistosomiasis using carbon particles [141], (d) hydrogen peroxide using HRP enzyme (reprinted with permission) [75] (e) markers causing Acute Febrile Illnesses using coloured latex beads [144]

2.4.5 Challenges Associated with LFAs for Anti-Doping

Although, LFAs are extremely promising, there are a few challenges that need to be surpassed to make this technology more reliable, popular and widely adapted for commercialization, especially for anti-doping purposes.

The first challenge concerns improving the sensitivity and specificity of the LFA platforms to match lab-based systems. There have been several developments in the past few years, which have allowed researchers to report sensitive detection limits without any sample pre-treatment.[54, 73, 147] However, most of these reports demonstrate high sensitivity levels in lab based controlled settings. On-field validation still remains a challenge for almost all such LFA platforms. On-site application implies limited availability of laboratory resources, because of which use of external equipment for pre-treatment, assay activation, signal detection and data analysis may not be possible. Therefore, strategies need to be devised to improve their sensitivity so that LFAs can compete with lab-based tests.

The next challenge is associated with the regulations governing LFAs. Currently there are limited regulations that commercial LFAs are mandated with and hence widespread variability in quality and performance of tests is observed.[58] This creates a sense of mistrust in potential users, as a result of which, LFAs have not seen widespread acceptance barring a few areas of application. Doping control is a fairly conservative area, whereby reliance on rapid detection is always sceptical. Although, an LFA cannot completely replace lab based analytical techniques, a proper set of guidelines detailing the usage and storage of LFAs; and regulatory approvals requiring stringent quality control checks can definitely improve the confidence on this technology, which can eventually lead to the acceptance of LFAs as reliable screening devices.

2.5 Sample Pre-treatment

Pre-treatment is mainly necessary when a sample has interfering matrix components that might result in false positives or negatives or the analyte concentration is too low for reliable detection. For instance, blood is a complex matrix consisting of cells, proteins, electrolytes etc., which can potentially interfere with the assay results. Hence, a lot of analytical tests are performed on serum or plasma, which are extracted from the whole blood samples. Although, serum and plasma, which do not contain cells and several proteins as compared to blood, are easier to analyse than blood itself, they still have several interferents such as salts, clotting factors, few proteins such as albumin etc.[148, 149] Other matrices like sweat and urine also contain interferents that can influence the LFA responses.

Most of WADA approved analytical methods are preceded by sample pre-treatment in order to improve sensitivity. For example, liquid-liquid extraction (LLE) is a conventional sample pre-concentration step, which is used in techniques such as GC-MS.[16, 150] It uses two immiscible solvents, usually a polar aqueous and a non-polar organic solvent, so that the analytes can migrate into a chemically more stable configuration. The solvent which becomes rich in the analyte is called the extraction phase, which is further concentrated by evaporating the solvents. Similarly, solid-phase extraction (SPE) is

another method which is used in several MS methods.[151] Here, a liquid sample is passed through a solid phase where the interfering compounds are separated as a result of their affinity towards the adsorbing solid. Various adsorbents like ethyl (C2), octyl (C8), octadecyl (C18), cyclohexyl (CH), phenyl (PH) cyanopropyl (CN), diol (2OH), aminopropyl (NH2) etc., have been used for SPE.[151-153] However, extensive instrumentation, high costs and long turnaround times imply that these techniques are not implemented at POC.

WADA has also approved membrane based sample purification techniques such as ultrafiltration (UF), which is a hydrostatic pressure induced filtration method.[56] Here, the sample is forced through a semi-permeable membrane to retain solids and solutes of high molecular weight, while allowing water and low molecular weight solutes to pass through. This is especially useful for blood samples, where filtering out cells and proteins is of paramount importance.[36] However, UF is a low efficiency separation method, which requires a long time. Moreover, use of a pressure pump is not too feasible in a resource-limited setting. Selective protein precipitation (SPP) is also used for purification of blood samples, especially before WADA approved techniques like IEF.[34] SPP is a method of protein recovery from a complex lysate to separate out one or more proteins through a purification step.[154] SPP can be specific or generic. Specific SPP uses an antibody-mediated precipitation, whereas a generic SPP depends on the physical and/or chemical interaction between a precipitating agent and the proteins that possess certain specific characteristics. In case of analyte extraction from a solution containing multiple proteins, a combination of different SPP protocols may be utilized to isolate at desired yields. However, this method is prone to yield variations across batches, consists of multiple tedious steps and is time consuming, all of which make it difficult to apply such techniques on-site. The limitations of all of these techniques have led researchers to look for simpler sample pre-treatment protocols, which have the potential to yield desired analytical results even in remote settings.

Two of the most promising techniques for on-site application are sample dilution and magnetic extraction. Sample dilution is a non-selective pre-treatment technique, which

involves dilution of sample solution in an appropriate solvent which does not affect the bioactivity of the analyte and has a relatively simpler composition as compared to the original matrix. The dilution factor can be as low as 1:1 or even as high as 1:100 or even more, depending on the concentration of analyte and the type of matrix.[16, 155] On the other hand, magnetic extraction is a selective sample pre-treatment method, which utilizes superparamagnetic beads of various sizes. These MBs can be composed of co-precipitated Fe_3O_4 particles (≤ 20nm) or spherical polymeric beads with embedded Fe_3O_4 (such as polystyrene beads, ~50 nm - 2.8 µm).[156, 157] MBs are homogenous, can be easily functionalized for attachment of different biomolecules and possess excellent magnetic properties. Therefore, they can be used to specifically bind analytes of interest by a simple incubation in a sample solution, following which, the conjugate formed can be easily extracted using an external magnetic field. The superparamagnetic nature ensures no remnant magnetic field remains upon removal of the field.[158] Sample extraction using MBs is quick and efficient and does not require any sophisticated instruments, except a magnet. Such extraction has been implemented for a wide range of assays used for detecting different analytes such as proteins [79], nucleic acids [159], bacterial cells [160] etc.

2.6 Research Model

2.6.1 Troponin

Troponin is a group of proteins, which is responsible for regulation and contraction of skeletal and cardiac muscles. There are three types of troponin proteins: Troponin I (TnI), Troponin C (TnC) and Troponin T (TnT). Usually a complex of Troponin consists of all the three forms and is present as Troponin ICT (TnICT). TnI is a 209 amino acid protein with a molecular weight of ~24 kDa, whereas, molecular weights of TnC and TnT are ~18 kDa and ~35 kDa respectively.[161, 162] High concentrations of Troponin in the body can be a direct indication of cardiac or skeletal muscle damage. TnC initiates contraction in muscles by binding calcium ions, which causes a conformational change and leads to movement of TnI. This causes the two proteins to pull the muscle fiber shorter and interact.

On the other hand, TnT anchors the troponin complex to the muscle fiber structure and together with the other troponins, regulates its contraction. TnI is the most important diagnostic marker for acute myocardial infarction (AMI). Cardiac TnI is produced in the cardiac muscle tissue and is specific to cardiac injury, making it important for detection during the onset of AMI. Troponin levels in blood for a healthy human are in the range of 20-30 pg/ml, whereas it increases rapidly after a heart attack, reaching a peak of ~50 ng/ml within 3-6 hours and 190-200 ng/ml after 11 h.[163-165] These levels stay elevated in the human body for around 6-8 days after which it starts lowering.[165] A different isoform of TnI is produced in skeletal muscles, which makes it possible to develop specific tests for cardiac and skeletal muscle injury. In sports, this is especially important to diagnose muscle damage and monitor recovery of athletes accurately.[166]

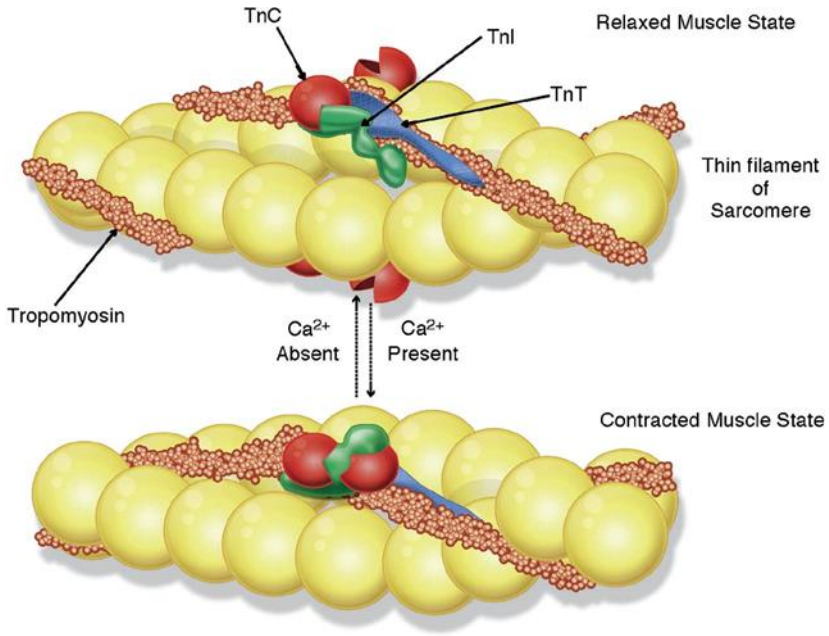

Fig 2.16: Schematic showing regulation of muscles by Troponin. TnC binds to Calcium ions to initiate muscle contraction and causes TnI to move. [166]

2.6.2 Insulin like Growth Factor-1

Insulin like Growth Factor-1 (IGF-1) is a 70-amino acid peptide hormone, secreted by the liver. It is a biomarker of Growth Hormone (GH), and is secreted as a response to pituitary

release or exogenous administration of GH. IGF-1, just like GH, is a prohibited substance as it provides unnatural performance enhancement to athletes. It has a molecular weight of 7.6 KDa. It has anabolic as well as insulin like metabolic activities and functions through the IGF-1 receptors. It can also bind with limited affinity to insulin receptors due to its structural and functional similarities to insulin. IGF-1 and GH work in conjunction to grow cartilage and build muscles. Additionally, IGF-1 signals regeneration of cells, helps increase bone density and helps in recovery of tissues. Most of the IGF-1 present in blood is bound to IGF binding protein (IGF-BP). This makes it more stable than GH and hence it has a longer half-life inside the body upon exogenous intake. Endogenous IGF-1 is generally dependent on age, with levels as high as 150-260 ng/ml in serum for an age group of 21-30 and less than 90 ng/ml beyond 80 years of age.[167, 168] The endogenous half-life of IGF-1 in plasma is 14-18 hours but can increase to around 4-5 days upon GH administration, thus increasing the window of detection for detection of GH doping.[49, 169]

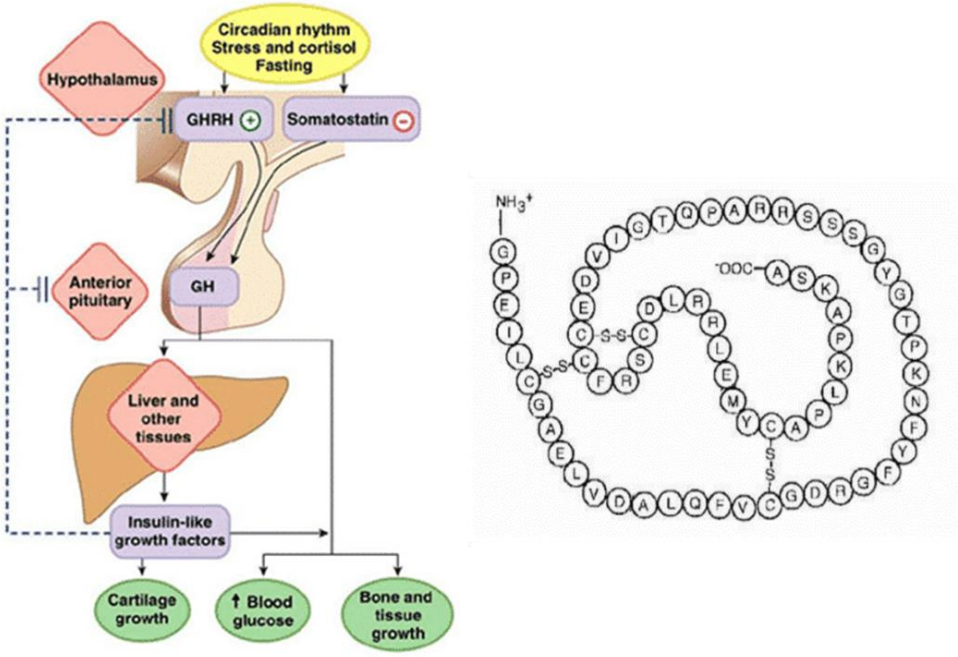

Fig 2.17: Schematic showing (a) IGF-1 release mechanism [170], (b) protein structure of IGF-1 [171]

2.6.3 Interlukin-8

Interlukin-8 (IL-8) is a chemokine, serving as an important mediator for inflammation in muscles and often serves as a biomarker for state of inflammation in athletes. It is produced by a variety of tissues and cell types within the body such as macrophages, epithelial cells and smooth muscle tissue. Structurally, IL-8 is a 72 amino acid protein, weighing ~8.4 kDa. Amongst the various pro-inflammatory cytokines, IL-8 has one of the longest half-life, implying that it can be detected in blood for a longer time period.[172] IL-8 can mediate inflammatory responses via neutrophils, activating them upon injury and causing them to migrate towards the site of inflammation.[173] Furthermore, studies have shown that urinary IL-8 levels can also be used to determine state of stress or fatigue.[174] As IL-8 is mostly released as an immune response, its baseline physiological levels are generally in trace quantities (~10 pg/ml).[175] However, upon intense fatigue, these levels can go up almost 10 folds.[175, 176]

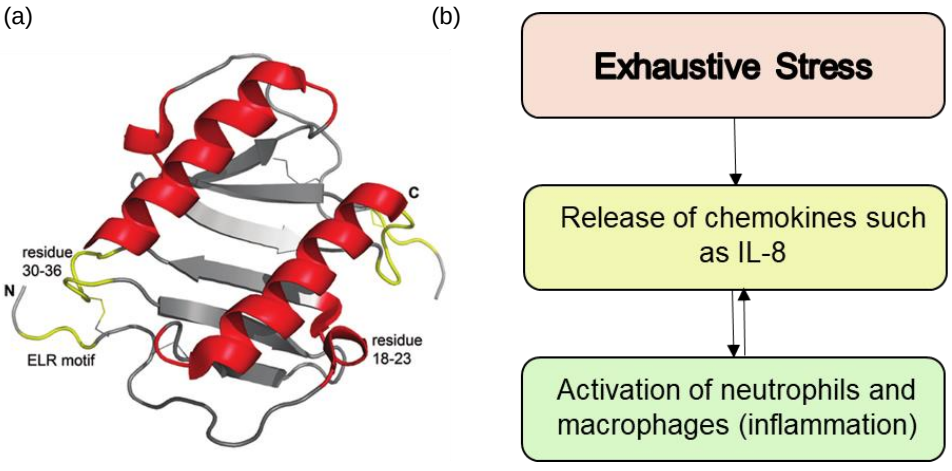

Fig 2.18: (a) A 3D structure of IL-8 as obtained by NMR spectroscopy [177] (b) Functioning pathway of IL-8. As stress is induced, more chemokines such as IL-8 are released which lead to transport of neutrophils to the site of inflammation.

2.7 Addressing Gaps in Literature Review

The phenomenon of doping in sports has existed since ages and is an evolving concept. The current day techniques to identify instances of doping have been found to be grossly inefficient due to the low frequency of testing, mostly due to a combination of factors such as high logistical costs involved in current testing mechanism, use of sophisticated and heavy instrumentation, and inability to conduct on-site tests. Therefore, POCT technologies such as LFAs need to developed and made more efficient for effective on site screening of athletes and a better doping control regime. However, the utilisation of LFAs in the field of sport science is still relatively nascent and there is a scope for extensive research to develop reliable LFA kits, especially for anti-doping markers. This thesis is an attempt to fill this gap in literature about the use of POCTs such as LFAs for reliable detection of anti-doping markers.

References

1. Taware, G.B. and D.G. Bansode, *Doping in sports.* National Journal of Basic Medical Sciences, 2015. **6**(2): p. 89-92.

2. Holt, R.I., I. Erotokritou-Mulligan, and P.H. Sönksen, *The history of doping and growth hormone abuse in sport.* Growth Hormone & IGF Research, 2009. **19**(4): p. 320-326.

3. Müller, R.K., *History of doping and doping control*, in *Doping in sports: Biochemical principles, effects and analysis*. 2010, Springer. p. 1-23.

4. Gandert, D., *The WADA code: the maximum extent of enforcement.* International Journal of Sport Policy and Politics, 2019. **11**(2): p. 275-293.

5. Catlin, D., K.D. Fitch, and A. Ljungqvist, *Medicine and science in the fight against doping in sport.* Journal Of Internal Medicine, 2008. **264**(2): p. 99-114.

6. Ulrich, R., et al., *Doping in two elite athletics competitions assessed by randomized-response surveys.* Sports Medicine, 2018. **48**(1): p. 211-219.

7. (WADA), W.A.-D.A. *The World Anti-Doping Code International Standard Prohibited List*. 2017; Available from: https://www.wada-

ama.org/sites/default/files/resources/files/2016-09-29_-_wada_prohibited_list_2017_eng_final.pdf.

8. Al Ghobain, M., et al., *Prevalence, knowledge and attitude of prohibited substances use (doping) among Saudi sport players.* Substance Abuse Treatment, Prevention, and Policy, 2016. **11**(1): p. 14.

9. Bowers, L.D., *The analytical chemistry of drug monitoring in athletes.* Annual Review Of Analytical Chemistry, 2009. **2**: p. 485-507.

10. WADA. *WADA Prohibited List 2020*. 2020 [cited 2020 18th May]; Available from: https://www.wada-ama.org/sites/default/files/wada_2020_english_prohibited_list_0.pdf.

11. Duclos, M., *Glucocorticoids: a doping agent?* Endocrinology and Metabolism Clinics, 2010. **39**(1): p. 107-126.

12. Kruse, P., et al., *Beta-blockade used in precision sports: effect on pistol shooting performance.* Journal of Applied Physiology, 1986. **61**(2): p. 417-420.

13. Sjöqvist, F., M. Garle, and A. Rane, *Use of doping agents, particularly anabolic steroids, in sports and society.* The Lancet, 2008. **371**(9627): p. 1872-1882.

14. Barnes, K.P. and C.R. Rainbow, *Update on banned substances 2013.* Sports health, 2013. **5**(5): p. 442-447.

15. Wagner, J.C., *Enhancement of athletic performance with drugs.* Sports Medicine, 1991. **12**(4): p. 250-265.

16. Nicoli, R., et al., *Analytical strategies for doping control purposes: needs, challenges, and perspectives.* Analytical Chemistry, 2016. **88**(1): p. 508-523.

17. Werner, T.C. and C.K. Hatton, *Performance-enhancing drugs in sports: how chemists catch users.* Journal of Chemical Education, 2011. **88**(1): p. 34-40.

18. WADA. *WADA International Standard for Testing and Investigations*. 2020 [cited 2020 19th May]; Available from: https://www.wada-ama.org/sites/default/files/resources/files/isti_march2019.pdf.

19. WADA. *WADA Accredited Laboratories*. [cited 2020 18th May]; Available from: https://www.wada-ama.org/en/what-we-do/science-medical/laboratories/accredited-laboratories.

20. Dass, C., *Fundamentals of contemporary mass spectrometry*. Vol. 16. 2007: John Wiley & Sons.

21. Hübschmann, H.-J., *Handbook of GC-MS: fundamentals and applications*. 2015: John Wiley & Sons.

22. Magalhães, W.S., et al., *Human Metabolism of the Anabolic Steroid Methasterone: Detection and Kinetic Excretion of New Phase I Urinary Metabolites and Investigation of Phase II Metabolism by GC-MS and UPLC-MS/MS.* Journal of the Brazilian Chemical Society, 2019. **30**(6): p. 1150-1160.

23. Magiera, S., et al., *GC–MS method for the simultaneous determination of β-blockers, flavonoids, isoflavones and their metabolites in human urine.* Journal Of Pharmaceutical And Biomedical Analysis, 2011. **56**(1): p. 93-102.

24. Brunelli, C., et al., *High-speed gas chromatography in doping control: Fast-GC and fast-GC/MS determination of β-adrenoceptor ligands and diuretics.* Journal Of Separation Science, 2006. **29**(18): p. 2765-2771.

25. UCLA. *GC/MS Schematic*. [cited 2020 18th May]; Available from: http://www.chem.ucla.edu/~harding/IGOC/G/gc_ms.html.

26. Matuszewski, B., M. Constanzer, and C. Chavez-Eng, *Strategies for the assessment of matrix effect in quantitative bioanalytical methods based on HPLC− MS/MS.* Analytical Chemistry, 2003. **75**(13): p. 3019-3030.

27. Thevis, M., A. Thomas, and W. Schänzer, *Current role of LC-MS (/MS) in doping control.* Analytical And Bioanalytical Chemistry, 2011. **401**(2): p. 405-420.

28. Zhou, B., *Computational Analysis of LC-MS/MS Data for Metabolite Identification*. 2011, Virginia Tech.

29. Ferrer, I. and E.M. Thurman, *Advanced techniques in gas chromatography-mass spectrometry (GC-MS-MS and GC-TOF-MS) for environmental chemistry*. 2013: Newnes.

30. Reporting, W., *evaluation guidance for testosterone, epitestosterone, T/E ratio and other endogenous steroids.* Technical document, vol. TD2004EAAS, 2004.

31. Aguilera, R., et al., *Performance characteristics of a carbon isotope ratio method for detecting doping with testosterone based on urine diols: controls and athletes with elevated testosterone/epitestosterone ratios.* Clinical Chemistry, 2001. **47**(2): p. 292-300.

32. WADA. *Detection of Synthetic Forms of Endogenous Anabolic Androgenic Steroids by GC/C/IRMS*. 2019 [cited 2020 18th May]; Available from: https://www.wada-ama.org/sites/default/files/td2019irms_final_eng_clean.pdf.

33. *Schemtaic of IRMS System*. [cited 2020 18th May]; Available from: http://www.wikiwand.com/en/Isotope-ratio_mass_spectrometry.

34. WADA. *WADA Technical Document – TD2014EPO*. 2014 [cited 2020 18th May]; Available from: https://www.wada-ama.org/sites/default/files/resources/files/WADA-TD2014EPO-v1-Harmonization-of-Analysis-and-Reporting-of-ESAs-by-Electrophoretic-Techniques-EN.pdf.

35. C. Ayotte, P.E.G., P. Desharnais *Purification of EPO in urine samples prior to detection by isoelectric focusing*. [cited 2020 18th May]; Available from: https://www.wada-ama.org/sites/default/files/resources/files/ayotte-purification_of_epo.pdf.

36. Harper, R.G., et al., *Low-molecular-weight human serum proteome using ultrafiltration, isoelectric focusing, and mass spectrometry*. Electrophoresis, 2004. **25**(9): p. 1299-1306.

37. Reihlen, P., et al., *Easy-to-use IEF compatible immunoaffinity purification of Erythropoietin from urine retentates.* Drug Testing And Analysis, 2012. **4**(11): p. 813-817.

38. *Reproduced with Permission from G.L. Jones, "Fig 6: The principle of isoelectric focusing", Elsevier Books*, in *Encyclopedia Of Separation Science*. 2000.

39. Kohler, M., et al., *Discrimination of recombinant and endogenous urinary erythropoietin by calculating relative mobility values from SDS gels.* International Journal Of Sports Medicine, 2008. **29**(01): p. 1-6.

40. Gwozdz, T. and K. Dorey, *Reprinted with permission. "Figure 6.2. Schematic of SDS-Page electrophoresis." Chapter 6 - Western Blot*, in *Basic Science Methods for Clinical Researchers*, M. Jalali, F.Y.L. Saldanha, and M. Jalali, Editors. 2017, Academic Press: Boston. p. 99-117.

41. Amino, N. and Y. Hidaka, *Various types of immunoassay.* Nihon rinsho. Japanese Journal Of Clinical Medicine, 1995. **53**(9): p. 2107-2111.

42. Eenoo, P.V. and F. Delbeke, *Detection of inhaled salbutamol in equine urine by ELISA and GC/MS2.* Biomedical Chromatography, 2002. **16**(8): p. 513-516.

43. Martin, L., A. Chaabo, and F. Lasne, *Detection of tetracosactide in plasma by enzyme-linked immunosorbent assay (ELISA).* Drug Testing And Analysis, 2015. **7**(6): p. 531-534.

44. Dr. Z. WU (Charite Campus Mitte, G. *Development of ultra sensitive duplex differential immunoassays for detection of doping with insulin analogues*. [cited 2020 18th May]; Available from: https://www.wada-ama.org/sites/default/files/resources/files/final_report_14b14zw_dr._wu.pdf.

45. WADA. *Technical Document – TD2015GH: HUMAN GROWTH HORMONE (hGH) ISOFORM DIFFERENTIAL IMMUNOASSAYS FOR DOPING CONTROL ANALYSES*. 2015 [cited 2020 19th May]; Available from: https://www.wada-ama.org/sites/default/files/resources/files/wada_td2015gh_hgh_isoform_diff_immunoassays_en.pdf.

46. Scientific, T. *Overview of ELISA*. [cited 2020 19th May]; Available from: https://www.thermofisher.com/sg/en/home/life-science/protein-biology/protein-biology-learning-center/protein-biology-resource-library/pierce-protein-methods/overview-elisa.html.

47. Ahuja, S. and M. Dong, *Handbook Of Pharmaceutical Analysis By HPLC*. 2005: Elsevier.

48. Konstantinov, K.B., et al., *Real-time compensation of the inner filter effect in high-density bioluminescent cultures.* Biotechnology And Bioengineering, 1993. **42**(10): p. 1190-1198.

49. Baumann, G.P., *Growth Hormone Doping in Sports: A Critical Review of Use and Detection Strategies.* Endocrine Reviews, 2012. **33**(2): p. 155-186.

50. Kuuranne, T., M. Saugy, and N. Baume, *Confounding factors and genetic polymorphism in the evaluation of individual steroid profiling.* Br J Sports Med, 2014. **48**(10): p. 848-855.

51. Sottas, P.-E., et al., *The athlete biological passport.* Clinical Chemistry, 2011. **57**(7): p. 969-976.

52. Drain, P.K., et al., *Diagnostic point-of-care tests in resource-limited settings.* The Lancet Infectious Diseases, 2014. **14**(3): p. 239-249.

53. Peeling, R. and D. Mabey, *Point-of-care tests for diagnosing infections in the developing world.* Clinical Microbiology And Infection, 2010. **16**(8): p. 1062-1069.

54. Zhang, D., et al., *Quantitative and ultrasensitive detection of multiplex cardiac biomarkers in lateral flow assay with core-shell SERS nanotags.* Biosensors and Bioelectronics, 2018. **106**: p. 204-211.

55. WADA. *WADA Technical Document – TD2014DL*. 2014 [cited 2020 20th May]; Available from: https://www.wada-ama.org/sites/default/files/resources/files/WADA-TD2014DL-v1-Decision-Limits-for-the-Quantification-of-Threshold-Substances-EN.pdf.

56. WADA. *WADA Technical Document – TD2014EPO*. 2014 [cited 2020 20th May]; Available from: https://www.wada-ama.org/sites/default/files/resources/files/WADA-TD2014EPO-v1-Harmonization-of-Analysis-and-Reporting-of-ESAs-by-Electrophoretic-Techniques-EN.pdf.

57. Yager, P., G.J. Domingo, and J. Gerdes, *Point-of-care diagnostics for global health.* Annual Review Of Biomedical Engineering, 2008. **10**.

58. Camacho-Ryan, O. and R. Bertholf, *Monitoring point-of-care testing compliance.* Clinical Laboratory News. American Association for Clinical Chemistry (AACC). https://www. aacc. org/publications/cln/articles/2016/february/monitoring-point-of-care-testing-compliance (Accesso 3 marzo 2018), 2016.

59. Carlson, D., *Point of care testing: regulation and accreditation.* Clinical laboratory science: Journal Of The American Society For Medical Technology, 1996. **9**(5): p. 298-302; quiz 303-4.

60. C. Harrison (San Diego State University, C., USA). *WADA Project Review: Blood Doping Screening through Capillary Electrophoresis*. [cited 2020 19th May]; Available from:https://www.wada ama.org/sites/default/files/resources/files/09a23ch_c._harrison.pdf.

61. St John, A. and C.P. Price, *Existing and emerging technologies for point-of-care testing.* The Clinical Biochemist Reviews, 2014. **35**(3): p. 155.

62. Soper, S.A., et al., *Point-of-care biosensor systems for cancer diagnostics/prognostics.* Biosensors and Bioelectronics, 2006. **21**(10): p. 1932-1942.

63. Myers, F.B., et al., *A handheld point-of-care genomic diagnostic system.* Plos One, 2013. **8**(8).

64. Sajid, M., A.-N. Kawde, and M. Daud, *Designs, formats and applications of lateral flow assay: A literature review.* Journal of Saudi Chemical Society, 2015. **19**(6): p. 689-705.

65. Devillé, W.L., et al., *The urine dipstick test useful to rule out infections. A meta-analysis of the accuracy.* BMC Urology, 2004. **4**(1): p. 4.

66. Xu, W. and Y. Lu, *Label-free fluorescent aptamer sensor based on regulation of malachite green fluorescence.* Analytical Chemistry, 2010. **82**(2): p. 574-578.

67. Chen, A. and S. Yang, *Replacing antibodies with aptamers in lateral flow immunoassay.* Biosensors And Bioelectronics, 2015. **71**: p. 230-242.

68. Liu, J., D. Mazumdar, and Y. Lu, *A simple and sensitive "dipstick" test in serum based on lateral flow separation of aptamer-linked nanostructures.* Angewandte Chemie International Edition, 2006. **45**(47): p. 7955-7959.

69. Michel, M.A., et al., *Ubiquitin linkage-specific affimers reveal insights into K6-linked ubiquitin signaling.* Molecular Cell, 2017. **68**(1): p. 233-246. e5.

70. Klont, F., et al., *Affimers as an Alternative to Antibodies in an Affinity LC–MS Assay for Quantification of the Soluble Receptor of Advanced Glycation End-Products (sRAGE) in Human Serum.* Journal Of Proteome Research, 2018. **17**(8): p. 2892-2899.

71. John, A.S., et al., *The use of urinary dipstick tests to exclude urinary tract infection: a systematic review of the literature.* American Journal Of Clinical Pathology, 2006. **126**(3): p. 428-436.

72. Hayden, J.A., M. Schmeling, and A.N. Hoofnagle, *Lot-to-lot variations in a qualitative lateral-flow immunoassay for chronic pain drug monitoring.* Clinical Chemistry, 2014. **60**(6): p. 896-897.

73. Choi, D.H., et al., *A dual gold nanoparticle conjugate-based lateral flow assay (LFA) method for the analysis of troponin I.* Biosensors and Bioelectronics, 2010. **25**(8): p. 1999-2002.

74. Leung, W., et al., *One-step quantitative cortisol dipstick with proportional reading.* Journal Of Immunological Methods, 2003. **281**(1-2): p. 109-118.

75. Fung, K.-K., C.P.-Y. Chan, and R. Renneberg, *Development of enzyme-based bar code-style lateral-flow assay for hydrogen peroxide determination.* Analytica Chimica Acta, 2009. **634**(1): p. 89-95.

76. Quesada-González, D. and A. Merkoçi, *Nanoparticle-based lateral flow biosensors.* Biosensors and Bioelectronics, 2015. **73**: p. 47-63.

77. Takalkar, S., K. Baryeh, and G. Liu, *Fluorescent carbon nanoparticle-based lateral flow biosensor for ultrasensitive detection of DNA.* Biosensors and Bioelectronics, 2017. **98**: p. 147-154.

78. Corstjens, P.L., et al., *Tools for diagnosis, monitoring and screening of Schistosoma infections utilizing lateral-flow based assays and upconverting phosphor labels.* Parasitology, 2014. **141**(14): p. 1841-1855.

79. Sharma, A., et al., *Magnetic field assisted preconcentration of biomolecules for lateral flow assaying.* Sensors and Actuators B: Chemical, 2019. **285**: p. 431-437.

80. Shim, W.-B., et al., *An aptamer-based dipstick assay for the rapid and simple detection of aflatoxin B1*. Biosensors and Bioelectronics, 2014. **62**: p. 288-294.

81. Altuntas, D.B., Y. Tepeli, and U. Anik, *Graphene-metallic nanocomposites as modifiers in electrochemical glucose biosensor transducers.* 2D Materials, 2016. **3**(3): p. 034001.

82. Levine, P.M., et al., *Real-time, multiplexed electrochemical DNA detection using an active complementary metal-oxide-semiconductor biosensor array with integrated sensor electronics.* Biosensors and Bioelectronics, 2009. **24**(7): p. 1995-2001.

83. Erdem, A., et al., *Detection of interaction between metal complex indicator and DNA by using electrochemical biosensor.* Electroanalysis: An International Journal Devoted to Fundamental and Practical Aspects of Electroanalysis, 1999. **11**(18): p. 1372-1376.

84. Wang, J., *Electrochemical biosensors: towards point-of-care cancer diagnostics.* Biosensors and Bioelectronics, 2006. **21**(10): p. 1887-1892.

85. Prakash, S., et al., *Polymer thin films embedded with metal nanoparticles for electrochemical biosensors applications.* Biosensors and Bioelectronics, 2013. **41**: p. 43-53.

86. Holford, T.R., F. Davis, and S.P. Higson, *Recent trends in antibody based sensors.* Biosensors and Bioelectronics, 2012. **34**(1): p. 12-24.

87. Lu, Y., et al., *Aptamer-based electrochemical sensors with aptamer–complementary DNA oligonucleotides as probe.* Analytical Chemistry, 2008. **80**(6): p. 1883-1890.

88. Wang, J. and M. Musameh, *Carbon nanotube/teflon composite electrochemical sensors and biosensors.* Analytical Chemistry, 2003. **75**(9): p. 2075-2079.

89. HEALTH, A. *Lateral FLow Assay*. [cited 2020 20th May]; Available from: https://www.abingdonhealth.com/contract-services/what-is-a-lateral-flow-immunoassay/.

90. Testing, F.C. *Strip Test*. [cited 2020 20th May]; Available from: http://www.gmotesting.com/Testing-Options/Immuno-analysis/Strip-Test.

91. AZoSensors. *A Guide to Understanding Blood Glucose Monitoring Sensors*. [cited 2020 20th May]; Available from: https://www.azosensors.com/article.aspx?ArticleID=30.

92. Geddes, L., *Wearable sweat sensor paves way for real-time analysis of body chemistry.* Nature: International Weekly Journal of Science, 2016.

93. Nie, Z., et al., *Electrochemical sensing in paper-based microfluidic devices.* Lab on a Chip, 2010. **10**(4): p. 477-483.

94. Kuswandi, B., J. Huskens, and W. Verboom, *Optical sensing systems for microfluidic devices: a review.* Analytica Chimica Acta, 2007. **601**(2): p. 141-155.

95. Giouroudi, I. and F. Keplinger, *Microfluidic biosensing systems using magnetic nanoparticles.* International Journal Of Molecular Sciences, 2013. **14**(9): p. 18535-18556.

96. Sonato, A., et al., *A surface acoustic wave (SAW)-enhanced grating-coupling phase-interrogation surface plasmon resonance (SPR) microfluidic biosensor.* Lab on a Chip, 2016. **16**(7): p. 1224-1233.

97. Yetisen, A.K., M.S. Akram, and C.R. Lowe, *based microfluidic point-of-care diagnostic devices.* Lab on a Chip, 2013. **13**(12): p. 2210-2251.

98. Dieterich, K., *Testing-paper and method of making same*. 1902, Google Patents.

99. Martinez, A.W., et al., *Patterned paper as a platform for inexpensive, low-volume, portable bioassays.* Angewandte Chemie International Edition, 2007. **46**(8): p. 1318-1320.

100. Bruzewicz, D.A., M. Reches, and G.M. Whitesides, *Low-cost printing of poly (dimethylsiloxane) barriers to define microchannels in paper.* Analytical Chemistry, 2008. **80**(9): p. 3387-3392.

101. Chitnis, G., et al., *Laser-treated hydrophobic paper: an inexpensive microfluidic platform.* Lab on a Chip, 2011. **11**(6): p. 1161-1165.

102. Carrilho, E., A.W. Martinez, and G.M. Whitesides, *Understanding wax printing: a simple micropatterning process for paper-based microfluidics.* Analytical Chemistry, 2009. **81**(16): p. 7091-7095.

103. Ratnarathorn, N., et al., *Reprinted with permission: Simple silver nanoparticle colorimetric sensing for copper by paper-based devices.* Talanta, 2012. **99**: p. 552-557.

104. Fan, S. *This One-Cent Lab-on-a-Chip Can Diagnose Cancer and Infections*. [cited 2020 20th May]; Available from: https://singularityhub.com/2017/02/19/one-cent-lab-on-a-chip-can-detect-cancer-and-infections/.

105. Gnoth, C. and S. Johnson, *Strips of hope: accuracy of home pregnancy tests and new developments.* Geburtshilfe und Frauenheilkunde, 2014. **74**(07): p. 661-669.

106. Koczula, K.M. and A. Gallotta, *Lateral flow assays.* Essays In Biochemistry, 2016. **60**(1): p. 111-120.

107. Eltzov, E., et al., *Lateral flow immunoassays–from paper strip to smartphone technology*. Electroanalysis, 2015. **27**(9): p. 2116-2130.

108. Yu, L., et al., *Disposable lateral flow-through strip for smartphone-camera to quantitatively detect alkaline phosphatase activity in milk.* Biosensors and Bioelectronics, 2015. **69**: p. 307-315.

109. Posthuma-Trumpie, G.A., J. Korf, and A. van Amerongen, *Lateral flow (immuno) assay: its strengths, weaknesses, opportunities and threats. A literature survey.* Analytical and Bioanalytical Chemistry, 2009. **393**(2): p. 569-582.

110. nanoComposix. *Introduction to Lateral Flow Rapid Test Diagnostics*. [cited 2020 23rd June]; Available from: https://nanocomposix.com/pages/introduction-to-lateral-flow-rapid-test-diagnostics.

111. Presta, L.G., *Antibody engineering.* Current Opinion In Biotechnology, 1992. **3**(4): p. 394-398.

112. Kennett, R.H. and T.J. MacKearn, *Monoclonal antibodies*. 1982: Springer.

113. Dunbar, B.S. and E.D. Schwoebel, *[49] Preparation of polyclonal antibodies*, in *Methods in enzymology*. 1990, Elsevier. p. 663-670.

114. Bioscience, J. *Antibodies*. [cited 2020 20th May]; Available from: https://www.jenabioscience.com/proteins/detection-analysis/antibodies.

115. Mascini, M., I. Palchetti, and S. Tombelli, *Nucleic acid and peptide aptamers: fundamentals and bioanalytical aspects.* Angewandte Chemie International Edition, 2012. **51**(6): p. 1316-1332.

116. Ni, X., et al., *Nucleic acid aptamers: clinical applications and promising new horizons.* Current Medicinal Chemistry, 2011. **18**(27): p. 4206-4214.

117. Ellington, A.D. and J.W. Szostak, *In vitro selection of RNA molecules that bind specific ligands.* Nature, 1990. **346**(6287): p. 818.

118. Tiede, C., et al., *Affimer proteins are versatile and renewable affinity reagents.* Elife, 2017. **6**: p. e24903.

119. Xie, C., et al., *Development of an Affimer-antibody combined immunological diagnosis kit for glypican-3.* Scientific Reports, 2017. **7**(1): p. 1-9.

120. Sharma, R., et al., *Label-free electrochemical impedance biosensor to detect human interleukin-8 in serum with sub-pg/ml sensitivity*. Biosensors and Bioelectronics, 2016. **80**: p. 607-613.

121. Tiede, C., et al., *Adhiron: a stable and versatile peptide display scaffold for molecular recognition applications.* Protein Engineering, Design and Selection, 2014. **27**(5): p. 145-155.

122. Woodman, R., et al., *Design and validation of a neutral protein scaffold for the presentation of peptide aptamers.* Journal Of Molecular Biology, 2005. **352**(5): p. 1118-1133.

123. Tasset, D.M., M.F. Kubik, and W. Steiner, *Reprined with permission: Oligonucleotide inhibitors of human thrombin that bind distinct epitopes.* Journal Of Molecular Biology, 1997. **272**(5): p. 688-698.

124. Wilson, C., J. Nix, and J. Szostak, *Functional requirements for specific ligand recognition by a biotin-binding RNA pseudoknot.* Biochemistry, 1998. **37**(41): p. 14410-14419.

125. Xu, H., et al., *Aptamer-Functionalized Gold Nanoparticles as Probes in a Dry-Reagent Strip Biosensor for Protein Analysis.* Analytical Chemistry, 2009. **81**(2): p. 669-675.

126. Media, E.N. *An affirmation of alternatives*. 2019 [cited 2020 1st July]; Available from: http://www.labnews.co.uk/article/2024916/an_affirmation_of_alternatives.

127. Ye, H. and X. Xia, *Enhancing the sensitivity of colorimetric lateral flow assay (CLFA) through signal amplification techniques.* Journal of Materials Chemistry B, 2018. **6**(44): p. 7102-7111.

128. Liu, L., et al., *Nanomaterials-based colorimetric immunoassays.* Nanomaterials, 2019. **9**(3): p. 316.

129. Sharma, A., et al., *Gold nanoparticle conjugated magnetic beads for extraction and nucleation based signal amplification in lateral flow assaying.* Sensors and Actuators B: Chemical, 2020: p. 127959.

130. Rivas, L., et al., *Lateral flow biosensors based on gold nanoparticles*, in *Comprehensive Analytical Chemistry*. 2014, Elsevier. p. 569-605.

131. Moyano, A., et al., *Magnetic Lateral Flow Immunoassays.* Diagnostics, 2020. **10**(5): p. 288.

132. Liu, C., et al., *Lateral flow immunochromatographic assay for sensitive pesticide detection by using Fe3O4 nanoparticle aggregates as color reagents.* Analytical chemistry, 2011. **83**(17): p. 6778-6784.

133. Biosciences, I. *Guide to Lateral Flow Immunoassays*. 2020 [cited 2020 21st May]; Available from: https://fnkprddata.blob.core.windows.net/domestic/download/pdf/IBS_A_guide_to_lateral_flow_immunoassays.pdf.

134. Nielsen, K., et al., *Prototype single step lateral flow technology for detection of avian influenza virus and chicken antibody to avian influenza virus.* Journal Of Immunoassay & Immunochemistry, 2007. **28**(4): p. 307-318.

135. Pan, R., et al., *Gold nanoparticle-based enhanced lateral flow immunoassay for detection of Cronobacter sakazakii in powdered infant formula.* Journal Of Dairy Science, 2018. **101**(5): p. 3835-3843.

136. Yu, Q., et al., *Gold nanoparticles-based lateral flow immunoassay with silver staining for simultaneous detection of fumonisin B1 and deoxynivalenol.* Food Control, 2015. **54**: p. 347-352.

137. Gao, Z., et al., *Platinum-decorated gold nanoparticles with dual functionalities for ultrasensitive colorimetric in vitro diagnostics.* Nano Letters, 2017. **17**(9): p. 5572-5579.

138. Fernández-Sánchez, C., et al., *One-step immunostrip test for the simultaneous detection of free and total prostate specific antigen in serum.* Journal Of Immunological Methods, 2005. **307**(1-2): p. 1-12.

139. Yan, L., et al., *Highly sensitive furazolidone monitoring in milk by a signal amplified lateral flow assay based on magnetite nanoparticles labeled dual-probe.* Food Chemistry, 2018. **261**: p. 131-138.

140. Abera, A. and J.-W. Choi, *Quantitative lateral flow immunosensor using carbon nanotubes as label.* Analytical Methods, 2010. **2**(11): p. 1819-1822.

141. Van Dam, G., et al., *Diagnosis of schistosomiasis by reagent strip test for detection of circulating cathodic antigen.* Journal Of Clinical Microbiology, 2004. **42**(12): p. 5458-5461.

142. van Amerongen, A., et al., *Quantitative computer image analysis of a human chorionic gonadotropin colloidal carbon dipstick assay.* Clinica Chimica Acta, 1994. **229**(1-2): p. 67-75.

143. Mao, X., W. Wang, and T.E. Du, *Dry-reagent nucleic acid biosensor based on blue dye doped latex beads and lateral flow strip.* Talanta, 2013. **114**: p. 248-253.

144. Lee, S., S. Mehta, and D. Erickson, *Two-color lateral flow assay for multiplex detection of causative agents behind acute febrile illnesses.* Analytical Chemistry, 2016. **88**(17): p. 8359-8363.

145. Cho, I.-H., et al., *Chemiluminometric enzyme-linked immunosorbent assays (ELISA)-on-a-chip biosensor based on cross-flow chromatography.* Analytica Chimica Acta, 2009. **632**(2): p. 247-255.

146. Kong, D., et al., *Development of ic-ELISA and lateral-flow immunochromatographic assay strip for the detection of citrinin in cereals.* Food and Agricultural Immunology, 2017. **28**(5): p. 754-766.

147. Jauset-Rubio, M., et al., *Ultrasensitive, rapid and inexpensive detection of DNA using paper based lateral flow assay.* Scientific Reports, 2016. **6**: p. 37732.

148. Mathew, J. and M. Varacallo, *Physiology, Blood Plasma*, in *StatPearls [Internet]*. 2019, StatPearls Publishing.

149. Silva, P., et al., *Blood serum components and serum protein test of Hybro-PG broilers of different ages.* Brazilian Journal of Poultry Science, 2007. **9**(4): p. 229-232.

150. Pedersen-Bjergaard, S. and K.E. Rasmussen, *Liquid-phase microextraction with porous hollow fibers, a miniaturized and highly flexible format for liquid–liquid extraction.* Journal of Chromatography A, 2008. **1184**(1-2): p. 132-142.

151. Thurman, E. and M. Mills, *Solid-phase extraction.* New York: John Wiley & Sons, 1998. **29**: p. 35-73.

152. Poole, C.F., *New trends in solid-phase extraction.* TrAC Trends in Analytical Chemistry, 2003. **22**(6): p. 362-373.

153. Simpson, N.J., *Solid-phase extraction: principles, techniques, and applications*. 2000: CRC press.

154. Matulis, D., *Selective precipitation of proteins.* Current Protocols In Protein Science, 2016. **83**(1): p. 4.5. 1-4.5. 37.

155. Smith, C., et al., *The antibody spectrum in individuals with defect expression of HLA class II and the LFA-1 glycoprotein family genes.* Clinical And Experimental Immunology, 1988. **74**(3): p. 449.

156. Do Kim, K., et al., *Formation and surface modification of Fe3O4 nanoparticles by co-precipitation and sol-gel method.* Journal of Industrial and Engineering Chemistry, 2007. **13**(7): p. 1137-1141.

157. Matsunaga, T., et al., *Fully automated immunoassay for detection of prostate-specific antigen using nano-magnetic beads and micro-polystyrene bead composites, 'Beads on Beads'.* Analytica Chimica Acta, 2007. **597**(2): p. 331-339.

158. Shevkoplyas, S.S., et al., *The force acting on a superparamagnetic bead due to an applied magnetic field.* Lab on a Chip, 2007. **7**(10): p. 1294-1302.

159. Levison, P.R., et al., *Recent developments of magnetic beads for use in nucleic acid purification.* Journal of Chromatography A, 1998. **816**(1): p. 107-111.

160. Chan, K.Y., et al., *Ultrasensitive detection of E. coli O157: H7 with biofunctional magnetic bead concentration via nanoporous membrane based electrochemical immunosensor.* Biosensors and Bioelectronics, 2013. **41**: p. 532-537.

161. Sundaralingam, M., et al., *Molecular structure of troponin C from chicken skeletal muscle at 3-angstrom resolution.* Science, 1985. **227**(4689): p. 945-948.

162. Tsukui, R. and S. EBASHI, *Cardiac troponin.* The Journal of Biochemistry, 1973. **73**(5): p. 1119-1121.

163. Bodor, G.S., et al., *Development of Monoclonal-Antibodies for an Assay of Cardiac Troponin-I and Preliminary-Results in Suspected Cases of Myocardial-Infarction.* Clinical Chemistry, 1992. **38**(11): p. 2203-2214.

164. Xu, Q.F., et al., *Development of lateral flow immunoassay system based on superparamagnetic nanobeads as labels for rapid quantitative detection of cardiac troponin I.* Materials Science & Engineering C-Biomimetic and Supramolecular Systems, 2009. **29**(3): p. 702-707.

165. Han, X., et al., *Recent development of cardiac troponin I detection.* Acs Sensors, 2016. **1**(2): p. 106-114.

166. Shave, R., et al., *Exercise-induced cardiac troponin elevation: evidence, mechanisms, and implications.* Journal of the American College of Cardiology, 2010. **56**(3): p. 169-176.

167. Svensson, J., et al., *Both low and high serum IGF-I levels associate with cancer mortality in older men.* The Journal of Clinical Endocrinology & Metabolism, 2012. **97**(12): p. 4623-4630.

168. Crowe, F.L., et al., *The association between diet and serum concentrations of IGF-I, IGFBP-1, IGFBP-2, and IGFBP-3 in the European Prospective Investigation into Cancer and Nutrition.* Cancer Epidemiology and Prevention Biomarkers, 2009. **18**(5): p. 1333-1340.

169. Powrie, J., et al., *Detection of growth hormone abuse in sport.* Growth Hormone & IGF Research, 2007. **17**(3): p. 220-226.

170. *Somatropin (Human Growth Hormone): Production & Function*. [cited 2020 23rd May]; Available from: https://schoolworkhelper.net/somatropin-human-growth-hormone-production-function/.

171. Peptide, M. *IGF-1 Protein*. 2013 [cited 2020 22nd May]; Available from: http://www.maximpeptide.com/research/wp-content/uploads/2014/07/Igf-1-Protein.pdf.

172. Bishara, N., *The use of biomarkers for detection of early-and late-onset neonatal sepsis.* Hematology, Immunology and Infectious Disease: Neonatology Questions and Controversies: Expert Consult-Online and Print, 2012: p. 303.

173. Bickel, M., *The role of interleukin-8 in inflammation and mechanisms of regulation.* Journal Of Periodontology, 1993. **64**(5 Suppl): p. 456-460.

174. Dutheil, F., et al., *Urinary interleukin-8 is a biomarker of stress in emergency physicians, especially with advancing age—the JOBSTRESS* randomized trial.* Plos One, 2013. **8**(8): p. e71658.

175. Zhang, J. and C. Bai, *Elevated serum interleukin-8 level as a preferable biomarker for identifying uncontrolled asthma and glucocorticosteroid responsiveness.* Tanaffos, 2017. **16**(4): p. 260.

176. Shin, Y.-O., et al., *Comparison of Interleukin-8 Levels in Long-Distance Runners and Healthy Sedentary Non-Athletic Control Subjects.* Korean Journal of Physiology & Pharmacology, 2007. **11**(6): p. 263-268.

177. Pichert, A., et al., *Functional aspects of the interaction between interleukin-8 and sulfated glycosaminoglycans.* Biomatter, 2012. **2**(3): p. 142-148.

Appendix:

Formula to calculate GH score as specified by WADA [55-56]:

GH-2000 score for males:

$-6.586 + 2.905 \cdot \ln(\text{P-III-NP}) + 2.100 \cdot \ln(\text{IGF-I}) - 101.737 / \text{age}$

GH-2000 score for females:

$-8.459 + 2.454 \cdot \ln(\text{P-III-NP}) + 2.195 \cdot \ln(\text{IGF-I}) - 73.666 / \text{age}$

Chapter 3

Experimental Methodology

This chapter contains description of the rationale behind selection of materials for the experiments, developed assay layouts and their protocols. The assay layouts have been explained using schematics and the LFA fabrication process has also been described in detail. The protocol related to colorimetric signal analysis and LOD calculation have then been elaborated. This section also describes the principles behind the characterization techniques used and the methodology used to perform them for the studies contained in it. Techniques such as SEM, EDX, DLS and UV-Vis have been utilized. Furthermore, the principles and protocols associated with protein quantification techniques such as BCA and ELISA have also been described.

*Materials and protocols were taken from: Sharma, A., et al., *Magnetic field assisted preconcentration of biomolecules for lateral flow assaying.* Sensors and Actuators B: Chemical, 2019. **285**: p. 431-437.; Sharma, A., et al., *Gold nanoparticle conjugated magnetic beads for extraction and nucleation based signal amplification in lateral flow assaying.* Sensors and Actuators B: Chemical, 2020: p. 127959.

3.1 Rationale for Selection of Materials

3.1.1 Membranes for LFA Fabrication

As mentioned in Section 2.4.1, an LFA strip consists of different membranes assembled together to perform analysis on a dispensed sample. Since each membrane constitutes a different functional zone, the properties required for each membrane also vary. Table 2.3 outlines the various types of membranes used in a typical LFA strip. The LFA layouts adopted in this thesis consist of two zones: the reaction zone containing the test line and the absorption pad.

The reaction zone is made up of nitrocellulose (NC) membranes. Nitrocellulose is a polymer prepared by nitrating cellulose through exposing it to a mixture of nitric acid and either hydrochloric or sulphuric acid. NC membranes are prepared through phase inversion of nitrocellulose solution.[1] In phase inversion technique, a highly concentrated liquid phase polymer solution inverts into a swollen solid 3-D macromolecular network by solvent evaporation.[2] It allows high degree of control over the morphology of the membrane, its internal structure and the overall porosity, all of which eventually define performance of the membrane and thus, the LFA strip. The control over the wicking time of a solution through the membrane defines the sensitivity of the LFA. Furthermore, nitrocellulose membranes have high protein binding ability, typically in the range of 80-100 $\mu g/cm^2$, which allows several immunological reactions to take place on its surface.[1, 3] This property, which is a resultant of hydrophobic interactions between protein and membrane surface, is important for having a test line composed of biomolecules in an LFA. The control over the properties of NC membranes have made them the most popular choice for LFAs. This has also led to widespread commercial availability of various types of NC membranes, providing flexibility in terms of LFA fabrication and its applications.

The absorption pad is composed of cellulose membrane. The main function of the absorption pad is to provide a wicking effect to direct capillary flow of reactant, sample and rinsing buffer solutions. Cellulose is a polysaccharide made up of a large number of

glucose molecules. It is synthesized by plants and it is one of the most abundantly present bio-macromolecules in the world. Cellulose chains are arranged in parallel arrays via Hydrogen (H) bonding to form structures known as microfibrils. These microfibrils, which are tough and inflexible, are bundled together to form larger structures called macrofibrils. Synthetic cellulose membranes, which are generally made of cellulose acetate blends, have a porous structure (pore size ~0.5 µm).[4, 5] The sugar molecules they contain can form H-bonds with water present in the sample, thus, allowing them to absorb substantial amounts. This property is highly desirable in a wicking membrane as a large absorbing capacity enable handling of large volumes of test samples.

3.1.2 Antibodies for Sensing

As mentioned in section 2.4.3, antibodies are the most widely used recognition molecules for detection and capturing of analytes in LFAs. The technology of antibodies dates back to more than six decades and has been studied extensively.[6, 7] It is one of the facile recognition systems utilized in biosensing applications. The widespread commercial availability and the abundance of literature makes it easy to test new LFA strategies on known model systems (such as Troponin or IGF-1 studied in this thesis) using high affinity antibodies. Furthermore advancement in technology such as use of recombinant forms, has enabled production of antibodies with better specificity, at a higher throughput, and with improved robustness and at manageable costs.[8, 9]

3.1.3 Signal Reporters

3.1.3.1 Magnetic Beads

Magnetic beads (MBs) have been extensively used in molecular biology for purposes such as sample purification [10, 11] and synthesis of nucleic acid aptamers via SELEX [12]. However, use of such MBs as colorimetric reporters has also been explored in the recent years. Commercially available magnetic beads, especially polymer beads with embedded superparamagnetic particles, ranging from a few nanometres to a few micrometres, have

several advantages. Such beads are biocompatible, possess low toxicity, are easy to prepare, and can be customized easily in terms of size, morphology, composition and surface chemistry to enable selective immobilization of biomolecules. Moreover, these magnetic beads (MBs) can be easily controlled in a solution by simply applying an external magnetic field. The superparamagnetic behaviour ensures that the remnant magnetic field completely dissipate when the external field is removed, thus ensuring that the particles are not flocculated.[13] MBs are especially favourable for sensing applications due to their properties such as high surface to volume ratio, which allows binding with a large number of functional groups on each bead, their colloidal stability in a wide range of media such as buffers, solvents etc., and the insusceptibility of their properties to reagent chemistries used for conjugation of biomolecules. Several different functionalisation strategies are possible on MBs using carboxyl, amine, maleimide or thiol anchors. Larger micron sized beads are typically used for extraction and amplification; whereas, smaller nanometre sized beads have been found to be more suitable for LFA applications, as smaller beads migrate efficiently and accumulate at the test line/control line as compared to micron sized beads [14-17]. MBs have been used for detection of several analytes such as proteins, enzymes, bacteria, toxins, viruses, etc.[17] The availability of a wide range of literature also helps to study newer LFA systems using well established model systems. Commercially available 200 nm polystyrene MBs are utilized in this thesis.

3.1.3.2 Gold Nanoparticle Conjugated Magnetic Beads

Although MBs are most useful for extraction and amplification, their use as optical reporters has not been investigated in detail. On the other hand, AuNPs are the most popular colorimetric reporters evaluated for applications in LFAs. The advantages of using AuNPs as optical reporters have already been discussed in section 2.4.4. However, concerns such as colloidal stability, and physisorption of biomolecules have limited their applications to assay complex matrices. Therefore, significant effort have been devoted to develop alternative reporters for optical detection in LFAs. Recently composite reporters comprising of magnetic particles and AuNP have been proposed for detection of biomolecules.[18-20] Such composites, with combined properties of AuNPs and MBs,

possess dual functionality in assaying. They not only enable analyte preconcentration, but also allow use of such particles as optical reporters for visual detection. These composite reporters offer high mechanical stability and excellent magnetic properties for efficient target analyte isolation in homogeneous assays.[20, 21] Co-precipitation is the commonly adopted approach for synthesis of these composites.[21] However, alternative synthesis protocols such as chemical bonding [20] and use of an intermediate layer [22] also have been explored. Therefore, this thesis explores the feasibility of using gold nanoparticle conjugated MBs (GMBs) for lateral flow assaying.

3.2 Synthesis of Reporter Conjugate

3.2.1 Synthesis of MB-Ab

EDC/NHS protocol [23] was adopted and optimized to conjugate antibodies to carboxylated magnetic beads. A 200 µl solution of magnetic beads (concentration 2.5 mg/ml) was prepared in 100 mM MES buffer (pH 5). The beads were washed twice with MES buffer prior to activation with EDC (400 mM) and NHS (300 mM) for 30 min. The excess of EDC and NHS was then removed by separating the beads using a magnetic separator followed by washing them twice with PBS. The beads were then re-suspended in 250 µl of antibody solution (100 µg/ml) and incubated for 2 h under gentle shaking. They were then separated and washed twice with PBS to remove the unbound antibodies followed by incubation in 1% BSA in PBS for 30 min in order to block any free and active carboxyl groups on the bead surface. The modified beads were eventually stored in a storage buffer consisting of PBS, 0.05% tween-20, 0.1% sodium azide and 1% BSA until use. Fig 3.1 represents a schematic of the conjugation process.

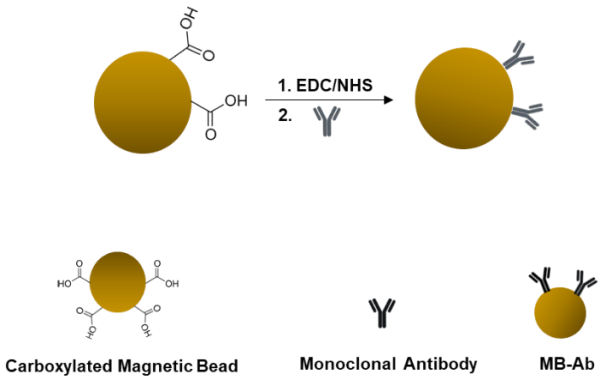

Fig 3.1: Schematic of MB-Ab synthesis protocol involving EDC/NHS activation of carboxylated MBs followed by immobilization of antibodies.

3.2.2 Synthesis of Ab-GMB complexes

The synthesis of Ab-GMB complexes consisted of two parts: synthesis of GMB reporter and conjugation of antibodies to GMB.

To synthesize GMB reporter, 500 µl solution of carboxylated magnetic beads (concentration 250 µg/ml) was prepared in 100 mM MES buffer (pH 5). The beads were washed thrice by magnetic separation with buffer replacement. EDC/NHS carbodiimide linkage protocol was utilized to conjugate cysteamine linker to MB. MBs were activated by a reaction in EDC (400 mM) and NHS (300 mM) for 30 min. The excess of EDC and NHS was then removed by separating the beads using a magnetic separator followed by washing them twice with PBS. The beads were then re-suspended in 500 µl of cysteamine solution and incubated for 1 h under gentle shaking, followed by washing five times with DI water to remove the unbound cysteamine. Tween 20 solution in DI water was then added to the vial containing the MB. AuNP solution (Sigma, OD 1) was introduced into the vial and incubated with the MB for 1 h under gentle shaking. The prepared GMB was stored in PBS-0.05% tween 20 (PBST).

EDC/NHS protocol used in section 3.2.1 was again adopted to conjugate the antibodies to the synthesized GMB. 500 µl solution of the synthesized GMB was prepared in 100 mM

MES buffer (pH 5). GMBs were washed thrice with MES and activated by a reaction in EDC (400 mM) and NHS (300 mM) for 30 min. The excess of EDC and NHS was then removed by separating the GMBs using a magnetic separator followed by washing them twice with PBS. The GMBs were then re-suspended in 250 µl of antibody solution (80 µg/ml) and incubated for 2 h under gentle shaking. The beads were then separated and washed twice with PBS to remove the unbound antibodies. These GMB-Ab conjugates were eventually stored in a storage buffer consisting of PBS, 0.05% tween-20, 0.1% sodium azide and 1% BSA until use. Fig 3.2 represents schematic of the GMB synthesis and Ab conjugation process.

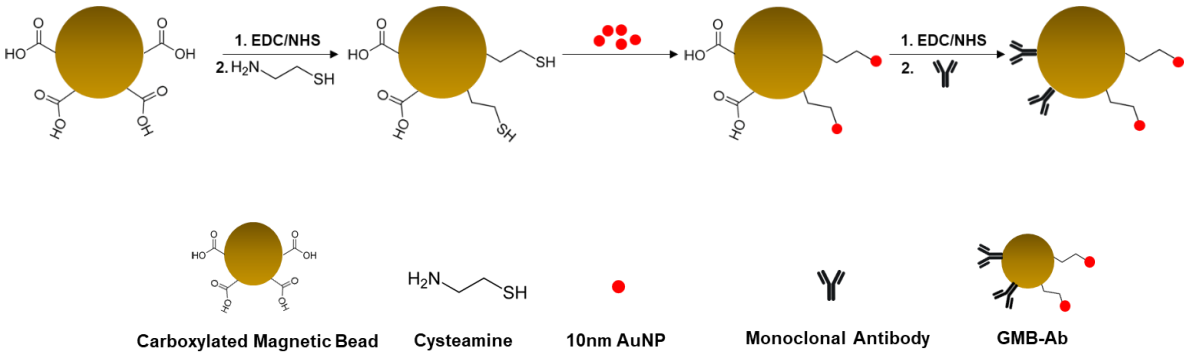

Fig 3.2: Schematic of GMB-Ab synthesis protocol. The carboxylated MBs were activated by EDC/NHS followed by exposure to cysteamine to yield MBs exposing free SH and COOH groups. The SH were reacted with gold NPs and the remaining COOH was activated via EDC/NHS for antibody immobilization.

3.3 Sample Preparation

Analyte solution was assayed in a concentration ranging from 0 to 1 µg/ml. The samples were prepared in two different matrices: PBS and plasma. Highest concentration of analyte was added to these matrices, followed by serial dilution to obtain test samples with varying concentrations of analyte. In case of plasma matrix, the samples were serially diluted in plasma to obtain lower test concentrations. 10 µl of these samples were diluted using 90 µl of PBS buffer followed by an incubation with 100 µl of antibody conjugated reporters (MB/GMB) for 15 min.

3.4 Assay Layout

The LFA strips were prepared by assembling a NC membrane (2.5 cm x 3 mm) and a cellulose absorbent pad (2 cm x 1 cm) with an overlap of 2 mm. The test line was manually deposited with 3 µl of capture antibody (1 mg/ml) over a width of 3 mm. The proposed layout does not require a control line because the bulk of GMB/MB reporter accumulates at cellulose absorbent pad forming a visible patch. Thus, the appearance of a visible patch at the absorbent pad is a clear indication that the reporters are migrating properly over the test band. In order to prevent non-specific adsorption of proteins, NC membranes were incubated with 1% BSA in PBS for 1 h at 37 ºC. Post BSA incubation, the strips were washed with PBS and dried. The strips were stored in dry conditions at 4ºC before use. Two main strategies, which have been explained in the subsections below, were explored using this layout.

3.4.1 Strategy 1: Incorporation of Sample Pretreatment with LFA

As illustrated in Fig 3.3, the assay layout consists of an LFA strip, a detachable magnet and a passivation layer. Typically, 100 µl of sample and anti-TnI conjugated magnetic beads (MB-Ab) mixture (1:1 ratio, prepared according to protocol in section 3.3) is dropped on to the strip for assaying. The magnetic field induced by the detachable magnet retains the MB-Ab-analyte complexes, if any, on the LFA membrane. The sample matrix components are subsequently channelized via a hydrophilic passivation layer to reach the absorbent pad. The channelling through the passivation layer allows the immobilized capture antibodies on the test line to be protected from the matrix solution. The magnet and passivation layer are then removed, followed by addition of 100 µl of PBS as the assay buffer. The captured MB-Ab then flows downstream, along the NC membrane and are specifically captured by the capture antibodies immobilized on the test line in the presence of analyte, yielding a visible brown band due to accumulation of magnetic beads on the test line. Images of the bands were then captured after 15 min for analysis.

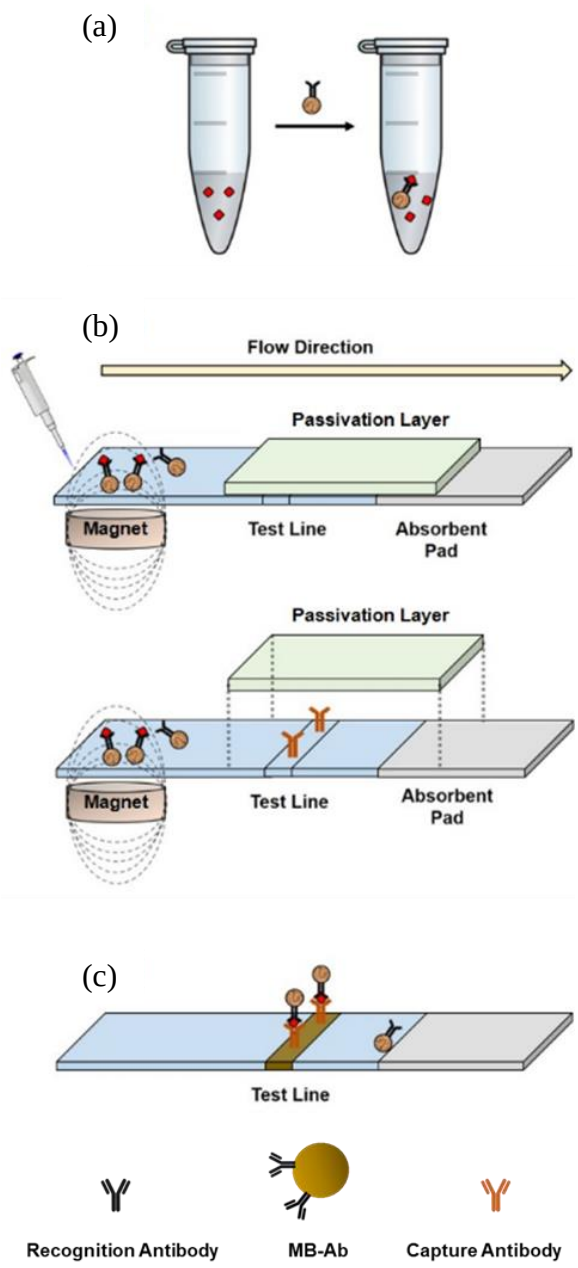

Fig 3.3: (a) Magnetic beads conjugated with antibodies are added to the sample matrix containing the analyte. (b) Use of magnetic field for isolation of analyte from the sample matrix and a hydrophilic passivation layer (glass fibre) to protect the test line from being exposed to the matrix. (c) Removal of passivation layer and magnetic field followed by release and capture of beads along the test line immobilized with anti-TnC antibodies.

3.4.1.1 Signal Enhancement

Since protein-A is known to bind to antibodies, a signal enhancement strategy utilizing protein-A conjugated magnetic bead (PMB) was explored. A 50 fold diluted stock solution of PMB was used for signal enhancement. Once the assay was complete, as described in Section 3.4.1, 5 µl of diluted PMB solution was dropped on the test line. After an incubation period of 10 min, 50 µl of PBS was used to rinse off the excess of PMB solution. Tests were carried out using strips corresponding to 1 ng/ml and 0.1 ng/ml analyte concentrations, with the use of passivation layer, in both PBS and plasma.

3.4.2 Strategy 2: Nucleation based signal amplification using GMB reporters

Analyte-antibody-GMB conjugates prepared according to section 3.3 was extracted from the solution using an external magnet. These conjugates were then introduced to a vial containing PBS buffer and subsequently 100 µl of this mixture was dispensed on the LFA strips to perform the assay, as shown in Fig 3.4 (a). As illustrated in Fig 3.4 (b-c), the sample solution is allowed to flow downstream till it reaches the absorbent pad. The analyte-Ab-GMB conjugates in the sample solution are specifically captured on the test line by the immobilized capture antibody, producing a brown band. Absence of analyte in the sample solution did not result in formation of the band. Images of the test zone were then captured after 15 min for analysis.

3.4.2.2 Signal Enhancement

The nucleation agent used for signal enhancement on the test line consists of a 10 mM citrate buffer solution (pH 4) containing 25 mM $HAuCl_4$ and 5 mM $NH_2OH.HCl$. 5 µl of this nucleation reagent was introduced on top of the test line and allowed to react with the captured GMB for 5 min, followed by rinsing with PBS, Fig 3.4 (c-d). This resulted in formation of larger gold clusters at the test line with enhanced visual contrast.

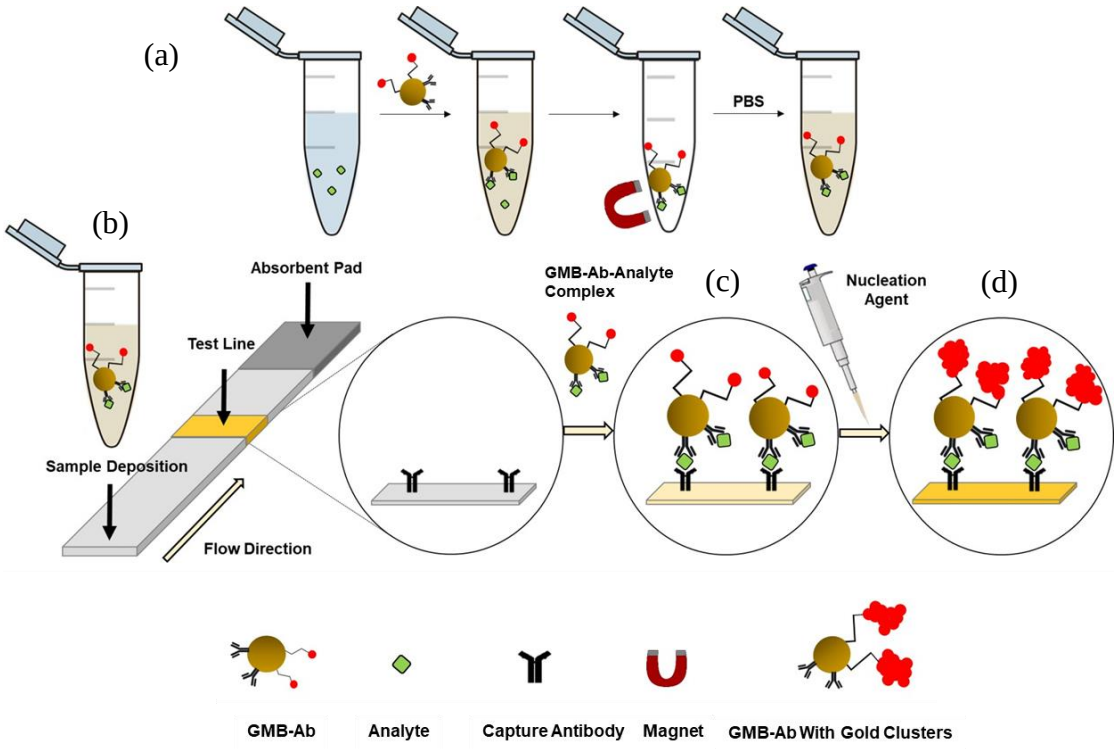

Fig 3.4: (a) GMB-Ab are added to the sample matrix containing the analyte and incubated for 15 min. The yellow coloration seen in the vial is due to the colour of the bead solution. The sample matrix is then replaced with PBS buffer by magnetic separation of beads. (b) The sample solution containing GMB-Ab-Analyte is introduced on the NC strip to initiate flow on the LFA strip. (c) Capture of GMB-Ab-Analyte at the test line produces a brown band. (d) Nucleation of gold nanoclusters on top of GMB for improving the contrast of the test band upon addition of nucleation reagent on the test line.

3.6 Analysis of Signal Readout

The visual detection limit (VDL) in this thesis has been defined as the concentration below which responses could not be observed visually at the test band. For quantitative analysis of the test bands, luminance values were considered. Luminance value is a weighted average of the red, blue and green (RBG) components of an image and it is inversely proportional to intensity.[24] A darker colour would result in a lower luminance while a higher luminance indicates a colour of lighter intensity. The entire region of test bands on the test strip was selected and analyzed by ImageJ software to acquire the luminance values. These luminance values were then normalized by calculating the relative

luminance, which refers to the change in luminance of the images that correspond to the analyte concentration from that of a reference luminance value, which is typically the control. These normalized values were then plotted to obtain the calibration curves. The limit of detection (LOD) was calculated using the 3σ/S approach.

3.7 Characterization Methods

3.7.1 Scanning Electron Microscopy (SEM)

Scanning Electron Microscopy (SEM) is an imaging technique that uses a focused electron beam to scan object surfaces to produce various signals, which are then used to gather information about the topography and composition of the material.[25] The electron beams interact with the atoms of the scanned object and produce the following products: secondary electrons (SE) which are a resultant of ionization of primary electrons near the metal surface; back scattered electrons (BSE) which are released due to elastic scattering of incident electrons from lower sub-surface levels; and characteristic X-rays, which are released as a result of ionization of sub-surface electrons. These signals are captured using different detectors and converted to readable outputs either in the form of digital images or scan plots. The amount of information gathered depends on several factors such as incident electron beam strength, scanning speed of the incident beam and even the scan area on the surface. SE and BSE are the most commonly used imaging modes in SEM for obtaining topographical information. Fig 3.5 shows a schematic of a typical SEM and the type of signals generated during imaging.

To image the synthesized GMB/MB particles, 5 µl of bead solution prepared was dropped on a quartz substrate and allowed to dry in air for 10 min, before desiccating the substrate overnight. SEM requires a conducting surface for imaging. A conducting surface prevents charge build-up and hence allows proper interaction of the incident beam with the surface electron. Since the samples imaged in this thesis are not conducting in nature, they have been coated with gold or platinum using a plasma sputter coater. Similarly, for imaging the membranes studied in this thesis, they were first cut into 0.5 cm x 0.5 cm pieces and then

sputter coated. Following this, the samples were imaged using a Field Emission SEM (FESEM). An FESEM is a type of high resolution SEM, which generates the electron beam using a field emission gun. The beam generated in an FESEM is of low energy, highly focused and requires a low potential for generation (≤5kV).[25]

3.7.2 Energy Dispersive X-Ray Photospectroscopy (EDX)

EDX is an analytical technique that uses the characteristic X-rays generated from a sample for chemical/elemental analysis. EDX may use a focused X-ray or electron beam to release and capture the characteristic x-rays from a sample.[26] When an incident beam interacts with electrons, some energy is transferred, which may lead to the electron to excite from its ground state and move to a nearby higher energy shell. The resulting vacancy in the lower energy shell is then filled up by a nearby electron from an outer higher energy shell. This movement from a higher energy shell to a lower energy shell produces X-rays, which are discrete and characteristic to the type of element. The energy of generated X-rays is detected externally to form a characteristic spectrum, which enables elemental analysis. Generally, an EDX detector can be attached to an SEM and the incident electron beam can be used as the source. Fig 3.5 (b) represents how an incident electron beam in an SEM can be used to perform an EDX analysis. For EDX analysis in this thesis, sample preparation was the same as described in section 3.7.1. However, the samples were not sputter coated before analysis to exclude undesired elemental peaks in the resultant spectrum.

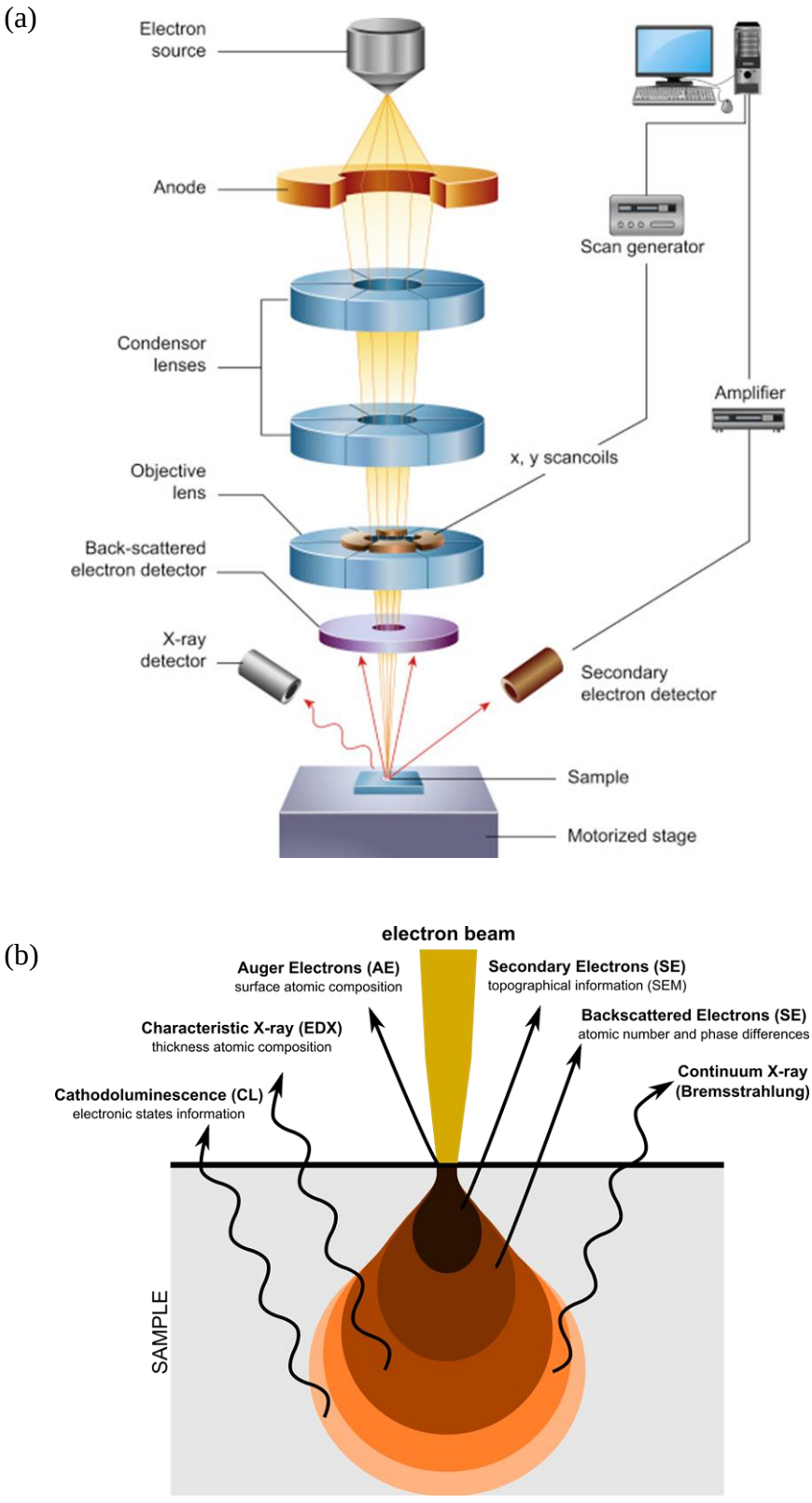

Fig 3.5: (a) Schematic of an SEM [25] (Reprinted with permission); (b) Types of signals generated in an SEM [27]

3.7.3 Dynamic Light Scattering (DLS)

DLS is an analytical technique used to analyze size distribution of particles in a solution. It measures the Brownian motion of particles in a suspension and uses the information to determine the hydrodynamic size of the particles. A monochromatic light source is illuminated at the sample, which leads to scattering of light in all directions by the component particles. The scattered light passes through a polarizer and is collected by a detector, and the resulting intensity is then used to plot the size profile of the particles. Since, the particles in a dispersion are constantly moving, the scattering caused is dynamic in nature, resulting in a dynamic intensity profile of the resultant light. Smaller particles show more rapid fluctuations due to faster diffusion in a solution, whereas larger particles show slower fluctuations.[28] This principle is used to determine the "correlation coefficient" for the intensity spectrum, which is then used to calculate the hydrodynamic size of the particles. DLS is useful for determining nanoparticle sizes in a wide range, from sub-nm to a few µm.[29] Fig 3.6 represents a schematic of the DLS process.

The nanoparticles used in this thesis were characterized using DLS for size measurement. The beads were washed thrice upon magnetic separation and resuspension in DI water. 1 ml of this solution was then used for analysis, which was stored at 4ºC before characterization.

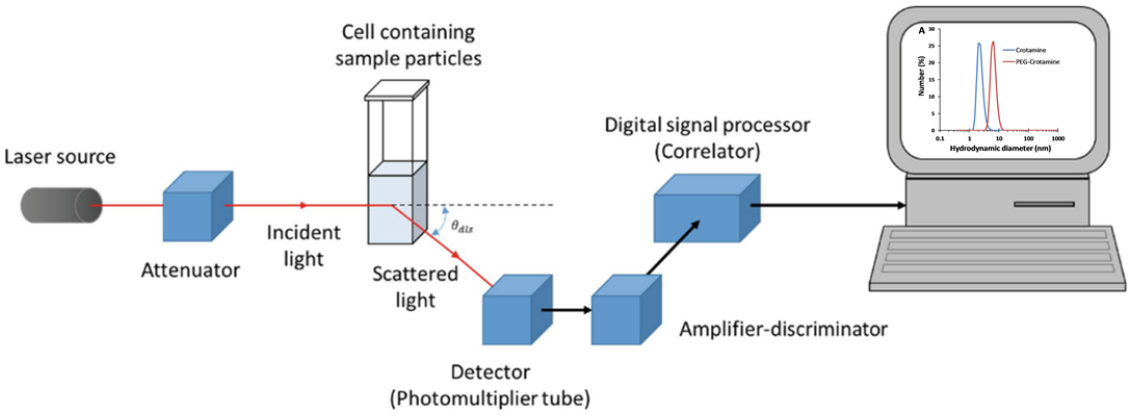

Fig 3.6: Schematic representation of DLS technique [30]

3.7.4 Ultraviolet-Visible Spectroscopy (UV-Vis)

UV-Vis is an absorption spectroscopic technique which utilizes wavelengths in part UV, full visible and the adjacent spectral regions (generally in the range of 200 nm-1100 nm).[31, 32] It uses the principle that when materials interact with light, they can absorb energy, provided that the incident light has sufficient energy to cause a possible electronic transition within the molecules of that material. The energy absorbed by the material is used by the electrons to transfer from a lower energy ground state to a higher energy excited state. A UV-Vis spectrophotometer measures that the amount of absorbed light in a sample at particular wavelengths. The result obtained is generally plotted as an absorbance vs wavelength graph. The amount of light absorbed is a function of the concentration of a sample and the path length through which light has to travel, whereas the characteristic absorbance peak is dependent on material properties, such as excitation state, size etc.[31, 32] For instance smaller AuNPs, when dispersed in a solution, absorb light near 520 nm, but as their size increases the characteristic absorption shifts towards higher wavelengths and the absorption peak becomes broader.[33] On the other hand, for the same path length, AuNPs of the same size would absorb at a particular wavelength irrespective of the concentration. UV-Vis is particularly useful for determining the concentrations of transition metal ions (such as copper, zinc iron etc.) in solutions and organic compounds (either in water for water soluble or ethanol for organic soluble).[34, 35] UV-Vis can be performed at a particular wavelength or as a scan over a wavelength range. The work in this thesis extensively uses UV-Vis for determination of protein binding on the reporters, monitoring analyte-antibody binding characteristics and for optimizing GMB synthesis protocol.

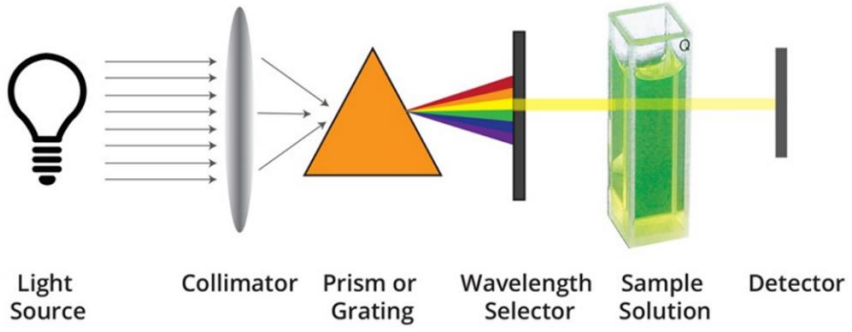

Fig 3.7: Schematic representation of a UV-Vis setup [36]

3.7.5 Bicinchoninic Acid Assay (BCA)

BCA is the one of the most commonly used colorimetric assay for determination of total protein amount in a sample.[37] The underlying principle of BCA is the reduction of Cu^{2+} to Cu^{+} by proteins via chelation in an alkaline solution. Cu^{+} subsequently forms a purple coloured complex with BCA reagent, which consists of an alkaline solution of bicinchoninic acid, sodium carbonate, sodium bicarbonate, sodium tartrate and copper (II) sulfate pentahydrate. The purple complex formed shows a characteristic absorption at 562 nm and the absorption intensity is directly proportional to the concentration of Cu^{+}, which in turn is proportional to the protein concentration. Generally, a BCA is performed on a standard protein such as BSA to obtain a calibration curve, using which absorption readouts from unknown samples can be converted to concentration readings. BCA is a sensitive, simple and a rapid method for total protein quantification. The linear range for BCA depends on the way it is performed.[37, 38] It may have a detection range of 0.1–1.0 mg/ml for a standard protocol or a range of 0.5–10 μg/ml for a micro-assay protocol.[37]

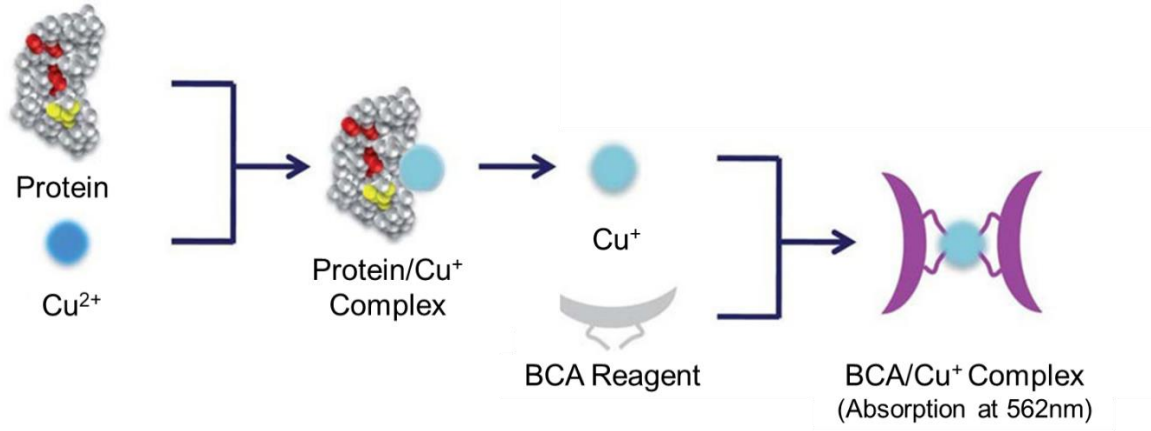

Fig 3.8: Schematic representation of protein quantification by BCA [39]

In this thesis, the antibody-reporter binding efficiency has been characterized using BCA. In the antibody conjugation protocol described in section 3.2, the supernatant post Ab incubation with activated carboxylated reporter beads was used as sample for BCA analysis. A commercial BCA kit was used for this purpose.[38] To prepare the working

reagent (WR), BCA reagent A and BCA reagent B, which were present in the kit, were mixed in 50:1 ratio. 9 BSA standard solutions were prepared according to instructions provided in the kit. 25 µl of each of these standard solutions were pipetted into different wells of a 96 well plate. 25 µl aliquots of the sample to be tested was pipetted into 3 wells for a triplicate measurement. 200 µl of WR was added to each of these wells. The well plate was covered and incubated at 37^{o}C for 30 min. The plate was then cooled to room temperature and absorbance was measured at 562 nm using a plate reader. The calibration curve was obtained using the absorbance readings of the BSA standards and the protein concentration of the samples was calculated using this curve. Since the total amount of antibodies incubated was known and the amount of antibodies in the supernatant post incubation was obtained by BCA, the amount of antibodies conjugated to the beads could be calculated using this information.

3.7.6 Enzyme Linked Immunosorbent Assay (ELISA)

ELISA is one of the most common type of immunoassay and an important technique for analytical measurements on samples. The functioning of ELISA has already been discussed in section 2.2.3. In this thesis, ELISA was used to study the model systems involved and to characterise the analyte-antibody binding. 100 µl of capture antibody solution at a concentration of 2µg/ml was added to individual wells of a transparent base 96 well plate. The plate was incubated overnight at 4^{o}C. The coating solution was removed the following day and the wells were washed three times with 100 µl of PBST (PBS + 0.05% v/v tween-20). The remaining protein binding sites in the coated wells were blocked by incubating them in a blocking solution of 1% BSA in PBS for 1 h. The incubation was done at room temperature and with gentle shaking. This was followed by washing the wells three times with 100 µl PBST. 100 µl of analyte solution at different dilutions were then added to the antibody coated-BSA blocked wells. The plate was then incubated for 2 h at 37^{o}C, followed by washing thrice with 100 µl of PBST. 100 µl of detection antibody solution at a concentration of 2 µg/ml was then added to each well and incubated at room temperature for 2 h. In case of IGF-1, biotinylated antibodies were used for this step, whereas in case of Troponin, HRP conjugated antibodies were used. The incubation was followed by

washing of each well thrice with 100 µl of PBST. In case of biotinylated antibodies, an additional step of room temperature incubation of each well with 100 µl HRP-Streptavidin solution (500 times diluted from stock solution) in 1% BSA-PBS was performed. After washing the wells again with 100 µl of PBST, 50µl of TMB substrate was added to each well and incubated for 30 min for sufficient colour development. This was followed by addition of 50 µl of a stop solution of 1N H_2SO_4. Absorbance was then measured at a wavelength of 450 nm.

References

1. Ahmad, A.L., et al., *Synthesis and characterization of polymeric nitrocellulose membranes: Influence of additives and pore formers on the membrane morphology*. Journal Of Applied Polymer Science, 2008. **108**(4): p. 2550-2557.

2. Pinnau, I. and W.J. Koros, *A qualitative skin layer formation mechanism for membranes made by dry/wet phase inversion.* Journal of Polymer Science Part B: Polymer Physics, 1993. **31**(4): p. 419-427.

3. Hoffman, W.L., et al., *Binding of antibodies and other proteins to nitrocellulose in acidic, basic, and chaotropic buffers.* Anal Biochem, 1991. **198**(1): p. 112-8.

4. Hydranautics, *Commercial RO Technology*. 2001.

5. Hubbe, M.A., et al., *Enhanced absorbent products incorporating cellulose and its derivatives: A review.* BioResources, 2013. **8**(4): p. 6556-6629.

6. Burnet, F.M., *The Production of Antibodies. A Review and a Theoretical Discussion.* The Production of Antibodies. A Review and a Theoretical Discussion., 1941.

7. Pauling, L., *A theory of the structure and process of formation of antibodies.* Journal of the American Chemical Society, 1940. **62**(10): p. 2643-2657.

8. Frenzel, A., M. Hust, and T. Schirrmann, *Expression of recombinant antibodies.* Frontiers In Immunology, 2013. **4**: p. 217.

9. Vink, T., et al., *A simple, robust and highly efficient transient expression system for producing antibodies.* Methods, 2014. **65**(1): p. 5-10.

10. Lien, K.-Y., et al., *Purification and enrichment of virus samples utilizing magnetic beads on a microfluidic system.* Lab on a Chip, 2007. **7**(7): p. 868-875.

11. Prioult, G., et al., *Rapid purification of nisin Z using specific monoclonal antibody-coated magnetic beads.* International Dairy Journal, 2000. **10**(9): p. 627-633.

12. Paul, A., et al., *Streptavidin-coated magnetic beads for DNA strand separation implicate a multitude of problems during cell-SELEX.* Oligonucleotides, 2009. **19**(3): p. 243-254.

13. Shevkoplyas, S.S., et al., *The force acting on a superparamagnetic bead due to an applied magnetic field.* Lab on a Chip, 2007. **7**(10): p. 1294-1302.

14. Jun, B.-H., et al., *Protein separation and identification using magnetic beads encoded with surface-enhanced Raman spectroscopy.* Analytical Biochemistry, 2009. **391**(1): p. 24-30.

15. Gomm, J.J., et al., *Isolation of pure populations of epithelial and myoepithelial cells from the normal human mammary gland using immunomagnetic separation with Dynabeads.* Analytical Biochemistry, 1995. **226**(1): p. 91-99.

16. Sharma, A., et al., *Magnetic field assisted preconcentration of biomolecules for lateral flow assaying.* Sensors and Actuators B: Chemical, 2019. **285**: p. 431-437.

17. Moyano, A., et al., *Magnetic Lateral Flow Immunoassays.* Diagnostics, 2020. **10**(5): p. 288.

18. Fan, A., C. Lau, and J. Lu, *Colloidal gold–polystyrene bead hybrid for chemiluminescent detection of sequence-specific DNA.* Analyst, 2008. **133**(2): p. 219-225.

19. Silva, S.M., et al., *Gold coated magnetic nanoparticles: from preparation to surface modification for analytical and biomedical applications.* Chemical Communications, 2016. **52**(48): p. 7528-7540.

20. Bao, J., et al., *Bifunctional Au-Fe3O4 nanoparticles for protein separation.* ACS nano, 2007. **1**(4): p. 293-298.

21. Karamipour, S., M. Sadjadi, and N. Farhadyar, *Fabrication and spectroscopic studies of folic acid-conjugated Fe3O4@ Au core–shell for targeted drug delivery application.* Spectrochimica Acta Part A: Molecular and Biomolecular Spectroscopy, 2015. **148**: p. 146-155.

22. Luo, Z., et al., *Fluorescent aptasensor for antibiotic detection using magnetic bead composites coated with gold nanoparticles and a nicking enzyme.* Analytica Chimica Acta, 2017. **984**: p. 177-184.

23. Sieben, S., et al., *Comparison of different particles and methods for magnetic isolation of circulating tumor cells.* Journal Of Magnetism And Magnetic Materials, 2001. **225**(1-2): p. 175-179.

24. Bezryadin, S., P. Bourov, and D. Ilinih. *Brightness calculation in digital image processing*. in *International symposium on technologies for digital photo fulfillment*. 2007. Society for Imaging Science and Technology.

25. Inkson, B., *Scanning electron microscopy (SEM) and transmission electron microscopy (TEM) for materials characterization*, in *Materials characterization using nondestructive evaluation (NDE) methods*. 2016, Elsevier. p. 17-43.

26. Ngo, P.D., *Energy dispersive spectroscopy*, in *Failure Analysis of Integrated Circuits*. 1999, Springer. p. 205-215.

27. Ezzahmouly, M., et al., *Micro-computed tomographic and SEM study of porous bioceramics using an adaptive method based on the mathematical morphological operations.* Heliyon, 2019. **5**(12): p. e02557.

28. Stetefeld, J., S.A. McKenna, and T.R. Patel, *Dynamic light scattering: a practical guide and applications in biomedical sciences.* Biophysical Reviews, 2016. **8**(4): p. 409-427.

29. Brown, W., *Dynamic light scattering: the method and some applications*. Vol. 313. 1993: Clarendon Press Oxford.

30. Leong, S.S., et al., *Dynamic Light Scattering: Effective Sizing Technique for Characterization of Magnetic Nanoparticles*, in *Handbook of Materials Characterization*. 2018, Springer. p. 77-111.

31. Weckhuysen, B.M., *Ultraviolet-Visible Spectroscopy*. 2004.

32. Upstone, S.L., *Ultraviolet/visible light absorption spectrophotometry in clinical chemistry.* Encyclopedia of Analytical Chemistry: Applications, Theory and Instrumentation, 2006.

33. Abdelhalim, M.A.K., M.M. Mady, and M.M. Ghannam, *Physical properties of different gold nanoparticles: ultraviolet-visible and fluorescence measurements.* J Nanomed Nanotechol, 2012. **3**(3): p. 178-194.

34. Fleming, I. and D.H. Williams, *Spectroscopic methods in organic chemistry*. 1966: McGraw-Hill New York.

35. Creighton, J.A. and D.G. Eadon, *Ultraviolet–visible absorption spectra of the colloidal metallic elements.* Journal of the Chemical Society, Faraday Transactions, 1991. **87**(24): p. 3881-3891.

36. Biotech, O. *Molecular analysis using UV/Visible spectroscopy*. 2006 [cited 2020 1st June]; Available from: https://orbitbiotech.com/molecular-analysis-using-uv-visible-spectroscopy-spectroscopy-uv-absorption-reflection-spectra-electromagnetic-radiation/.

37. Walker, J.M., *The bicinchoninic acid (BCA) assay for protein quantitation*, in *The protein protocols handbook.* 2009, Springer. p. 11-15.

38. Scientific, T., *Pierce BCA protein assay kit.* Pierce BCA 449 Protein Assay Kit, 2013.

39. OneLab. *BCA Colorimetric Protein Assay*. [cited 2020 2nd June]; Available from: https://onelab.andrewalliance.com/library/bca-colorimetric-protein-assay-X5nPg0gP.

Chapter 4

Characterization and Optimization of LFA Components

This chapter lays the foundation of the LFA layouts studied in the subsequent chapters. The various parameters associated with the functioning of the proposed layouts, such as membranes for the different functional zones, reporters for signal generation and the model systems used have been studied and characterized. Moreover, optimization of these parameters has also been carried out to maximise the efficiency of the assay. The first set of optimization experiments are related to the membranes used and to underline the importance of using a blocking agent in an LFA. Furthermore, the next set of optimizations is to determine the concentration of the MB reporters for an optimal signal readout. Finally, characterization of the analyte-antibody model systems is performed to test the viability of these systems.

4.1 Introduction

LFAs are composed of different functional zones. Each functional zone is modified to carry out a designated function. For instance, Nitrocellulose (NC) membranes are modified to immobilize capture biomolecules at the test line and blocked with BSA to prevent non-specific adsorption of proteins. On the other hand, absorption pads are made up of cellulose, which generally do not require any functionalisation but are mounted on the backing pads to increase the robustness of LFA device. These membranes are then assembled to fabricate the overall LFA device. Several parameters of these functional zones should be optimized to improve the LFA performance.[1, 2] For instance, there are several pore size variants of commercial NC membranes.[3, 4] Pore size is an important feature in determining the sensitivity of an LFA device.[5, 6] This is because a large pore size implies a faster flow rate of sample on the device and therefore less time for the capture biomolecules to interact with it, whereas a smaller pore size leads to a slower flow rate and allows for a longer interaction time between the sample solution and the capture biomolecules.

Hydrophobic membranes such as PVDF and Fusion-5 have been tested over the years for use in test zones in LFAs.[7, 8] For use as absorbent pads, mostly hydrophilic membranes such as glass fibre and cellulose have been tested.[9] Absorption pads are responsible for wicking the sample solution and thus should possess a good absorption capability, which is another important parameter to be optimized. Other parameters such as degree of blocking required to prevent non-specific adsorption and the type of blocking agent used also influence the sensitivity of LFAs. Blocking agents also help control the porosity of the membranes and thus regulate flow. The compatibility of a blocking agent with the model system being studied is very important for proper functionality of an LFA.

Apart from the properties of the membranes, the other important aspects affecting sensitivity of the LFAs are the reporter properties and the biomolecules used, which in this work implies antibody-analyte binding characteristics. The colour intensity of the magnetic beads at the test line is an essential parameter, which directly affects the sensitivity of the

assay.[10] Hence, the concentration of magnetic beads used for signal generation needs to be optimized for a viable naked eye readout, especially at low concentrations of analytes. Similarly, the antibodies used in the assay should be able to bind to low analyte concentrations for an optimal signal readout, implying that characterisation of the interactions between the antibodies and analyte is an essential part of an LFA study.

This chapter contains results pertaining to the various optimization experiments for fabrication of the LFA devices to be studied in this thesis. The first set of experiments are on the various potential membrane types for the different functional zones in the LFA layout. The flow characteristics and the microstructure of the membranes have been studied to explain the rationale behind choosing the membranes. Secondly, the optimizations regarding MBs have also been performed to have sufficient beads on the strip for obtaining a naked eye observable band even at low concentrations of analytes. Thirdly, the antibody-analyte model systems have been characterized using ELISA to ensure their immunoreactivity, which would be eventually utilized in the proposed LFA systems.

4.2 Reagents, Membranes and Apparatus

PBS, BSA (Lyophilized) and tween 20 were purchased from Sigma-Aldrich. Troponin I-C-T complex (cTnICT, 100 µg/ml), anti-TnI and anti-TnC antibodies were purchased from Hytest Inc. Recombinant human IGF-1 protein, biotinylated anti-IGF-1 antibody (anti-IGF-1(b)) and anti-IGF-1 antibody (anti-IGF-1) were purchased from Abcam Inc. Commercially available superparamagnetic carboxylated polystyrene beads (200 nm) purchased from Chemicell were used in this study. NC membrane cards (Hi-Flow Plus 75, 135 and 180 variants), glass fibre membranes and cellulose pads were obtained from Merck-Millipore, whereas Fusion-5 and CF-4 were purchased from GE. Images of strips were captured by Sony Alpha a7R III and processed in Sony Imaging Edge Edit RAW software. SEM was performed using a JEOL 6340 FESEM.

4.3 Results and Discussions

4.3.1 Membrane Characterization

4.3.1.1 Flow Behaviour

The flow behaviour on different membranes was studied using 2 cm x 0.3 cm membrane strips by flowing 100 µl of PBS buffer through them. The sample deposition (in this case a buffer solution) and strip blocking was done according to the protocol described in Section 3.4 of the previous chapter. The time taken for the buffer solution to flow through the entire length of the strips was noted and compared. Nitrocellulose, cellulose, glass fibre, Fusion 5 and CF4 membranes were tested. Nitrocellulose membranes are protein binding, hydrophobic membranes, which are synthesized by phase inversion of nitrocellulose polymer solution.[11] Cellulose (C) membranes, on the other hand, are water wicking and hydrophilic in nature.[12] Similarly, glass fibre (GF) membranes are hydrophilic in nature as well and are made up of aluminosilicates, mostly using phase inversion technique.[13] On the other hand, the recently developed Fusion 5 (F5) and CF4 are proprietary membranes from GE Healthcare. F5 is a single layer matrix membrane consisting of glass fibre and organic binders, whereas CF4 is made of medium weight, cotton liner material.[8, 14] The time taken to flow PBS buffer solution across these membranes under various blocking conditions has been shown in Fig 4.1.

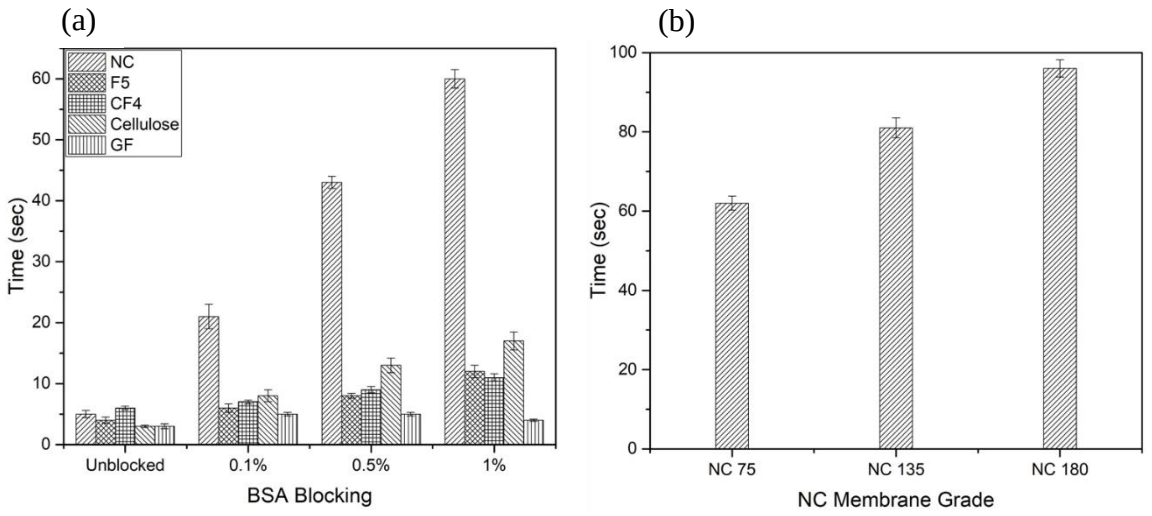

Fig 4.1: (a) Flow rate of different membranes under various blocking conditions (b) Flow rate of different NC membrane grades with 1% BSA blocking. Flow rate here refers to the time required for sample buffer to cross a length of 2 cm on the membranes (represented by the Y-axis).

The flow rate is a key factor which determines the sensitivity of an assay. Higher flow rate would mean less time for interactions between analyte molecules in the sample and the capture biomolecules on the strip, whereas low flow rate would lose the advantage of a rapid turnaround time. Therefore, an optimal flow rate is necessary for a successful assay. One way of achieving this is by blocking of membranes. Blocking proteins such as BSA not just prevent non-specific binding of analyte proteins on membranes but also tend to fill up the pores of these membranes, which leads to a slower flow of solutions through them, thus providing a better control over the flow properties. This behaviour can be seen in Fig 4.1, which shows that the flow rate through the membranes decrease after BSA blocking.

The biggest effect of BSA blocking can be seen in case of the NC membranes, which when unblocked, let the entire buffer volume flow through in ~5 sec (Fig 4.1(a)). In case the membranes are blocked, the flow rate becomes slower as the amount of blocking agent used increases. This can be clearly seen in Fig 4.1(a), where the buffer volume flows through in ~20 sec when 0.1% BSA is used, whereas almost 60 sec is needed for it to flow through when 1% BSA is used.

The Hi-Flow Plus 75 grade of NC membranes, with the largest pore size amongst the three grades tested, was used initially for comparing with other membranes. Since NC is known to bind to protein molecules via hydrophobic interactions, the binding efficiency of a blocking protein to such membranes is high. This leads to further narrowing of the pores, which eventually lowers the flow rate of solutions through a membrane. This behaviour makes NC membranes highly suited for protein immobilisation, making them the ideal choice for a reaction zone which requires immobilization of capture antibodies at the test line and a controlled flow rate for an efficient immunoreaction between capture antibodies and incoming analyte molecules. The decrease in flow rate post blocking in other membranes is not significant as compared to NC, indicating that the flow characteristics of other membranes tested are influenced by only by their pore sizes.

On the other hand, GF has the highest flow rate amongst the tested membranes, and it remained almost unchanged even after blocking. The flow through time was typically ~5 sec regardless of blocking. The large pore size of ~0.7 µm and minimal interaction with proteins due to a hydrophilic surface, helps the flow through of solutions. Thus, glass fibre membranes are ideal for use as passivation layers pertaining to layout for strategy 1 (Chapter 3, Section 3.4).

In case of cellulose, the dispensed buffer solution immediately dissipated into the membrane upon application. Cellulose membranes have a porous structure (pore size ~0.5 µm) and contain sugar building block, which can form H bonds with water present in the sample.[12, 15] Thus, they can absorb substantial amounts of aqueous solutions. This property is highly desirable in a wicking membrane as a large absorbing capacity can direct capillary flow better. Fusion 5 and CF4 also showed a similar behaviour but were not as efficient as cellulose. However, these membranes have been used in LFA studies as sample pads, conjugate pads or even blood separators for their excellent hydrophilicity, wicking characteristics and non-aging behaviour.[8, 14] However, protein immobilisation is a challenging task on these membranes, because of which NC membranes are still the most widely preferred choice for test zones in LFAs. Table 4.1 provides a summary of the tested membranes.

Table 4.1: Summary of the tested membranes

Membrane Tested	Manufacturer	Wetting Behaviour	Protein Binding Ability	Pore size	Use in LFA
Nitrocellulose	Merck-Millipore	Hydrophobic	High	0.2-0.5 µm	Test Zone
Glass Fibre		Hydrophilic	Low	~ 50 µm	Sample Pad/Passivation Layer
Cellulose		Hydrophilic	Low	~ 0.5 µm	Absorption Pad
CF4	GE Healthcare	Hydrophilic	Low		Absorption/Sample Pad
Fusion 5		Hydrophilic	Low	~ 2.5 µm	Absorption/Sample Pad

Fig 4.1(b) shows a comparison between the different pore sizes of the NC membranes used. NC 180 has the smallest porosity and hence the slowest flow rate (~100 sec for buffer to flow through), whereas NC 75 has the largest porosity and the highest flow rate (~60 sec for buffer to flow through). However, NC 135, because of an intermediate flow rate (~80 sec for buffer to flow through) and its ability to flow through 200 nm MBs with ease, was eventually used for all subsequent studies of the proposed LFA layouts in this thesis.

4.3.1.2 Topography in SEM

SEM imaging was performed according to the protocol described in section 3.7.1, to observe the topography of the membranes used for the proposed LFA layouts. NC, GF and cellulose membranes were imaged. Since these membranes were non-conducting, sputter coating of gold was needed to obtain high resolution images. The results are shown in Fig 4.2. From the SEM micrographs, it can be clearly seen that NC membrane is the least porous amongst the three. The glass fibres are random in nature and much thinner than the cellulose fibres, which are flat shaped and large. The cellulose membrane has a high porosity because of the low fibre density.

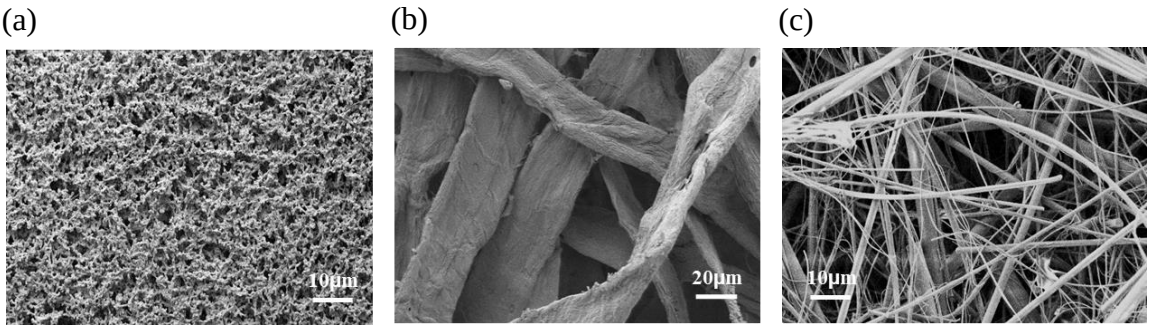

Fig 4.2: SEM images of (a) NC 135, (b) cellulose and (c) GF membranes

4.3.2 Magnetic Bead Characterization

4.3.2.1 Magnetic Separation and Resuspension

Superparamagnetic polystyrene beads were used as reporters for the proposed LFAs. The MBs used were highly homogenous and well distributed in solution form. The beads separated with a high degree of efficiency upon application of external magnetic field, which was provided using a magnetic rack. The superparamagnetic nature of the beads ensured they were quickly recovered into a dispersed phase after removal of the external magnetic field. However, mild shaking was required to re-achieve homogeneity. Fig 4.3 shows the magnetic separation of 5 µl of stock bead solution (~10^{11} beads/ml) in 1 ml PBS buffer solution.

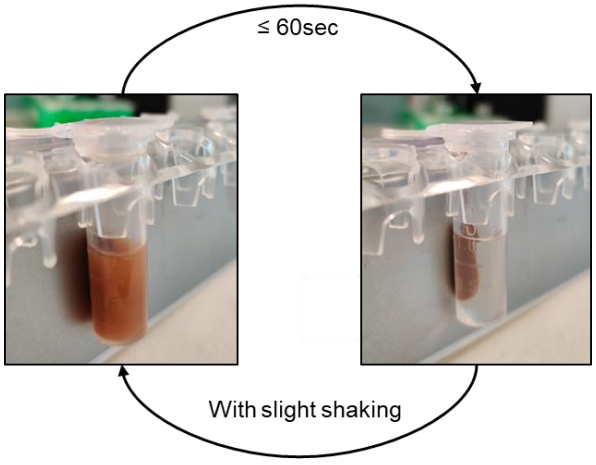

Fig 4.3: Magnetic separation of MBs from a PBS solution using a magnetic rack

4.3.2.2 Size Characterization

DLS was performed according to the protocol described in section 3.7.3 to obtain the hydrodynamic radius of the MBs. A DLS peak at ~200 nm (Fig. 4.4) is an indication of the hydrodynamic radius of the MBs. The homogeneity of the bead solution was evident from the poly dispersity index (PDI) of 0.1. PDI is an indicator of the size distribution of particles and a measure to describe the non-uniformity of any solution. Mathematically, PDI is described as square of the standard deviation divided by the square of the mean of a particular peak. It can have a value between 0 and 1. A low PDI (0-0.1) indicates that a solution is highly homogenous or monodisperse. On the other hand, a PDI above 0.5 indicates a solution is polydisperse and has particles of varying size distributions.

The findings of DLS was also verified using SEM imaging (Fig 4.4 inset). The beads, when dried on a quartz surface tend to aggregate into a solid mass. However, upon observing a few isolated particles, the MB diameters could be estimated to be around 200 nm, which was in agreement with the DLS data.

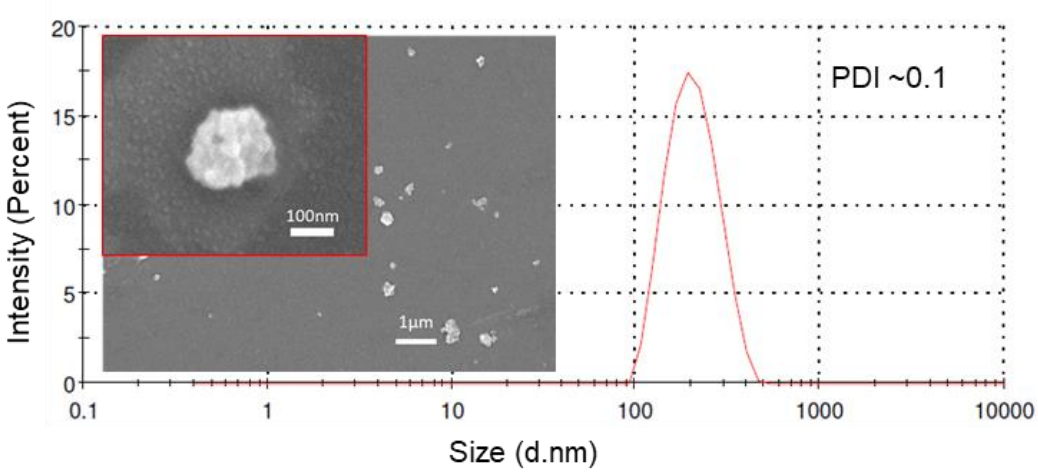

Fig 4.4: DLS plot for MBs. Inset shows the morphology of an MB as observed under SEM

4.3.3 Optimization of Magnetic Bead Flow

The main objective in optimizing the concentration of MB solution, to be used in the proposed LFA layouts, is to ensure that MBs do not physically adsorb on the NC membrane

surface, while providing a sufficiently strong signal when captured at the test line. To achieve a strong colorimetric signal, the number of MBs need to be maximised, albeit the number needs to be small enough to avoid physisorption. Thus, various dilutions of MB stock solution was dispensed on an LFA strip to estimate their optimal concentration. The proposed strip assembly layout, as described in section 3.5, was tested with 100 µl MB solution. 100 µl of PBS rinsing buffer was dispensed to wash off the beads after 10 min, once the MB solution flowed through, followed by capturing of images after 5 minutes.

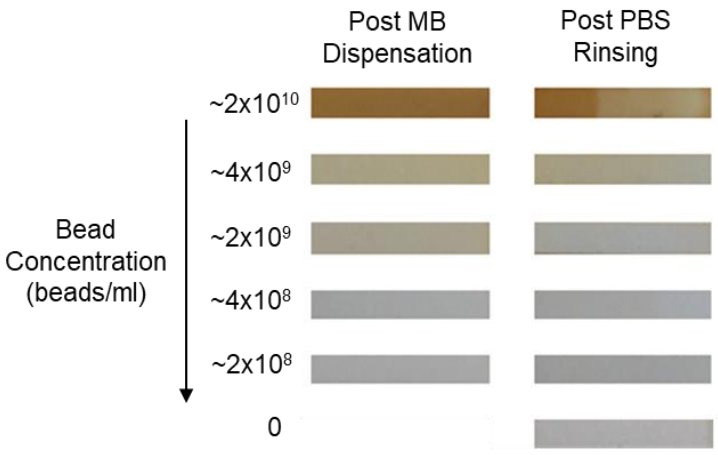

Fig 4.5: Photographs of NC strips showing effect of dispensing varying concentration of MB solutions and subsequent wash off with PBS

Figure 4.5 clearly shows that at high concentration of beads i.e. ≥ ~$2x10^9$ beads/ml, physisorption is high, which can be easily visualised from the brown colouration seen on the NC membranes. This brown colouration seems to disappear upon rinsing with PBS buffer. However, at concentrations levels ≥ ~$4x10^9$ beads/ml, the reduction in colour after rinsing is insignificant. Under optimized conditions, the NC membranes should release almost all of the captured beads upon rinsing with buffer. This behaviour was observed at concentration levels of ~$2x10^9$ beads/ml or lower. Upon rinsing, the strips corresponding to these concentration levels appear identical to the control strip, where no MBs were dispensed (0 beads/ml), but only rinsed with PBS buffer. Therefore, for all subsequent LFA experiments, an MB concentration of not more than ~$2x10^9$ beads/ml was used.

4.3.4 Antibody-Analyte Binding Characteristics

ELISA was performed on both model systems, cTnICT and IGF-1, according to the protocol described in section 3.7.6. ELISA uses HRP labelled antibodies to bind to antigens in a well plate and the subsequent colour change upon substrate addition to identify and/or determine the concentration of an antigen. The capture antibody and recognition antibody concentrations were kept constant, while varying the analyte concentrations to obtain a concentration dependent response plot by acquiring absorbance at 450 nm upon completion of the ELISA protocol. The absorbance values were then normalized prior to plotting.

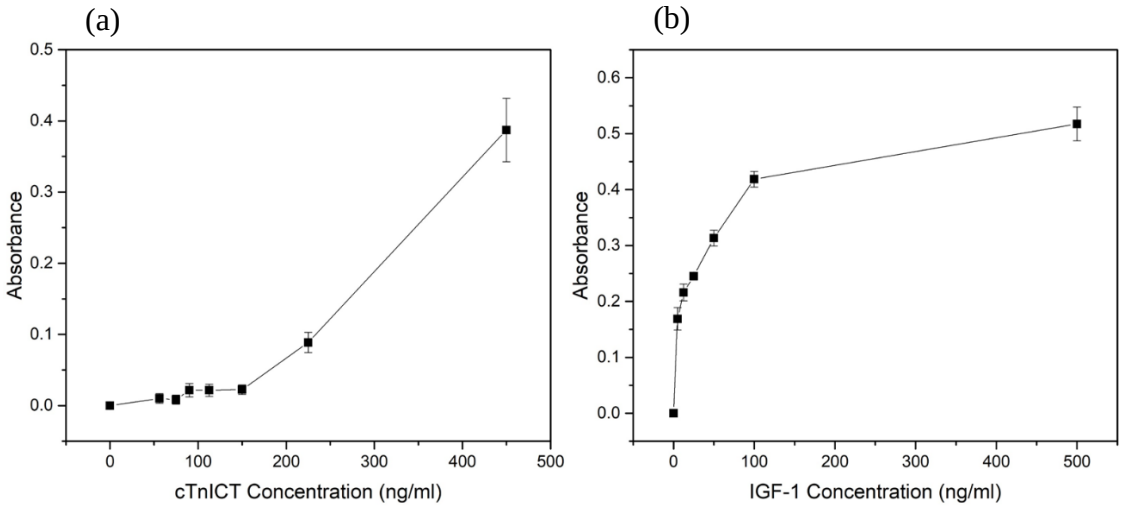

Fig 4.6: ELISA plots showing concentration dependent response of (a) cTnICT and (b) IGF-1

The plots in Fig 4.6 show an increasing trend, which means that as the analyte concentration increases, the signal readout increases. The cTnICT system shows a sharp rise in signal output beyond 200 ng/ml, whereas in case of IGF-1 the signal output starts increasing at much lower concentrations (≥ 10 ng/ml). The trends seen in both the cases validate the antibody-antigen binding and the viability of these model systems for use in LFA. The obtained varying concentration dependent response is an indication of the difference in antibody-analyte affinity of the two systems.

4.4 Conclusion

This chapter lays the foundation of the LFA studies to be conducted in the subsequent chapters. Various parameters associated with the proposed LFA device and their influence on the assay performance have been investigated and optimized to maximise the overall performance of the LFA device. Different potential membranes which can constitute the functional zones of the proposed layouts: the test zone, the absorbent pad and the passivation layer, have been studied. NC membranes with a high degree of protein binding was the most suitable for use in the test zone, cellulose with a very good absorption and wicking behaviour for solutions was the ideal choice for an absorbent pad and the highly porous and hydrophilic GF membranes, which could easily let sample solutions to flow through was the ideal choice for the passivation layer. The functioning of these membranes will be explained in the next chapter. The effect of a blocking agent, BSA, was systematically investigated. The sensitivity of the device is highly dependent on the MB reporters and hence, knowing its physical characteristics such as size and microstructure is essential. This was achieved through DLS and SEM characterisation of the beads. These beads showed an excellent magnetic behaviour, separating from a solution in less than a minute and completely dispersing back with just mild shaking. The optimal concentration of beads was obtained by flowing through different concentrations of MB solution on the LFA strip. Finally, the working and viability of the proposed model systems: cTnICT and IGF-1, were validated by ELISA. The difference in signal readouts, especially at low concentration ranges, implied a difference in the antibody-analyte affinity of the two systems.

References

1. Koczula, K.M. and A. Gallotta, *Lateral flow assays.* Essays In Biochemistry, 2016. **60**(1): p. 111-120.

2. Bahadır, E.B. and M.K. Sezgintürk, *Lateral flow assays: Principles, designs and labels.* TrAC Trends in Analytical Chemistry, 2016. **82**: p. 286-306.

3. Lin, W. and H. Kasamatsu, *On the electrotransfer of polypeptides from gels to nitrocellulose membranes.* Analytical Biochemistry, 1983. **128**(2): p. 302-311.

4. Champion, H.M., J.J. Pierog, and J.E. Peters, *Multiwell membrane filtration apparatus*. 1988, Google Patents.

5. Sharma, A., et al., *Magnetic field assisted preconcentration of biomolecules for lateral flow assaying.* Sensors and Actuators B: Chemical, 2019. **285**: p. 431-437.

6. Sharma, A., et al., *Gold nanoparticle conjugated magnetic beads for extraction and nucleation based signal amplification in lateral flow assaying.* Sensors and Actuators B: Chemical, 2020: p. 127959.

7. Wen, H.-W., et al., *Development of a competitive liposome-based lateral flow assay for the rapid detection of the allergenic peanut protein Ara h1*. Analytical And Bioanalytical Chemistry, 2005. **382**(5): p. 1217-1226.

8. Jones, K., *FUSION 5: a new platform for lateral flow immunoassay tests*, in *Lateral Flow Immunoassay*. 2009, Springer. p. 1-15.

9. St John, A. and C.P. Price, *Existing and emerging technologies for point-of-care testing.* The Clinical Biochemist Reviews, 2014. **35**(3): p. 155.

10. Moyano, A., et al., *Magnetic Lateral Flow Immunoassays.* Diagnostics, 2020. **10**(5): p. 288.

11. Ahmad, A.L., et al., *Synthesis and characterization of polymeric nitrocellulose membranes: Influence of additives and pore formers on the membrane morphology.* Journal Of Applied Polymer Science, 2008. **108**(4): p. 2550-2557.

12. Hubbe, M.A., et al., *Enhanced absorbent products incorporating cellulose and its derivatives: A review*. BioResources, 2013. **8**(4): p. 6556-6629.

13. Makhtar, S.N.N.M., et al., *Preparation and characterization of glass hollow fiber membrane for water purification applications.* Environmental Science and Pollution Research, 2017. **24**(19): p. 15918-15928.

14. Lifesciences), C.P.G.H. *CF-4 Membranes*. [cited 2020 6th June]; Available from: https://www.cytivalifesciences.com/en/us/shop/whatman-laboratory-filtration/whatman-dx-components/flow-through-pads/cf4-p-00786.

15. Hydranautics, *Commercial RO Technology*. 2001.

Chapter 5

Incorporation of Magnetic Field Assisted Sample Pre-treatment with LFA Device

Typically, LFA responses are influenced by the complexity of sample matrices containing analogues or molecules that may potentially yield non-specific responses, for instance, when assaying of biomarkers in blood, serum and plasma. Therefore, isolation of analytes of interest from sample matrices would significantly improve the LFA responses. In this chapter, a magnetic field assisted preconcentration approach for extraction and assaying of cardiac Troponin-I-C-T (cTnICT) complex in an LFA format is discussed. The proposed approach yields pM level limit of detection within 15 min using very low sample volumes (<100 µL), and with possibilities for signal enhancement, therefore offering a promising avenue for sensitive detection of troponin and similar targets in complex matrices at clinically relevant concentration levels without requiring tedious sample pre-treatment protocols.

*This section published substantially as: Sharma, A., et al., *Magnetic field assisted preconcentration of biomolecules for lateral flow assaying.* Sensors and Actuators B: Chemical, 2019. **285**: p. 431-437.

5.1 Introduction

Point-of-care (POC) assaying of biomolecules in complex matrices has attracted significant research interest over the past few decades. LFAs being one of the most promising POC assay formats, has been widely explored for this purpose. However, in clinical applications, LFAs have been limited by two main challenges; sensitivity and specificity, owing to the interferences associated with the complexity of sample matrices such as whole blood [1-3], serum [4, 5] and plasma [6]. Therefore, efforts have been devoted to exploring methodologies such as sample extraction/preconcentration, antifouling surface treatment, use of reporter molecules with improved optical properties and efficient read out strategies in order to overcome the limitations of LFA.

Typical LFA utilizes gold nanoparticles (AuNP) as optical reporters.[7-9] Although AuNPs possess advantages such as good biocompatibility, high surface-to-volume ratio and high intensity signal readouts [9, 10], their colloidal stability in complex matrices often causes an inhibitory effect on the performance of LFAs.[11, 12] Therefore, alternative reporters including composites such as gold-silver [13], gold-iron [14] and gold-graphene oxide [15] have been investigated for sensitive detection of analytes. However, synthesis of these composite materials is cumbersome and often yield a broad distribution of particles with non-homogenous surface areas for conjugation, which significantly influences the performance of the assay. Polystyrene-magnetic beads have been reported for detection of several biomolecules such as proteins and nucleic acids.[16-18] As explained in section 3.1.3.1, these beads are homogenous, stable and bear functional groups that can be modified and effectively conjugated to recognition molecules, such as antibodies and aptamers. Magnetic beads provide an additional advantage of spatial control with application of an external magnetic field, enabling efficient biomolecule extraction from a complex matrix.[18] Studies involving magnetic separation of analyte molecules have shown significant enhancement in sensitivity and specificity of such assays.[19, 20] Most of these assays follow a layout wherein the antibody conjugated magnetic beads are added to a matrix consisting of the analyte and incubated for a certain period of time for antigen-antibody binding, followed by extraction using an external magnetic field. The separated

beads are then re-suspended in a buffer solution (PBS, DI water, etc.) for assaying. This approach, although effective, involves external instrumentation and tedious extraction protocols such as several intermediate centrifugation or vortexing and pipette-based transfers of reagents, which may result in artefacts influencing the assay reproducibility.

This chapter aims to study a facile extraction and assaying approach using polystyrene magnetic beads (MB) under a magnetic field for preconcentration of biomolecule and for subsequent concentration-dependent visual detection of biomolecules. The proposed LFA consists of a backing pad incorporated with a nitrocellulose (NC) membrane and a detachable magnet for preconcentration of target biomolecules. The sample containing the target analyte is added to a vial containing the target specific antibody-conjugated magnetic beads. The assay layout has been represented through a schematic in Fig 3.3 of chapter 3. The magnetic field of the detachable magnet is utilized to retain the magnetic beads on the LFA, enabling preconcentration of the bound analytes. The magnet is then detached from LFA to release the captured magnetic beads once the matrix solution has flown across the test zone on the NC membrane into the absorbent pad. A hydrophilic passivation layer has been evaluated for channelizing the sample matrix solution, and for protecting the test zone from non-specific adsorption of molecules present in complex sample matrices.

Cardiac Troponin I-C-T complex (cTnICT), a biomarker for contractile regulation of cardiac and skeletal muscles, has been used as a model system for validation of the proposed approach.[21] In healthy humans, cTnI levels in blood are in the range of 20-30 pg/ml, whereas it increases rapidly after a heart attack [22, 23], reaching a peak of 190-200 ng/ml after 11 h [23, 24], thus serving as an important marker for diagnosis of acute myocardial infarction (AMI). Currently most LFA devices for colorimetric detection of Troponin mainly rely on tedious sample pre-treatment protocols to achieve the required detection limits, resulting in a long turnaround time for assaying, thereby preventing early diagnosis of AMI. The proposed assay strategy demonstrates a facile approach to isolate target proteins on an LFA membrane for sensitive and specific evaluation of cTnICT concentrations within a short time span and with a clinically relevant visual detection limit (VDL). Moreover, an approach involving protein-A conjugated magnetic beads has been

evaluated for further enhancing the VDL. The simplicity of the proposed approach facilitates point of care assaying of analytes in complex matrices. Another advantage offered by the proposed methodology is the generic approach of the assay, which could be translated for detection of other biomarkers in complex matrices.

5.2 Reagents, Membranes and Apparatus

PBS, BSA (Lyophilized), sodium azide and tween 20 were purchased from Sigma-Aldrich. Troponin I-C-T complex (cTnICT, 100 µg/ml), recognition anti-TnI and capture anti-TnC antibodies were purchased from Hytest Inc. Commercially available superparamagnetic carboxylated polystyrene be (b) 00nm) purchased from Chemicell were used in this study. EDC (1-ethyl-3-[3-dimethylaminopropyl] carbodiimide hydrochloride) and sulfo-NHS (*N*-Hydroxysuccinimide) were purchased from Sigma-Aldrich. PMB of size 1 µm was procured from Thermo Scientific. NC membrane cards (Hi-Flow Plus 75), glass fibre membranes and cellulose absorbent pads were obtained from Merck-Millipore. Images of strips were captured by Sony Alpha a7R III and processed in Sony Imaging Edge Edit RAW software. A permanent neodymium-iron-boron magnet (LifeSep 96F) purchased from Sigma Aldrich was used for the assay. The magnetic strength was measured using an ESCO Tesla/Gauss meter (EA703G-11).

5.3 Results and Discussion

5.3.1 Principle of Assay

An LFA layout incorporating a magnetic field assisted sample preconcentration step has been proposed here to isolate analyte molecules from complex matrices. Carboxylated polystyrene magnetic beads conjugated with anti-TnI monoclonal antibodies were utilized to specifically capture cTnICT. These MB-Ab complexes were used to capture cTnICT from the matrix solution in a vial (Fig 3.3(a)). An incubation time of 10 min was provided to ensure efficient binding between cTnICT and anti-TnI Ab to form MB-Ab-cTnICT complexes. It should be emphasized that the number of conjugated antibodies available for

binding were maintained in excess to the typical cTnICT levels in clinical samples, in order to ensure that no free cTnICT remains in the sample solution.

The solution containing the MB-Ab-cTnICT complexes, when transferred to the LFA strip, starts flowing along the NC membrane. However, the magnetic field in the sample injection area induced by a magnet retains the MB-Ab-cTnICT complex, enabling isolation of the bound cTnICT from the matrix on the LFA membrane. A glass fiber membrane was evaluated as a passivation layer to channelize the matrix solution and to protect the test line comprising of pre-immobilized anti-TnC antibodies from non-specific adsorption of the sample matrix components. The passivation layer shown in Fig 3.3(b and c), channelizes the flow of matrix solution, owing to it superior hydrophilicity as compared to that of the NC membrane, thereby minimizing exposure of the sample matrix to the test line. To release the MB-Ab-cTnICT complexes, the magnet was detached, and an assay buffer was added on the strip to facilitate the flow. The passivation layer was simultaneously peeled off to reveal the test line for capturing the MB-Ab-cTnICT complexes using the immobilized anti-TnC antibodies. A characteristic brownish band was observed on the test line for samples containing cTnICT and the intensity of the band correlated with cTnICT concentrations. Qualitative analysis was then carried out by visual observation of the band intensity, followed by a quantitative analysis using ImageJ for ascertaining the visual estimation of cTnICT concentrations.

5.3.2 Effect of Magnetic Field on the Flow of Magnetic Beads

Magnetic fields of different strengths were applied on the LFA strip to evaluate the retaining efficiency of the magnetic beads. The strength of the applied magnetic field was controlled by adjusting the distance between the strip and the magnet (Fig 5.1(a)) and the magnetic field strength was measured using a Gauss meter. As illustrated in Fig 5.1(b), a dark brownish coloration of NC membrane was observed near the sample injection area in the presence of a magnetic field, which is due to capture and accumulation of magnetic beads. However, the beads could not be released upon removal of magnet, which is attributed to extensive penetration of the beads into the NC membrane owing to the

magnetic attraction. For instance, magnetic field with strengths of 200 mT (strip placed directly on the magnet) (Fig 5.1(b)) and 100 mT (corresponding to 3 mm distance between magnet and the strip) (Fig 5.1(c)) lead to significant adhesion of beads to the NC membrane. In this case, a lesser number of beads flow through to reach the test line leading to formation of band with low intensity. On the other hand, if the magnetic field is too weak, almost all the beads flow through due to insufficient retaining of magnetic beads in sample injection area, inhibiting isolation of the analyte from the sample matrix. This was visualized on the strip where a 20 mT field strength was applied, that corresponded to a distance of 9 mm between the strip and magnet (Fig 5.1(e)). A distance of 6 mm between the strip and the magnet yielded an optimized magnetic field of ~ 40 mT (Fig 5.1(d)) for retaining and release of beads in the presence and absence of magnetic field, respectively. At this optimized magnetic field, the magnetic beads are retained near the surface and when assisted by a liquid medium they flow through towards the test line, without significant adhesion onto the NC membrane, upon removal of magnetic field.

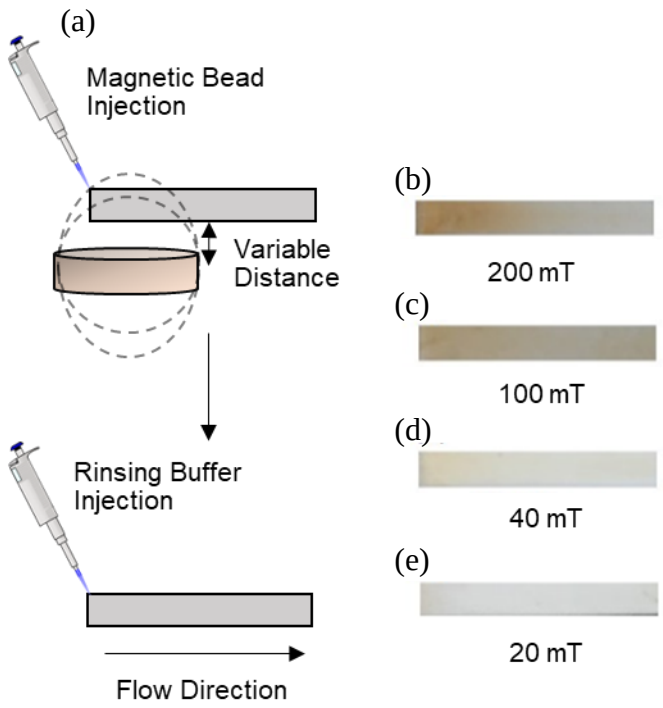

Fig 5.1: (a) Schematic NC strip before flowing MB-Ab complexes and the approach adopted for controlling the magnetic field strength. (b)-(e) Photographs of NC strips showing effect of varying magnetic field strength on the flow of MB-Ab complexes

5.3.3 Antibody-Magnetic Bead Conjugation

The MB-Ab conjugation efficiency was studied by a BCA analysis of the Ab supernatant post its incubation with carboxyl activated MBs and its extraction from the reaction vial (MB-Ab binding protocol described in section 3.2.1 of Chapter 3). Fig 5.2(b) shows the antibody concentration in the reaction vial before and after the incubation with MBs, which has been calculated using the equation of standard BCA plot obtained in Fig 5.2(a). The amount of antibodies conjugated to the MB is predominantly controlled by the availability of free carboxyl groups on the surface and is inversely proportional to the amount of antibodies left in the supernatant. Upon subtracting the number of antibodies in the supernatant post-incubation from the pre-incubation solution of antibodies, it is observed that ~25.2 µg of antibodies could be conjugated per 125 µg of MB (~5 µl of stock solution).

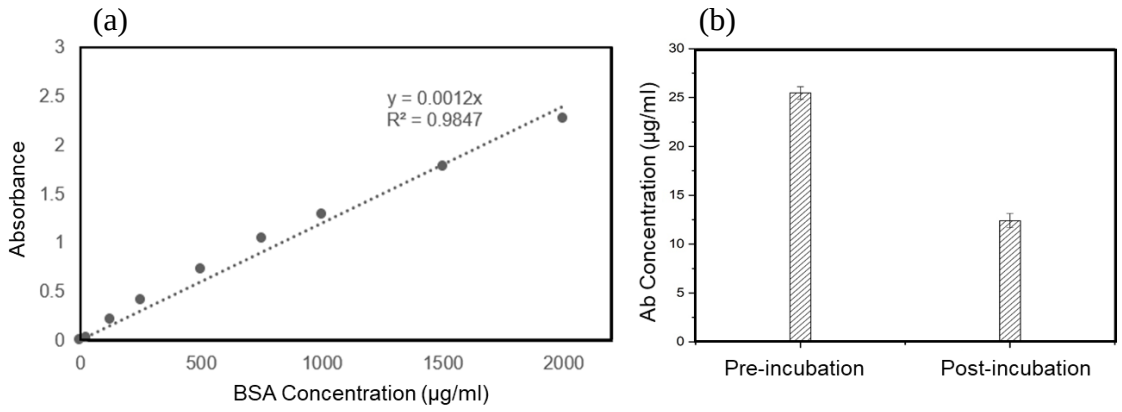

Fig 5.2: (a) BCA standard plot for calculation of antibody concentration; and (b) Bar graph showing pre-incubation antibody concentration in reaction vial and post-incubation antibody concentration left in supernatant after MB extraction.

5.3.4 Assay Performance

5.3.4.1 Assay in Buffer and Plasma without Passivation Layer

Figure 5.4(a-b) show the test bands obtained for different concentration of cTnICT in buffer and in 10x diluted plasma, without the use of the passivation layer, respectively. A sample volume of 100 µl was necessary for obtaining a distinct band. Once the sample matrix solution reaches the absorbent pad, another 100 µl of PBS was added as a rinsing buffer to release the MB complexes from the sample injection area (magnet removed). The signal read out was observed at a fixed time frame of 15 min after adding PBS. A test band was visually observed for assay in PBS, at a concentration ≥ 1 ng/ml, which was considered as the VDL, without involving any instrumentation for analysis. In the absence of cTnICT, no band was observed at the test line, showing minimal non-specific adsorption of the MB-Ab complexes (without bound cTnICT) on the test line.

For the assay in 10x diluted plasma, experimental parameters such as the sample and rinsing volumes were the same as that of assay in buffer. Visual observation for bands at cTnICT concentrations between 0 and 1000 ng/ml illustrates that the LFA responses in 10x

diluted plasma correlate with that of responses obtained using the buffer solution. Fig 5.3(b) shows a dark band for 10x diluted plasma spiked with 1000 ng/ml of cTnICT. As the cTnICT concentration decreases, the bands become less observable and below 100 ng/ml, the band could not be observed by naked eye, indicating a VDL of 100 ng/ml for assay in 10x diluted plasma samples.

5.3.4.2 Influence of Passivation Layer

The 100 ng/ml VDL obtained in plasma is significantly higher than the 1 ng/ml VDL obtained in PBS and could be attributed to interferences present in the matrix solution. Interferences such as dissolved proteins, clotting factors, electrolytes, etc., in plasma could inhibit the binding of MB-Ab-cTnICT complexes to the anti-TnC antibodies deposited on test line. This inhibitory effect can be reduced significantly if the interaction of the matrix solution with the test line antibodies is minimized. Thus, a hydrophilic passivation layer was incorporated with the proposed assay to channelize the flow of matrix solution over the test line. Glass fiber membrane was used as a passivation layer in this study. The hydrophilic nature of the membrane enables channelization of flow of sample matrix, thus protecting the capturing antibodies in the test line. Figure 5.3(c-d) illustrate the LFA responses in buffer and 10x plasma, respectively, with the passivation layer. It is evident that the band for 1 ng/ml cTnICT in buffer is more distinct in the presence of a passivation layer compared to the band obtained without the passivation layer (Fig 5.3(a)). The influence of passivation layer is best visualized for the assay in 10x diluted plasma (Fig 5.3(d)). A band is visually observed for 10 ng/ml, unlike the responses without the passivation layer (Fig 5.3(b)), where a band was visually observed only up to 100 ng/ml.

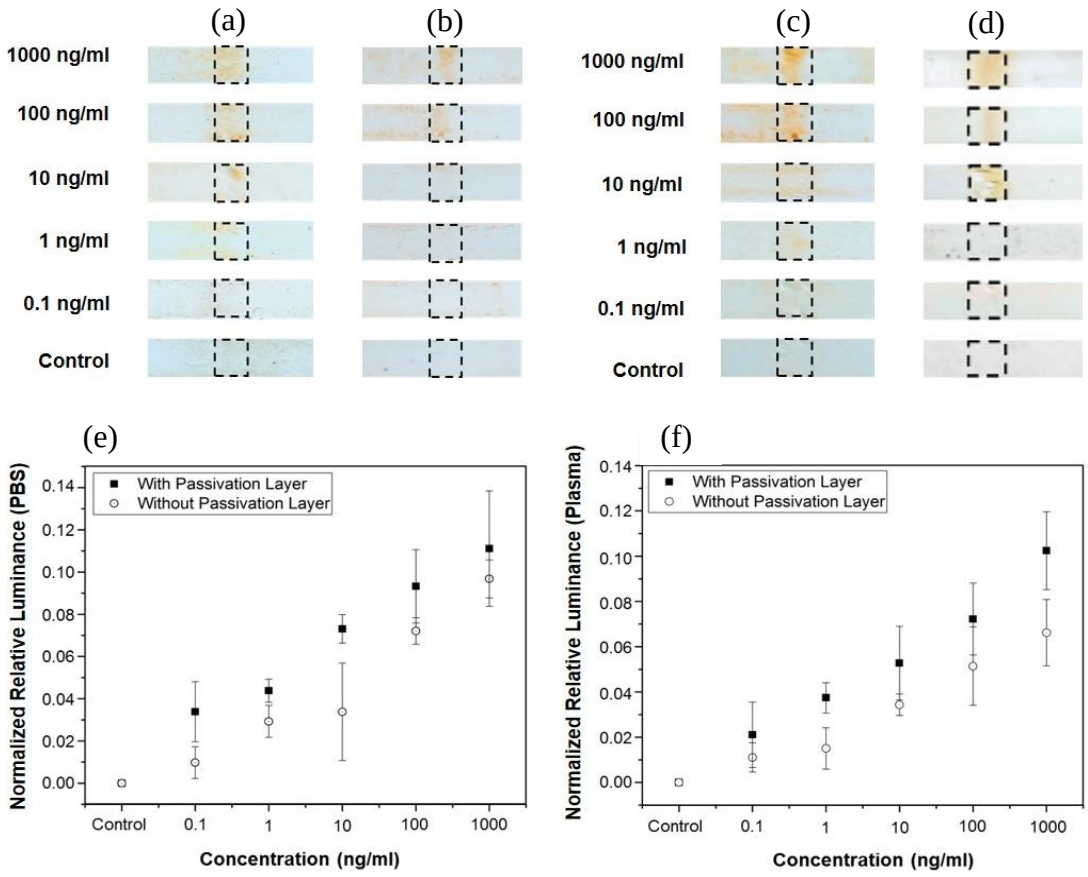

Fig 5.3: Photographs of NC membranes showing the test bands for assay without passivation layer in buffer (a) and 10x diluted plasma (b); and with passivation layer in buffer (c) and 10x diluted plasma (d), respectively. Quantification of colour intensities via measurement of normalized relative luminance of test bands for assay in buffer (e) and 10x diluted plasma (f). Here, "Control" refers to absence of cTnICT in sample matrix. Relative luminance has been calculated with respect to the control.

5.3.4.3 Calibration Curves in Buffer and 10x Plasma

Calibration curves between 0 and 1000 ng/ml (Fig. 5.4 (e-f)) were plotted for all the assay configurations (Fig 5.3(a-d)) using the normalized relative luminance values obtained via image analysis using ImageJ software. The luminance value is a weighted average of the red, blue and green components of an image and it is inversely proportional to the intensity of the band.[25] Thus, the band at 1000 ng/ml being the darkest in coloration, yield the lowest luminance and highest relative luminance, whereas, band that are difficult to visualize with naked eye (for instance, 1 ng/ml), yield a higher luminance value and a lower

relative luminance. As observed from Fig 5.3(e) and 5.4(f), concentration dependent normalized relative luminance responses are obtained for cTnICT, which correlate well with the visual observations for all the assay configurations, illustrating that quantification of cTnICT concentrations is feasible by the proposed methodology. The effect of the passivation layer in buffer and 10x plasma also can be seen in the normalized relative luminance read outs. For all test concentrations, the normalized relative luminance value increases upon incorporation of passivation layer as compared to the read outs without the passivation layer (Fig 5.3(e-f). This observation suggests that interferences from plasma, that affect the binding ability of MB-Ab-cTnICT complexes to the antibodies deposited on the test line, are significantly reduced by employing a glass fiber passivation layer.

5.3.4.4 Signal Enhancement Approach

A signal enhancement approach based on PMB was explored to enhance the sensitivity of the assay. Protein-A can bind to the recognition antibodies (anti-TnI) attached to the MBs captured on the test line, thus, allowing localization of PMBs at the test line. The aggregate of beads (PMBs and MBs) at the test line would be helpful to visualize low concentrations, whereby lesser amount of MBs are captured at the test line. As observed from Fig 5.4(a), the bands obtained upon assaying appear darker after treatment with PMB complexes. In case of assay in PBS, a band is observed at a cTnICT concentration of 0.1 ng/ml, implying that the VDL could be improved up to 10-fold. In case of assay in plasma, the band corresponding to 1 ng/ml is visible upon PMB treatment, thus improving the VDL to 1 ng/ml in plasma. These results correlate with the normalized relative luminance plot, which shows an increase in normalized relative luminance values at all concentrations of cTnICT. (Fig. 5.5(b)) However, the relative luminance at 0.1 ng/ml of plasma concentration is still quite low to be visually identifiable in the form of a band. The absence of any band at low plasma concentrations and the control strip indicates that PMB complexes do not adsorb on test line nor bind to the anti-TnC antibodies immobilized along the test line.

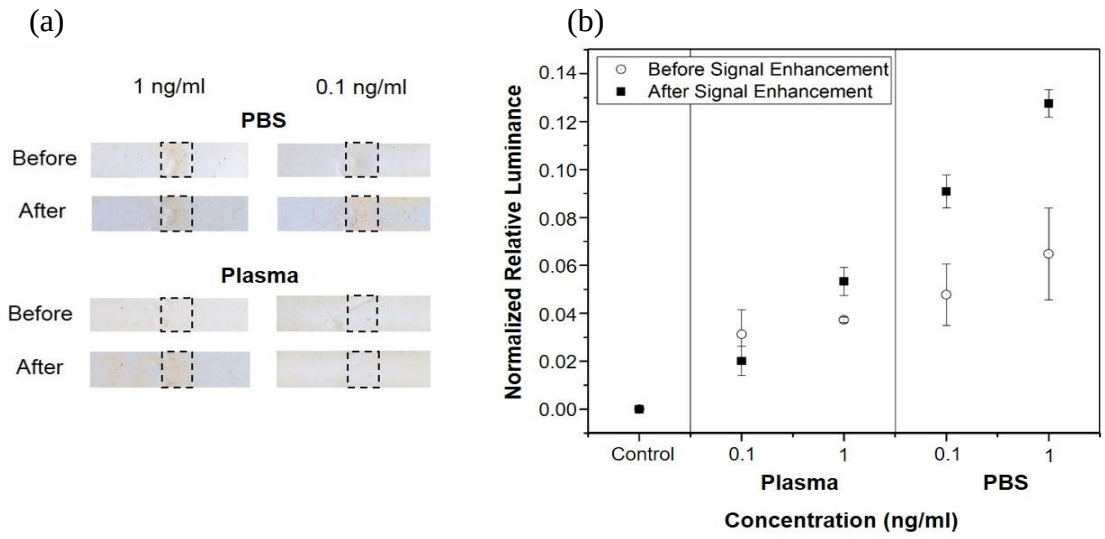

Fig 5.4: (a) Comparison of strips before and after signal enhancement, in PBS and 10x plasma. (b) Normalized relative luminance plot before and after signal enhancement. Here, "Control" corresponds to absence of cTnICT in sample matrix.

5.3.4.5 Benchmarking against Reported cTnICT Colorimetric LFA

As illustrated in Table 5.1, other colorimetric LFA assays have been reported with better sensitivities by employing optical and enzymatic signal enhancement protocols. For example, signal enhancement approaches using a secondary Au nanoparticle have been reported to yield good sensitivities.[26, 27] Apart from nanoparticles, enzymatic assays using HRP have also been reported to be sensitive.[28] Although these methods are sensitive, they require either cumbersome particle synthesis or tedious LFA fabrication protocols [36, 38] with elaborate signal enhancement approaches.[26]

Taken together, the proposed methodology of using magnetic beads as optical reporters is facile and cost effective as it requires neither signal enhancement nor sample pre-treatment to reach clinically relevant concentration ranges in complex matrices such as plasma. In addition, it should be noted that the proposed methodology demonstrates assaying in plasma (Table 5.1), which is a more complicated matrix than serum that is utilized in most of the existing approaches with better LODs.

Table 5.1: Performance characteristics of colorimetric LFAs for Cardiac Troponin

Matrix	Label	Assay Time	LOD	Pros	Cons
Serum	Dual AuNP	10 min	0.01 ng/ml [26]	Sensitive Demonstrated efficacy in clinical samples	Elaborate synthesis and LFA fabrication protocols Requirement of additional reagents for signal amplification
	Dual AuNP	15 min	1 ng/l [27]	Sensitive Multiplexed detection	Elaborate synthesis and LFA fabrication protocols
	AuNP	20 min	0.24 ng/ml [29]	Sensitive	Complex device fabrication
	HRP	20 min	0.027 ng/ml [28]	Sensitive	Requirement of reagents for signal amplification
Plasma	MB	15 min	10 ng/ml [This work]	Facile fabrication Cost effective, minimal reagents required	Further optimisations needed to improve sensitivity
Plasma (with signal enhancement)		25 min	1 ng/ml [This work]	Sensitive Facile fabrication	Requirement of additional reagents for signal amplification

5.3.4.6 Limitations and Scope for Improvement

Although the proposed approach enables assaying at clinically relevant levels, further optimizations are required to achieve a lower VDL in plasma samples, given than 10x diluted plasma has been utilized as a proof of concept in this study. The addition of a signal enhancement step is feasible, but this approach influences the complexity, leading to an increased overall cost and turnaround time for assaying. This may also limit its applicability for point of care (POC) assaying. Hence, there is a need for making the assay more competitive, without compromising the assay performance. Exploration of composite materials as reporters is a feasible approach for sensitivity enhancement, which constitutes the work in the next chapter of this thesis. Moreover, the uniformity and intensity of bands can be improved by immobilization of the test line antibodies using an LFA dispenser. Uniformity in test line, optimization of the MB complex-protein concentrations and

binding protocols as well as novel composite materials can provide an avenue for further improving the detection limits of the proposed LFA strategy.

5.4 Conclusions

In this chapter, an approach to incorporate extraction and assaying of a model target protein (cTnICT) on an LFA strip has been studied. The LFA layout comprised of an external magnet that assisted in capturing of anti-TnI antibody conjugated magnetic bead complexes. The effect of varying magnetic fields on the capture and release of these bead complexes on the strip was studied and optimized. The binding capacity of the capturing antibodies in the test zone was preserved by the use of a hydrophilic passivation layer that protected the test zone by channelizing the flow of sample matrix. The layout was tested against cTnICT spiked in PBS as well as 10x diluted plasma. The VDLs achieved were 1 ng/ml and 10 ng/ml in buffer and 10x plasma, respectively before signal enhancement, which meets the requirement for clinical assaying of cTnICT. A 10-fold improvement of VDL to 0.1 ng/ml and 1 ng/ml in buffer and 10x plasma, respectively, after signal enhancement by subsequent exposure of Protein A modified magnetic beads to the test line was demonstrated. The proposed methodology could serve as a facile and appealing alternative to the current LFA schemes and as an approach towards the development of an LFA device that does not require tedious sample pre-treatment protocols. Furthermore, the generic approach of the proposed methodology allows translation to detect several other relevant biomolecules of interest.

References

1. Schramm, E.C., et al., *A quantitative lateral flow assay to detect complement activation in blood.* Analytical Biochemistry, 2015. **477**: p. 78-85.

2. Chan, C.P.Y., et al., *Development of a quantitative lateral-flow assay for rapid detection of fatty acid-binding protein.* Journal of Immunological Methods, 2003. **279**(1-2): p. 91-100.

3. Ang, S.H., et al., *Quantitative, single-step dual measurement of hemoglobin A1c and total hemoglobin in human whole blood using a gold sandwich immunochromatographic assay for personalized medicine.* Biosensors & Bioelectronics, 2016. **78**: p. 187-193.

4. Corstjens, P.L.A.M., et al., *Lateral flow assay for simultaneous detection of cellular- and humoral immune responses.* Clinical Biochemistry, 2011. **44**(14-15): p. 1241-1246.

5. Magambo, K.A., et al., *Utility of urine and serum lateral flow assays to determine the prevalence and predictors of cryptococcal antigenemia in HIV-positive outpatients beginning antiretroviral therapy in Mwanza, Tanzania.* J Int AIDS Soc, 2014. **17**: p. 19040.

6. Schramm, E.C., et al., *A quantitative lateral flow assay to detect complement activation in blood.* Anal Biochem, 2015. **477**: p. 78-85.

7. Rong-Hwa, S., et al., *Gold nanoparticle-based lateral flow assay for detection of staphylococcal enterotoxin B.* Food Chemistry, 2010. **118**(2): p. 462-466.

8. Rivas, L., et al., *Improving sensitivity of gold nanoparticle-based lateral flow assays by using wax-printed pillars as delay barriers of microfluidics.* Lab on a Chip, 2014. **14**(22): p. 4406-4414.

9. Choi, D.H., et al., *A dual gold nanoparticle conjugate-based lateral flow assay (LFA) method for the analysis of troponin I.* Biosensors & Bioelectronics, 2010. **25**(8): p. 1999-2002.

10. Delmulle, B.S., et al., *Development of an immunoassay-based lateral flow dipstick for the rapid detection of aflatoxin B1 in pig feed.* J Agric Food Chem, 2005. **53**(9): p. 3364-8.

11. Wang, A.W., et al., *Gold Nanoparticles: Synthesis, Stability Test, and Application for the Rice Growth.* Journal of Nanomaterials, 2014.

12. Makhsin, S.R., et al., *The effects of size and synthesis methods of gold nanoparticle-conjugated MαHIgG4 for use in an immunochromatographic strip test to detect brugian filariasis.* Nanotechnology, 2012. **23**(49): p. 495719.

13. Gao, Z.Q., et al., *High-Resolution Colorimetric Assay for Rapid Visual Readout of Phosphatase Activity Based on Gold/Silver Core/Shell Nanorod.* ACS Applied Materials & Interfaces, 2014. **6**(20): p. 18243-18250.

14. Liang, C.-H., et al., *Iron oxide/gold core/shell nanoparticles for ultrasensitive detection of carbohydrate− protein interactions.* Analytical Chemistry, 2009. **81**(18): p. 7750-7756.

15. Kim, T.-H., K.-B. Lee, and J.-W. Choi, *3D graphene oxide-encapsulated gold nanoparticles to detect neural stem cell differentiation.* Biomaterials, 2013. **34**(34): p. 8660-8670.

16. Paleček, E. and M. Fojta, *Magnetic beads as versatile tools for electrochemical DNA and protein biosensing.* Talanta, 2007. **74**(3): p. 276-290.

17. Tang, D., et al., *Multiplexed electrochemical immunoassay of biomarkers using metal sulfide quantum dot nanolabels and trifunctionalized magnetic beads.* Biosensors and Bioelectronics, 2013. **46**: p. 37-43.

18. Berensmeier, S., *Magnetic particles for the separation and purification of nucleic acids.* Applied Microbiology And Biotechnology, 2006. **73**(3): p. 495-504.

19. Huang, Y., et al., *Magnetized carbon nanotubes for visual detection of proteins directly in whole blood.* Analytica Chimica Acta, 2017. **993**: p. 79-86.

20. Olsvik, O., et al., *Magnetic separation techniques in diagnostic microbiology.* Clinical Microbiology Reviews, 1994. **7**(1): p. 43-54.

21. Katrukha, I.A., *Human cardiac troponin complex. Structure and functions.* Biochemistry (Mosc), 2013. **78**(13): p. 1447-65.

22. Bertinchant, J.P., et al., *Diagnostic value of human cardiac troponin I assay in acute myocardial infarction.* Archives Des Maladies Du Coeur Et Des Vaisseaux, 1996. **89**(1): p. 63-68.

23. Xu, Q.F., et al., *Development of lateral flow immunoassay system based on superparamagnetic nanobeads as labels for rapid quantitative detection of cardiac*

troponin I. Materials Science & Engineering C-Biomimetic and Supramolecular Systems, 2009. **29**(3): p. 702-707.

24. Bodor, G.S., et al., *Development of Monoclonal-Antibodies for an Assay of Cardiac Troponin-I and Preliminary-Results in Suspected Cases of Myocardial-Infarction.* Clinical Chemistry, 1992. **38**(11): p. 2203-2214.

25. Bezryadin, S., P. Bourov, and D. Ilinih. *Brightness calculation in digital image processing*. in *International symposium on technologies for digital photo fulfillment*. 2007. Society for Imaging Science and Technology.

26. Choi, D.H., et al., *A dual gold nanoparticle conjugate-based lateral flow assay (LFA) method for the analysis of troponin I.* Biosensors and Bioelectronics, 2010. **25**(8): p. 1999-2002.

27. Zhu, J., et al., *Simultaneous detection of high-sensitivity cardiac troponin I and myoglobin by modified sandwich lateral flow immunoassay: proof of principle.* Clinical Chemistry, 2011: p. clinchem. 2011.171694.

28. Cho, I.-H., et al., *Chemiluminometric enzyme-linked immunosorbent assays (ELISA)-on-a-chip biosensor based on cross-flow chromatography.* Analytica Chimica Acta, 2009. **632**(2): p. 247-255.

29. Kim, W., S. Lee, and S. Jeon, *Enhanced sensitivity of lateral flow immunoassays by using water-soluble nanofibers and silver-enhancement reactions.* Sensors and Actuators B: Chemical, 2018. **273**: p. 1323-1327.

Chapter 6

Sample Extraction and Nucleation Based Signal Amplification in Lateral Flow Assaying Using Gold Nanoparticle Conjugated Magnetic Bead Reporters

In this chapter, an approach utilising a gold nanoparticle conjugated magnetic beads (GMB) in LFAs for extraction and sensitive visual assaying of proteins has been studied. To validate this approach GMB, conjugated with anti-Troponin I antibodies, is used to capture cardiac marker Troponin I-C-T (cTnICT) in plasma that subsequently flows through on LFA membrane via a test zone containing anti-Troponin C antibodies. The capture of cTnICT-GMB complexes at the test zone produces a characteristic brownish band, enabling concentration dependent visual detection of cTnICT. Subsequently, contrast of these bands is enhanced by a nucleation approach that utilizes the gold nanoparticles on GMB in the test bands as seed materials for growth of more visible gold clusters, improving visual detection limit of the assay. This assay offers a promising avenue for sensitive detection of analytes in complex matrices at clinically relevant concentrations without requiring tedious sample pre-treatment protocols.

---

*This section published substantially as: Sharma, A., et al., *Gold nanoparticle conjugated magnetic beads for extraction and nucleation based signal amplification in lateral flow assaying.* Sensors and Actuators B: Chemical, 2020: p. 127959.

6.1. Introduction

Over the past few decades, various lateral flow assays (LFA) have been reported for POC assaying. Sample solutions, when flown over LFAs, activate the dried reagents contained within the LFA membranes and emanate qualitative signals that can be subsequently quantified.[1, 2] Typical LFAs that make use of visual readouts as signals are widely reported for POC applications.[3, 4] Additionally, LFAs are easy to fabricate and do not require sophisticated instrumentation, which make such devices cost effective and facile to use.[5, 6] However, the use of LFA for clinical applications has been limited by two main challenges; sensitivity and specificity [7], mainly owing to the interferences associated with the complexity of sample matrices such as whole blood [8, 9], serum [10] or plasma [8]. Therefore, efforts have been devoted to improve performance of such assays by adopting sample extraction or preconcentration protocols for removal of analogues and interferents present in complex matrices that may yield false positives.[6, 11, 12]

Polystyrene magnetic beads (MB) have been utilized for extraction of target biomolecules such as proteins or nucleic acids from complex matrices.[13-15] These MBs are homogeneous, stable in suspension and have been utilized as reporters for detection of several biomolecules.[13, 16, 17] However, most of the existing reports monitor the magnetic flux variations of MBs for sensitive detection of analytes, which involve the use of sophisticated instrumentation, thereby inhibiting their applicability for POC assays. On the other hand, a sensitive optical reporter for naked eye detection, widely used in LFAs, is colloidal gold nanoparticles (AuNPs).[18-20] Although AuNPs have several advantages such as good biocompatibility and high surface-to-volume ratio, they do not possess extraction capabilities as compared to MBs for analyte preconcentration. Moreover, at low concentrations, the optical signal strengths emanated by AuNPs are weak and hence they are often engineered to provide signal amplification in LFAs. Amplification strategies such as silver amplification [21, 22], dual gold conjugation [23] and use of gold aggregates [24] have been explored. However, most of these approaches involve complicated synthesis protocols and are prone to aggregation and formation of large clusters, thereby compromising the assay performance.

Recently composite reporters comprising of magnetic particles and AuNPs have been reported for detection of biomolecules.[25-27] Such composites, with combined properties of AuNPs and magnetic particles, possess dual functionality in assaying that enable analyte preconcentration and also serve as optical reporters for visual detection. These composite reporters have been shown to possess high mechanical stability and excellent magnetic properties for efficient target analyte isolation in homogeneous assays.[27, 28] Co-precipitation [28] is the commonly adopted approach for synthesis of these composites, however, their heterogeneous size distribution and lack of long term stability limit their applicability for on-site assaying. Therefore, alternative synthesis protocols such as chemical bonding [27] and use of an intermediate layer [29] have been explored. The applications of these composites in LFA is limited mainly by the weak optical signal strengths that does not yield visual responses, especially at low analyte concentrations. Furthermore, most of the existing reports rely on qualitative responses and require instrumentation for achieving competitive limits of detection (LODs). Hence, there is a need to evaluate strategies to improve the performance of composite reporters for application in LFAs.

In this chapter, an LFA approach based on sample extraction, assaying and signal amplification using gold nanoparticle conjugated MB (GMB) composites as reporters for visual detection of cTnICT has been studied. cTnICT, as explained in the previous chapters, is an important biomarker for contractile regulation of cardiac and skeletal muscles; and serves as an important biomarker for early diagnosis of acute myocardial infarction (AMI).[30] cTnI levels in a healthy human blood is in the range of 20-30 pg/ml, whereas it increases rapidly after a heart attack [31, 32], peaking to the range of 190-200 ng/ml after ~11 h [32, 33]. MBs are conjugated with AuNPs via linker molecules, for subsequent conjugation with anti-TnI antibodies (anti-TnI). These anti-TnI antibody conjugated GMBs are then used to capture target analyte (cTnICT) in a sample matrix, followed by extraction from the matrix, prior assay using a LFA strip. The proposed approach further emphasizes on a signal amplification protocol, wherein the gold nanoparticles of the GMB reporters are utilized as seed materials. The growth of gold clusters on AuNPs improves the contrast of the test band, yielding a significant

improvement in the visual read-out and thereby improving the visual detection limit (VDL) by approximately 10-fold. The proposed nucleation-based signal amplification methodology is facile and an effective approach for achieving competitive LODs. Unlike typical nanoparticle based signal amplification approaches that may compromise assay performance due to uncontrolled migration of large complexes on LFA membranes,[23, 24] the proposed strategy utilizes the nanoparticles that are already captured on the test line, yielding a reproducible 10 fold signal amplification within 5 min. Optimization of parameters such as the volume of the nucleation reagent resulted in a VDL of 0.1 ng/ml of cTnICT in both buffer and plasma, post signal amplification. The proposed assay serves to provide a sensitive and specific detection of cTnICT in a complex matrix such as plasma, with a total assay time of ~20 min, inclusive of nucleation-based amplification. Furthermore, the proposed assay is facile and has a generic approach for POC assaying of other biomolecules in complex matrices.

6.2 Reagents, Membranes and Apparatus

10 nm AuNPs colloidal solution, cysteamine, Tris (2-carboxyethyl) phosphine *(*TCEP), chloroauric acid ($HAuCl_4.xH2O$), hydroxylamine hydrochloride ($NH_2OH.HCl$), PBS (pH 7.4), BSA (Lyophilized), sodium azide and tween 20 were purchased from Sigma-Aldrich. Troponin I-C-T (cTnICT, 100 µg/ml), recognition antibody: anti-Troponin I (anti-TnI), and capture antibody: anti-Troponin C (anti-TnC), were purchased from Hytest Inc. Commercially available superparamagnetic carboxylated polystyrene beads (200 nm) purchased from Chemicell were used in this study. EDC (1-ethyl-3-[3-dimethylaminopropyl] carbodiimide hydrochloride) and sulfo-NHS (*N*-Hydroxysuccinimide) were purchased from Sigma-Aldrich. NC membrane cards (Hi-Flow Plus 135), glass fibre membranes and cellulose absorbent pads were obtained from Merck-Millipore. Images of strips were captured using a Sony Alpha a7R III digital camera and were processed by Sony Imaging Edge Edit RAW software.

6.3 Results and Discussion

6.3.1 Principle of Assay

The proposed assay comprises of a facile sample pre-treatment protocol and a novel nucleation-based approach for signal amplification using a composite GMB reporter. The GMB is prepared by conjugating commercially available MB with AuNPs using cysteamine linker molecules. The sample preconcentration is based on efficient analyte extraction owing to the specific binding between cTnICT and monoclonal anti-TnI antibodies conjugated with the synthesized GMB. Upon addition of sample to Ab-GMB solution, an incubation time of 15 min was provided to ensure efficient binding between cTnICT and Ab-GMB. The concentration of GMB conjugated capture antibodies were maintained in excess of typical cTnICT analytical concentrations in order to maximize the capturing of cTnICT in the sample solution. After binding, the cTnICT-Ab-GMB complexes were separated from the sample matrix using a magnetic rack followed by rinsing and resuspension in PBS, Fig 3.4(a) of chapter 3. The prepared sample solution would then be free of the interferents associated with the plasma matrix.

The sample, when introduced on the NC membrane, starts flowing downstream to reach the absorbent pad. [1, 7]. NC membrane of a low porosity (Merck 135NC) was utilized in this study to ensure a controlled flow of the sample solution over the test band, thereby providing sufficient time for cTnICT-Ab-GMB complexes to react at the test line. In order to prevent non-specific binding of proteins on the membrane surface, the strips were blocked with 1% BSA in PBS [1, 15, 20].The capture of cTnICT-Ab-GMB by anti-TnC antibody at test line led to formation of a dark brown band, with an intensity that could be correlated to the concentration of cTnICT in the sample matrix. The control experiments without cTnICT did not yield a band at the test line. Qualitative analysis was then carried out by visual observation of the band intensity, followed by a quantitative analysis using ImageJ for ascertaining the cTnICT concentrations estimated visually.

6.3.2 Optimization of GMB Synthesis Protocol

6.3.2.1 Optimization of Gold Nanoparticle and Linker Concentration

The GMB was synthesized by linking carboxylated polystyrene magnetic beads (200 nm) with gold nanoparticles (10 nm) using cysteamine linkers. Cysteamine solution was incubated with 5 mM TCEP solution for 10 min to inhibit the formation of cysteamine disulfide bonds. The carboxyl group on the MB could be activated by EDC-NHS treatment for conjugation with the amine group of the cysteamine linkers. Subsequently, thiolated MBs could be easily conjugated with AuNPs via Au-thiol linkage.[34] The number of AuNPs used in the synthesis is maintained 100 times in excess of the MB to ensure sufficient access of AuNPs for an optimal binding to the MBs. In order to minimize the physisorption of AuNPs on MB surface, a surfactant (tween-20) was introduced into the reaction vial. The amount of tween-20 was optimized by checking physisorption of AuNPs on non-activated MB. An increased binding of AuNPs on MB surface would imply a lower concentration of AuNPs in the supernatant with a lower optical density (OD). The supernatant was obtained by extracting the AuNPs-MB complexes from the reaction vial. As illustrated in the absorption spectra (Fig 6.1(a)), a tween-20 concentration of 0.1% yielded an overlapping absorption spectrum with that of AuNPs solution prior incubation with MBs. Therefore, 0.1% tween-20 was chosen as the optimal concentration for the synthesis process as no physisorption was observed at or above this concentration.

The absorption spectra of post incubation supernatants, shown in Fig 6.1(b), further revealed that that an increasing linker concentration led to an increased amount of AuNPs conjugation with the MBs. However, this increment of AuNP conjugation onto the MBs approached a saturation beyond a threshold cysteamine concentration, indicating that no more activated carboxyl groups were available for binding with cysteamine. A high amount of cysteamine, for instance, 100 µM (Fig 6.1(b)), would imply that an increasing amount of the activated carboxyl groups on MB surface is replaced with thiols. This would allow for more AuNPs to bind to MB, thus lowering the concentration of free AuNPs in the supernatant, yielding a lower (OD). Conversely, lesser amount of cysteamine, for instance,

1 µM (Fig 6.1(b)), revealed limited binding of AuNPs on MB surface and a higher AuNPs concentration in the supernatant with a higher OD. This hypothesis is in agreement with the obtained absorption spectra, where conjugation between AuNPs and MBs at 1 µM cysteamine concentration yielded a supernatant solution with an OD of 0.3, whereas an OD of 0.24 is observed for 100 µM cysteamine linker concentration. Based on these observations, an intermediate concentration of 30 µM cysteamine, showing an OD of 0.27, was used for the conjugation of AuNPs with MBs. This intermediate concertation would ensure that there are optimal number of thiol groups on the surface to provide an efficient AuNPs conjugation with MBs and at the same time, a sufficient number of activated carboxyl groups are available for subsequent conjugation with anti-TnI-antibody via EDC/NHS linkage.

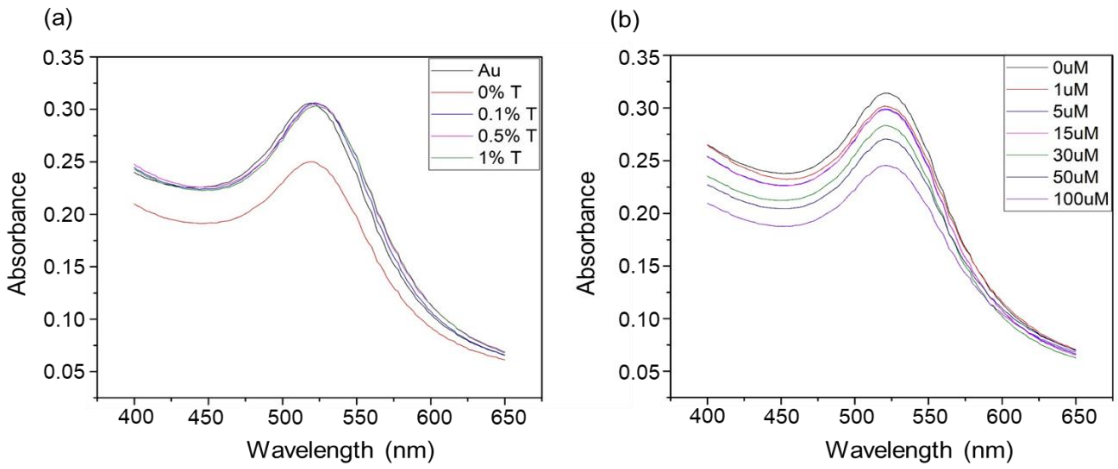

Fig 6.1: Absorption spectra of supernatant solutions upon magnetic separation of AuNPs-MB complexes for; (a) different tween 20 concentrations and (b) varying cysteamine concentrations.

Subsequently, the synthesized GMB was conjugated to anti-TnI antibody by using free carboxyl groups on the GMB surface after the MB-AuNPs conjugation. Antibody conjugation efficiency of the GMBs was then evaluated for varying cysteamine linker concentrations by a BCA analysis. It could be observed that the amount of antibodies conjugated to the GMB is predominantly controlled by the availability of free carboxyl groups after MB conjugation with AuNPs via cysteamine linker molecules. A lower

amount of cysteamine would imply lesser AuNPs conjugation and a higher availability of carboxyl groups for antibody binding, whereas high cysteamine linker concentration implies lower availability of carboxyl groups and hence lower Ab binding. A cysteamine linker concentration of 30 µM yielded ~9 µg of antibodies per 125 µg of beads, whereas 5 µM cysteamine yielded ~15 µg of antibodies per 125 µg of beads (Fig 6.2(b)). Although, the amount of antibody conjugated was lower for 30 µM cysteamine linker, the higher amount of conjugated AuNPs could yield improved contrast upon signal amplification via nucleation. Therefore, cysteamine concentration has been optimized to accommodate both gold nanoparticles and antibodies in appropriate stoichiometric ratios so that: 1. there are enough AuNPs on MB surface to provide effective signal enhancement post nucleation and, 2. there are sufficient conjugated antibodies to effectively bind even trace amounts of analytes from sample solution.

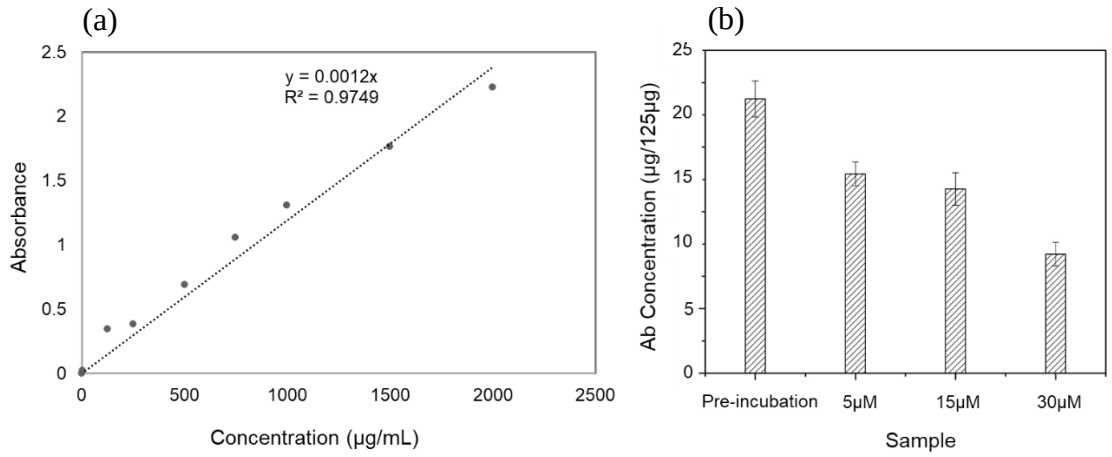

Fig 6.2: (a) BCA standard plot for calculation of antibody concentration; and (b) Bar graph showing pre-incubation antibody concentration in reaction vial and post-incubation antibody concentration left in supernatant after GMB extraction, corresponding to various cysteamine concentrations.

6.3.2.2 Nucleation in Solution State

The phenomenon of nucleation is first evaluated in solution state by adding 10 µL of nucleation reagent to 500 µL of the synthesized GMB (5x diluted in PBS). The AuNPs present on the surface of GMB acts as seed material on which gold salt reduces in the presence of a reducing agent.[35, 36] This leads to the formation of gold clusters on the

GMB and thereby to an increase in overall size of the composite, Fig 3.4(d) of chapter 3. This effect offers an increase in contrast due to a higher optical signal strength emanated by the gold clusters on the surface of the GMB. Figure 6.4(b) shows that the colour intensities of the vials marginally increase before addition of the nucleation reagents. However, upon addition of the nucleation reagents, the vials corresponding to higher cysteamine amounts appear darker, as observed from Fig 6.3(c). This observation could be attributed to the presence of higher amounts of gold in the GMB, which facilitates growth of gold clusters, as the cysteamine amount increases. It should be noted that post nucleation, no noticeable difference occurs in the vials with only MB and without cysteamine (Fig 6.3(b-c)). In the absence of AuNPs, the nucleation behaviour of the composite is not observed as the nucleation process is suppressed without a seed material. Thus, within the observed time frame, gold clusters are not formed on MB surface and hence no significant variation in the colour intensity of the vial without cysteamine was observed. This observation is further verified by plotting luminance values of the different vials, obtained using ImageJ. It could be observed from Fig 6.3(a) that there are no significant variations in the luminance values (below 10 units of luminance values) of MBs and 0 μM vials, indicating almost no gold cluster formation on MBs without AuNPs post nucleation, whereas, larger changes in luminance values (25 and above) are noticed for all the other vials with varying concentration of cysteamine linkers. The decrease in luminance post nucleation implies darkening of the solution due to formation of gold clusters on the seed AuNPs. As the concentration of cysteamine increases, a larger decrease in luminance is observed further indicating that gold clusters formation is proportional to concentration of AuNPs on the MBs. Since this nucleation behaviour requires the presence of AuNPs and MBs, it could be envisioned to amplify LFA responses upon capturing GMB on the test band. The darkening of GMB would enable visual differentiation of the colour of the test bands, especially at low analyte concentrations.

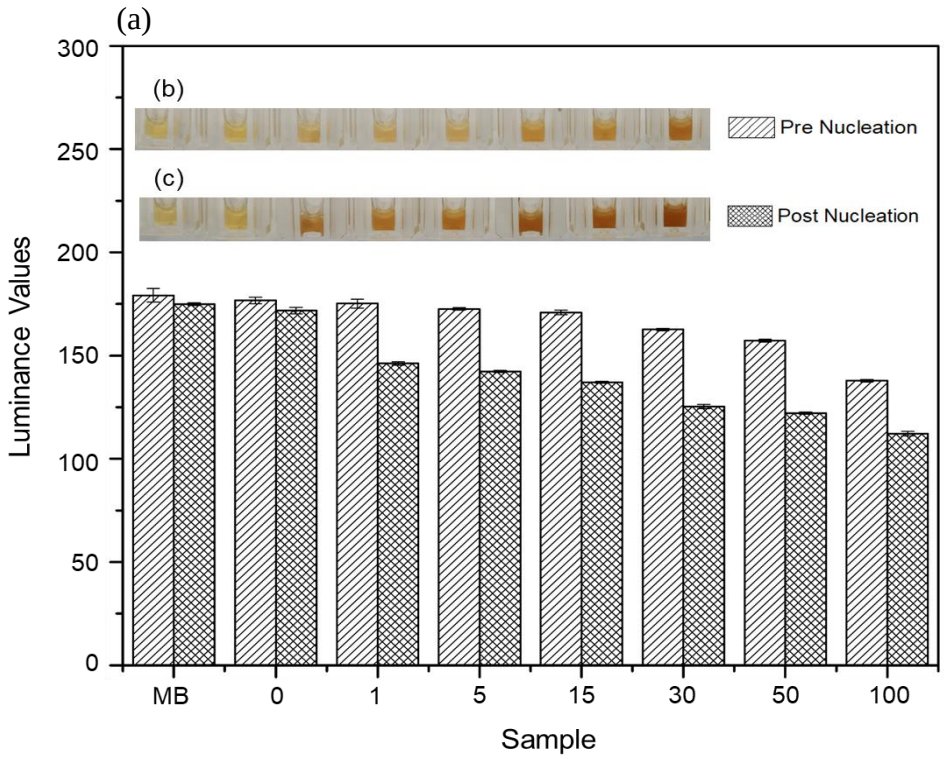

Fig 6.3: (a) Bar graph showing luminance values corresponding to vials in (b)-(c). Lower luminance implies darker colour in the vial. Inset images: (b) GMB with varying cysteamine concentrations. (c) GMB, 5 minutes after addition of nucleation reagents. From left to right (concentration of cysteamine in µM): MB, 0, 1, 5, 15, 30, 50, 100.

6.3.2.3 Study of GMB Construct

The synthesized GMB using 30 µM cysteamine linker concentration was characterized using DLS, SEM and EDX to observe its topographical properties and size distribution. Naked eye observation suggested that the GMBs were homogenous in distribution. DLS data, shown in Fig 6.4, revealed that the peak corresponding to 200 nm of MB shifts to around 240 nm after conjugation with AuNPs. A marginal increase from 0.1 to 0.3, in the PDI is observed as AuNPs is conjugated to MB, indicating a change in the size distribution.

Post-nucleation, upon formation of clusters of AuNPs, the hydrodynamic radius increases further to around 440 nm. The presence of multiple peaks in the solution containing nucleated GMB illustrates the formation of gold clusters of varying sizes with a PDI of ~0.8.

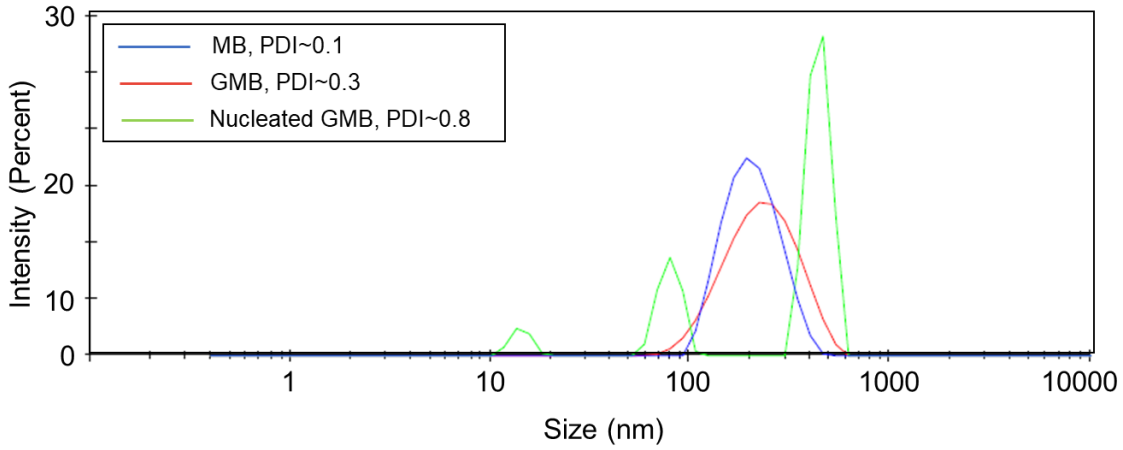

Fig 6.4: DLS plots of MB, GMB and nucleated GMB

SEM was performed as described in section 3.7.1 of chapter 3. The beads (MB, GMB and nucleated GMB), when dried on a quartz surface tend to aggregate. However, in order to show the morphology and approximate size of the beads, isolated particles were selected for imaging. Fig 6.5 (a) shows the MBs dried on quartz surface. The MB diameters could be estimated to be around 200 nm, in agreement with the DLS data shown in Fig 6.4. Upon conjugation with AuNPs, no significant variations on particle diameters were observed (Fig 6.5 (b)), however clustering of AuNPs around the MB core could be seen. Post-nucleation on GMB, the size increases significantly, as evident from Fig 6.5 (c). The successful formation of GMB was also confirmed using EDX analysis, whereby Au characteristic peaks were observed as shown in Fig 6.5 (d).

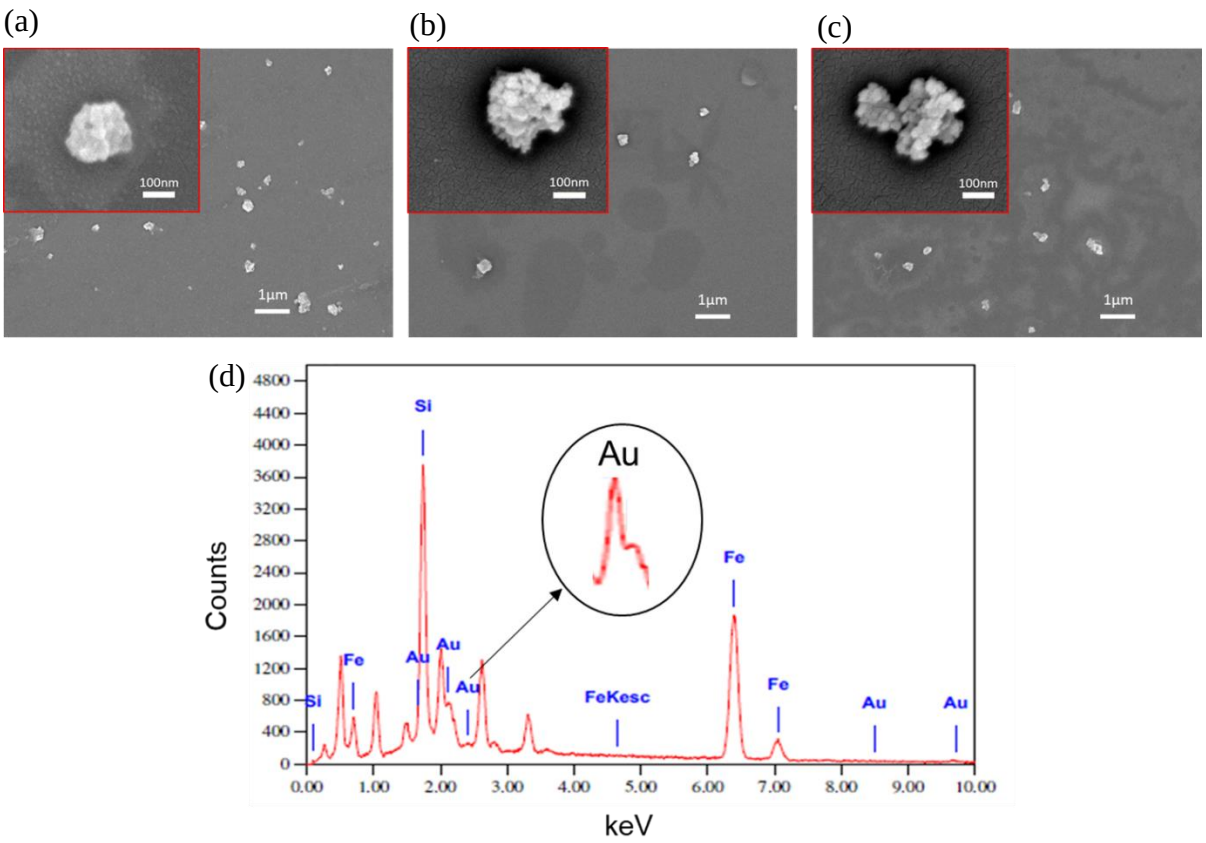

Fig 6.5: SEM images of (a) MB, (b) GMB and (c) Nucleated GMB. Inset images (red boxes) show individual construct of the particles; (d) EDX scan of GMB

6.3.3 Assay Performance

6.3.3.1 Assay Performance in Buffer and Plasma

The test bands obtained, before nucleation, for different concentrations of cTnICT are shown in insets of Fig 6.6 (a) and (b) for buffer and plasma, respectively. A sample volume of 100 µL was used to achieve a sufficiently distinct band. The images were recorded after 15 min upon sample introduction. Test bands were visually observed at cTnICT concentrations ≥ 0.1ng/ml in case of assay in PBS (Fig 6(a) left inset), whereas in case of plasma, test bands were observed at cTnICT concentrations ≥1 ng/ml (Fig 6(b) left inset). These concentration levels were considered as the VDLs in respective matrices below which no distinct test band could be observed without using any instrumentation for

analysis. No band was observed in case of the control experiment without cTnICT. The response for the control strip further indicated minimal non-specific adsorption of the Ab-GMB complexes on the test line. Although, the concentration dependent responses of the test strips could be observed visually, the contrast of the test bands can be improved with further optimizations, such as in capture antibody immobilization, GMB synthesis etc.

6.3.3.2 Effect of Nucleation based Signal Amplification

Upon recording assay responses, signal amplification was performed to improve the contrast of the test bands. 5 µL of the nucleation reagent was found to be sufficient to provide significant nucleation of gold on Au containing GMB that are captured on the test line. The responses were recorded for analysis after 5 min from the addition of nucleation reagent. Formation of gold clusters enhances the size of GMB (refer go Fig. 6.5 and 6.6), yielding a composite that appear darker in colour, thus significantly improving the visual contrast of the test band. This phenomenon, as observed in right insets of Fig 6.6 (a-b), yielded test bands that are more distinct for visual assaying, especially at lower concentrations, where the bands are not visible prior amplification. It can be observed from Fig 6.6 (a) that post the amplification step, the band corresponding to a concentration ≥0.1 ng/ml in the PBS became more intense, indicating that the contrast of the test bands were significantly improved.

In case of plasma, the experimental parameters were the same as that of assay in PBS. Similar to responses in PBS, amplification was observed where the test bands appeared darker in colour and showed a correlation between 0 and 1000 ng/ml (right inset of Fig 6.6 (b)). However, a test band appeared at a cTnICT concentration ≥0.1 ng/ml, illustrating a 10-fold improvement of the VDL with respect to pre-nucleation. It is evident from Fig 6.6 (b) that below 0.1 ng/ml, the test bands were not visually observable. The higher VDL in case of plasma prior signal amplification, when compared to PBS, could be due to the residual interferences present in plasma such as electrolytes, clotting factors, dissolved proteins etc., even after magnetic separation, which could inhibit the binding of cTnICT-Ab-GMB onto the test line anti-TnC antibodies. It is to be emphasized that this additional

nucleation step for signal amplification, with an addition of 5 min to the overall assay time, did not involve migration of any larger complexes, a concern that compromises the assay performance in typical nanoparticle based amplification approaches. Although the NC strips are blocked with BSA, some inevitable residual physisorption of GMB during the assay lead to marginal variations in coloration of the strips, especially after nucleation. Furthermore, the nucleation-based amplification is a remarkably facile approach consisting of only two steps; introduction of the nucleation reagent on the test band followed by rinsing with the buffer solution.

The proposed layout does not require a control line because the bulk of GMB accumulates at the interface between NC test strip and absorbent pad forming a brownish band as well as a light brownish patch over the absorbent pad (see dashed box in Fig 6.6 inset), thus indicating that the magnetic beads are successfully migrating over the test band and that the assay is working. Furthermore, the obtained concentration dependent responses at the test line ascertains proper functionalisation of the GMB.

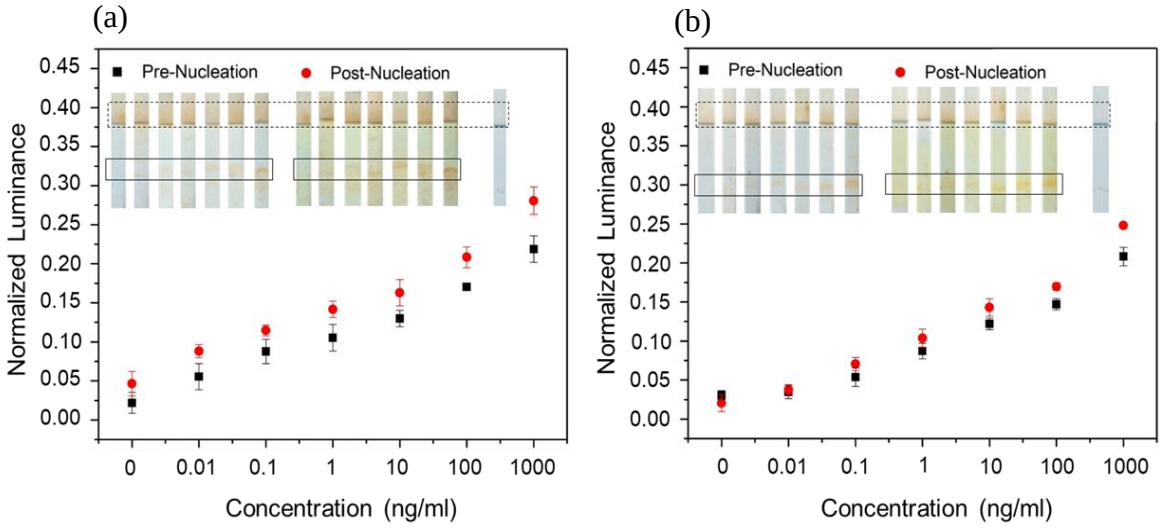

Fig 6.6: Quantification of colour intensities via measurement of normalized relative luminance of test bands for assay in (a) buffer and (b) plasma. Normalized relative luminance was measured with respect to reference LFA strip. Inset images: photographs of LFA strips showing the test bands (within solid box) and the control patches (within dashed box) for assay before nucleation (left) and after nucleation (right). From left to right: 0 ng/ml, 0.01 ng/ml, 0.1 ng/ml, 1 ng/ml, 10 ng/ml, 100 ng/ml, 1000 ng/ml, reference LFA strip without GMB flow.

6.3.3.3 Calibration Curves

Figure 6.6 (a-b) show the calibration curves for cTnICT concentrations between 0 and 1000 ng/ml, plotted for both assay matrices. These curves were plotted using the normalized relative luminance values obtained via image analysis using ImageJ software. The luminance readouts for various cTnICT concentrations correlate well with the visual observations. The concentration dependent responses illustrated in the calibration curves indicate that the proposed approach can be used for quantification of analyte concentrations. The relative luminance values increase after nucleation of gold (Fig 6.6 (a-b)), indicating that the bands are of higher visual contrasts. Furthermore, the improvement of the VDL as quantified by the calibration curves, supports the efficacy of the proposed assay and signal amplification approach.

6.3.3.4 Benchmarking against Reported cTnICT Colorimetric LFA

Most of the colorimetric assays reported for Troponin have utilized signal amplification protocols. Dual gold amplification, making use of two different sizes of gold nanoparticles was first reported by Choi et.al.[20] with an LOD of 0.01 ng/ml. Similar efforts have been undertaken in several follow up studies.[37] Although good LODs have been obtained, these approaches involve complicated synthesis protocol and tedious LFA fabrication processes. More importantly, since only AuNPs have been used as reporters in these studies, facile sample preconcentration is not possible. Kim et.al reported an LOD of 0.24 ng/ml using silver amplification of AuNPs reporters.[22] However, the fabrication and use of electrospun fibres in their LFA strip increases the complexity of LFA fabrication and the overall cost of the assay. Other strategies such as enzyme based amplification using HRP was reported by Cho et.al with an LOD of 0.027 ng/ml.[38] All of these studies have reported LODs in serum. In this work, we have reported a VDL of 0.1 ng/ml in plasma, which is a more complicated matrix as compared to serum (due to the presence of additional components such as fibrinogen etc.). However, the proposed approach ensures facile extraction and preconcentration of analytes from matrices even at extremely low amounts of target analytes. Furthermore, the LFA device fabrication is facile and cost

effective. Moreover, the proposed signal amplification protocol does not involve migration of large complexes as it utilizes the captured GMB on the test line, thereby yielding reproducible responses.

6.3.3.5 Limitations and Scope for Improvement

The proposed approach is an illustration of a possibility for the development of sensitive and specific LFAs. The achieved VDL in a complex matrix such as plasma is not just clinically relevant but also competitive. Although the use of a dual functional reporter can aid sample pre-treatment as well as signal amplification, additional steps of nucleation may increase overall cost of the assay. Therefore, exploring approach for incorporating signal amplification step within the current assay platform could be a possible solution. One possible direction could involve incorporation of a pad that elutes the nucleation reagent into the LFA membrane. Moreover, the bands obtained could be made more uniform and intense by use of a lateral flow dispenser to deposit the test line antibodies, rather than manual deposition. Additionally, optimization of the Ab-GMB synthesis protocols to provide a better size control without compromising the antibody binding efficiency, could provide an avenue for further improving the detection limits of the proposed assay. Size control also could ensure that the beads flow uniformly and the physical adsorption on the membrane surface is minimized.

6.4 Conclusion

In this chapter, a GMB reporter-based approach has been studied for extraction and assaying of Troponin in complex matrix. A facile nucleation-based signal amplification strategy for applications in LFA is further demonstrated. cTnICT was used as a model target analyte and the assay was carried out in both PBS and plasma. The approach captures cTnICT from a sample matrix using anti-TnI antibody conjugated GMB, followed by its extraction and assaying on an LFA strip consisting of anti-TnC antibody for capturing the analyte-antibody-GMB complexes. The signal amplification was carried out using a nucleation reagent consisting of a gold salt and a reducing agent. The effect of this

nucleation reagent on the synthesized GMP was studied in solution state, before optimizing the process parameters for the LFA. A VDL of 0.1 ng/ml was achieved in plasma, post signal amplification, which is a 10-fold improvement as compared to LFA results without signal amplification (Chapter 5). The achieved VDL easily meets the requirement for clinically relevant assaying of cTnICT and at least 10 times better than the reported visual LODs of assays involving magnetic beads for assaying in complex matrices.[15, 39] The proposed methodology provides a signal amplification strategy using a dual-functional composite reporter molecule, thus providing an appealing alternative to the existing LFA strategies. The signal amplification is easy to perform, does not involve migration of large complexes and yields reproducible responses. Moreover, facile device fabrication makes this LFA cost effective. The proposed assay possesses the potential to enable sensitive and specific detection of cTnICT with a total assay time of ~20 min. Furthermore, the assay has a generic approach enabling facile translation of the proposed methodology to detect several other relevant biomolecules of interest in complex matrices such as whole blood.

References

1. Koczula, K.M. and A. Gallotta, *Lateral flow assays.* Essays In Biochemistry, 2016. **60**(1): p. 111-120.

2. You, D.J., T. San Park, and J.-Y. Yoon, *Cell-phone-based measurement of TSH using Mie scatter optimized lateral flow assays.* Biosensors and Bioelectronics, 2013. **40**(1): p. 180-185.

3. Quesada-González, D. and A. Merkoçi, *Nanoparticle-based lateral flow biosensors.* Biosensors and Bioelectronics, 2015. **73**: p. 47-63.

4. Yoo, S.M. and S.Y. Lee, *Optical biosensors for the detection of pathogenic microorganisms.* Trends In Biotechnology, 2016. **34**(1): p. 7-25.

5. Li, Z., et al., *Rapid and sensitive detection of protein biomarker using a portable fluorescence biosensor based on quantum dots and a lateral flow test strip.* Analytical Chemistry, 2010. **82**(16): p. 7008-7014.

6. Sajid, M., A.-N. Kawde, and M. Daud, *Designs, formats and applications of lateral flow assay: A literature review.* Journal of Saudi Chemical Society, 2015. **19**(6): p. 689-705.

7. Posthuma-Trumpie, G.A., J. Korf, and A. van Amerongen, *Lateral flow (immuno) assay: its strengths, weaknesses, opportunities and threats. A literature survey.* Analytical And Bioanalytical Chemistry, 2009. **393**(2): p. 569-582.

8. Schramm, E.C., et al., *A quantitative lateral flow assay to detect complement activation in blood.* Analytical Biochemistry, 2015. **477**: p. 78-85.

9. Chan, C.P., et al., *Development of a quantitative lateral-flow assay for rapid detection of fatty acid-binding protein.* Journal Of Immunological Methods, 2003. **279**(1-2): p. 91-100.

10. Corstjens, P.L., et al., *Lateral flow assay for simultaneous detection of cellular-and humoral immune responses.* Clinical Biochemistry, 2011. **44**(14-15): p. 1241-1246.

11. van Dam, G.J., et al., *A robust dry reagent lateral flow assay for diagnosis of active schistosomiasis by detection of Schistosoma circulating anodic antigen.* Experimental Parasitology, 2013. **135**(2): p. 274-282.

12. Corstjens, P.L., et al., *Up-converting phosphor technology-based lateral flow assay for detection of Schistosoma circulating anodic antigen in serum.* Journal Of Clinical Microbiology, 2008. **46**(1): p. 171-176.

13. Berensmeier, S., *Magnetic particles for the separation and purification of nucleic acids.* Applied Microbiology And Biotechnology, 2006. **73**(3): p. 495-504.

14. Shikida, M., et al., *Using wettability and interfacial tension to handle droplets of magnetic beads in a micro-chemical-analysis system.* Sensors and Actuators B: Chemical, 2006. **113**(1): p. 563-569.

15. Sharma, A., et al., *Magnetic field assisted preconcentration of biomolecules for lateral flow assaying.* Sensors and Actuators B: Chemical, 2019. **285**: p. 431-437.

16. Paleček, E. and M. Fojta, *Magnetic beads as versatile tools for electrochemical DNA and protein biosensing.* Talanta, 2007. **74**(3): p. 276-290.

17. Tang, D., et al., *Multiplexed electrochemical immunoassay of biomarkers using metal sulfide quantum dot nanolabels and trifunctionalized magnetic beads.* Biosensors And Bioelectronics, 2013. **46**: p. 37-43.

18. Rong-Hwa, S., et al., *Gold nanoparticle-based lateral flow assay for detection of staphylococcal enterotoxin B.* Food Chemistry, 2010. **118**(2): p. 462-466.

19. Rivas, L., et al., *Improving sensitivity of gold nanoparticle-based lateral flow assays by using wax-printed pillars as delay barriers of microfluidics.* Lab on a Chip, 2014. **14**(22): p. 4406-4414.

20. Choi, D.H., et al., *A dual gold nanoparticle conjugate-based lateral flow assay (LFA) method for the analysis of troponin I.* Biosensors and Bioelectronics, 2010. **25**(8): p. 1999-2002.

21. Ye, H. and X. Xia, *Enhancing the sensitivity of colorimetric lateral flow assay (CLFA) through signal amplification techniques.* Journal of Materials Chemistry B, 2018. **6**(44): p. 7102-7111.

22. Kim, W., S. Lee, and S. Jeon, *Enhanced sensitivity of lateral flow immunoassays by using water-soluble nanofibers and silver-enhancement reactions.* Sensors and Actuators B: Chemical, 2018. **273**: p. 1323-1327.

23. Xu, Q., et al., *Development of lateral flow immunoassay system based on superparamagnetic nanobeads as labels for rapid quantitative detection of cardiac troponin I.* Materials Science and Engineering: C, 2009. **29**(3): p. 702-707.

24. Hu, J., et al., *Oligonucleotide-linked gold nanoparticle aggregates for enhanced sensitivity in lateral flow assays.* Lab on a Chip, 2013. **13**(22): p. 4352-4357.

25. Fan, A., C. Lau, and J. Lu, *Colloidal gold–polystyrene bead hybrid for chemiluminescent detection of sequence-specific DNA.* Analyst, 2008. **133**(2): p. 219-225.

26. Silva, S.M., et al., *Gold coated magnetic nanoparticles: from preparation to surface modification for analytical and biomedical applications.* Chemical Communications, 2016. **52**(48): p. 7528-7540.

27. Bao, J., et al., *Bifunctional Au-Fe3O4 nanoparticles for protein separation.* ACS Nano, 2007. **1**(4): p. 293-298.

28. Karamipour, S., M. Sadjadi, and N. Farhadyar, *Fabrication and spectroscopic studies of folic acid-conjugated Fe3O4@ Au core–shell for targeted drug delivery application.* Spectrochimica Acta Part A: Molecular and Biomolecular Spectroscopy, 2015. **148**: p. 146-155.

29. Luo, Z., et al., *Fluorescent aptasensor for antibiotic detection using magnetic bead composites coated with gold nanoparticles and a nicking enzyme.* Analytica Chimica Acta, 2017. **984**: p. 177-184.

30. Katrukha, I.A., *Human cardiac troponin complex. Structure and functions.* Biochemistry (Mosc), 2013. **78**(13): p. 1447-65.

31. Bertinchant, J.P., et al., *Diagnostic value of human cardiac troponin I assay in acute myocardial infarction.* Archives Des Maladies Du Coeur Et Des Vaisseaux, 1996. **89**(1): p. 63-68.

32. Xu, Q.F., et al., *Development of lateral flow immunoassay system based on superparamagnetic nanobeads as labels for rapid quantitative detection of cardiac troponin I.* Materials Science & Engineering C-Biomimetic and Supramolecular Systems, 2009. **29**(3): p. 702-707.

33. Bodor, G.S., et al., *Development of Monoclonal-Antibodies for an Assay of Cardiac Troponin-I and Preliminary-Results in Suspected Cases of Myocardial-Infarction.* Clinical Chemistry, 1992. **38**(11): p. 2203-2214.

34. Pensa, E., et al., *The chemistry of the sulfur–gold interface: in search of a unified model.* Accounts Of Chemical Research, 2012. **45**(8): p. 1183-1192.

35. Shi, W., et al., *Gold nanoshells on polystyrene cores for control of surface plasmon resonance.* Langmuir, 2005. **21**(4): p. 1610-1617.

36. Sung, Y.J., et al., *Novel antibody/gold nanoparticle/magnetic nanoparticle nanocomposites for immunomagnetic separation and rapid colorimetric detection of Staphylococcus aureus in milk.* Biosensors and Bioelectronics, 2013. **43**: p. 432-439.

37. Zhu, J., et al., *Simultaneous detection of high-sensitivity cardiac troponin I and myoglobin by modified sandwich lateral flow immunoassay: proof of principle.* Clinical Chemistry, 2011: P. Clinchem. 2011.171694.

38. Cho, I.-H., et al., *Chemiluminometric enzyme-linked immunosorbent assays (ELISA)-on-a-chip biosensor based on cross-flow chromatography.* Analytica Chimica Acta, 2009. **632**(2): p. 247-255.

39. Moyano, A., et al., *Magnetic Lateral Flow Immunoassays.* Diagnostics, 2020. **10**(5): p. 288.

Chapter 7

Proof-of-Concept LFAs for Detection of Sports Markers: IGF-1 and IL-8

In this chapter, proof of concept LFAs have been demonstrated for assaying of sports markers using two model systems: Insulin like Growth Factor-1 (IGF-1) and Interlukin-8 (IL-8). IGF-1 is a prohibited substance for athletes and serves as a biomarker for GH, whereas IL-8 is a well-known inflammation mediator and stress marker in athletes. The LFA strategies developed in Chapter 5 and 6 have been adapted for assaying IGF-1 using anti-IGF-1 antibodies. The feasibility of utilizing affimers as recognition molecules also has been investigated to assay IL-8 on an LFA strip, with an intention of replacing antibodies for development of a more robust assay. The preliminary results are promising for both systems and therefore lay the foundation for a robust and sensitive LFA for on-site detection of various sports markers.

7.1 Introduction

As explained in the earlier chapters, one of the biggest challenges in POC testing of physiological markers is the interference from the components of a complex matrix. For example, blood is a relatively viscous liquid containing various cells, proteins such as albumins and clotting factors. Plasma and serum also have a similar composition as blood but are devoid of the cells. Sweat and urine consist of various salts and enzymes, which can easily mask trace levels of analytes. The problems associated with these complex matrices become even more prominent while detecting the various sports related biomarkers, which includes the prohibited substances as well. Most physiological markers associated to doping are present in trace quantities and even a slight change in their levels can make a difference between testing positive or negative for doping.[1-3] As a result, sample pre-treatment becomes extremely important for testing any such substances. Therefore, the LFA layouts developed in chapter 5 and 6 become even more relevant in this context, demonstrating an efficient detection strategy for trace levels of analytes without complicated sample pre-treatment protocols.

IGF-1 has been classified as a prohibited substance by WADA due to its anabolic effects.[4] IGF-1 also serves as a biomarker for GH doping, as its physiological levels in the blood stream elevates upon GH intake.[5] The first set of results in this chapter deals with translating the developed LFA strategies to detect IGF-1. IGF-1 antibodies have been used to fabricate a sandwich LFA in the same manner as described in the previous chapters. Preliminary results show a promising concentration dependent response, yielding a VDL of 1 µg/ml using strategy 1, which utilizes MB reporters and a VDL of 0.1 µg /ml post signal amplification using strategy 2, which utilizes GMB reporters.

As already mentioned, these strategies incorporate antibodies as capture and recognition biomolecules. However, antibodies have several limitations, the most important being long term stability.[6, 7] A robust LFA requires a mechanism, which does not deteriorate with time. In resource limited settings, proper storage facilities may not be available, which may affect the performance of an LFA in the long run. Therefore, researchers have studied

various alternative recognition molecules to replace antibodies in LFAs.[8-10] Affimer, which is a small protein similar to antibodies but with several advantages over them, is one such viable alternative. Affimers have come to light very recently and have not yet been fully explored for incorporation into LFAs. The next set of results in this chapter showcase an attempt to fabricate one such robust LFA by replacing antibodies with affimers. IL-8, which is another well-known sports biomarker for inflammation and fatigue, has been used as a model system for this study. The preliminary results have been achieved using an MB reporter based LFA in a buffer solution and show a concentration dependent response for IL-8 with a VDL of 1 ng/ml, however further optimizations are still needed to make this system more sensitive and reliable.

7.2 Materials and Methods

7.2.1 Reagents, Membranes and Apparatus

10 nm AuNPs colloidal solution, cysteamine, *Tris (2-carboxyethyl) phosphine* (TCEP), chloroauric acid ($HAuCl_4.xH2O$), hydroxylamine hydrochloride ($NH_2OH.HCl$), PBS (pH 7.4), BSA (Lyophilized), sodium azide and tween 20 were purchased from Sigma-Aldrich. IGF-1 (product 9573), recognition antibody: anti-IGF-1 Ab (product 9572), and capture antibody: biotinylated anti-IGF-1 Ab (product 83137), were purchased from Abcam Ltd. IL-8, recognition affimer: anti-IL-8 aff and capture affimer: biotinylated anti-IL8 aff were purchased from Avacta Life Sciences Ltd. Commercially available superparamagnetic carboxylated polystyrene beads (200 nm) purchased from Chemicell were used in this study. Neutravidin, EDC (1-ethyl-3-[3-dimethylaminopropyl] carbodiimide hydrochloride) and sulfo-NHS (*N*-Hydroxysuccinimide) were purchased from Sigma-Aldrich. NC membrane cards (Hi-Flow Plus 135), glass fibre membranes and cellulose absorbent pads were obtained from Merck-Millipore. Images of strips were captured using a Sony Alpha a7R III digital camera and were processed by Sony Imaging Edit RAW software. ImageJ software was used to analyse the images.

7.2.2 Conjugation of Biomolecules with MB/GMB

The conjugation protocols described in section 3.2 with slight modifications were followed for conjugating IGF-1 and IL-8 to the reporter molecules. Upon activation of 1 ml bead solution (100x diluted in MES) using EDC/NHS protocol and subsequent washing, a 500 µl solution (concentration 10 µg /ml) of recognition anti-IGF-1 Ab was incubated with activated MB/GMB. On the other hand, for IL-8 affimer conjugation, the same volumes were used but the concentration of incubated affimer solution was adjusted to 50 µg/ml before incubation with activated MB.

7.2.3 Affimer-Streptavidin Conjugation

The capture biotinylated anti-IL-8 affirmer was conjugated onto a larger molecule, Neutravidin, before immobilising on the LFA strip using Biotin-Neutravidin conjugation chemistry.[11] 250 µl (0.9 mg/ml) of biotinylated anti-IL-8 solution was incubated with 250 µl (1 mg/ml) of Neutravidin solution in PBS. The volumes were chosen such that the Neutravidin to biotin molar ratio was maintained at ~1:4 during conjugation. Post incubation, the solution was dialysed twice in PBS at 5000 g using a centrifugal filter (30 kDa) to obtain a final concentration of ~500 µg /ml of biotinylated anti-IL-8-Neutravidin solution.

7.3 Results and Discussion

7.3.1 IGF-1 LFA Performance

IGF-1 assay was performed using the layouts described in chapter 5 and 6, utilising MBs and GMBs as reporter molecules respectively. Capture anti-IGF-1 Ab was immobilised on each strip using 100 µg/ml (~3 µl/strip). The assay results in plasma are shown in Fig 7.1(a-b). A sample volume of 100 µl was used to achieve a sufficiently distinct band. In case of strategy 1 (Fig 7.1(a)), whereby a passivation layer was used, the images were recorded after 15 min upon sample introduction. Test bands could be visually observed for IGF-1

concentrations ≥ 1 µg /ml (Fig 7.1(a) inset), which was considered as the VDL. No band was observed in case of the control experiment without IGF-1, which further indicated minimal non-specific adsorption of the Ab-MB complexes on the test line.

In case of strategy 2, wherein GMB reporters are used for signal amplification, the images were recorded after 25 min upon sample introduction. The longer time is to incorporate the nucleation step. The responses for this assay were better than the first strategy and the test bands could be visually observed at IGF-1 concentrations ≥ 100 ng/ml (Fig 7.1(b) inset), which was considered as the VDL. The use of GMB reporter, which has a higher contrast than MB and the subsequent nucleation step allowed for the 10-fold improvement in VDL for this strategy. However, the test bands for both assays appear to be of lower contrast than the bands obtained for Troponin assay (as shown in chapter 5, Fig 5.4 and chapter 6, Fig 6.7). These results imply that the assay still requires improvement via further optimisations using a higher concentration of recognition Ab during MB conjugation or immobilising capture Ab on the test lines at a higher concentration.

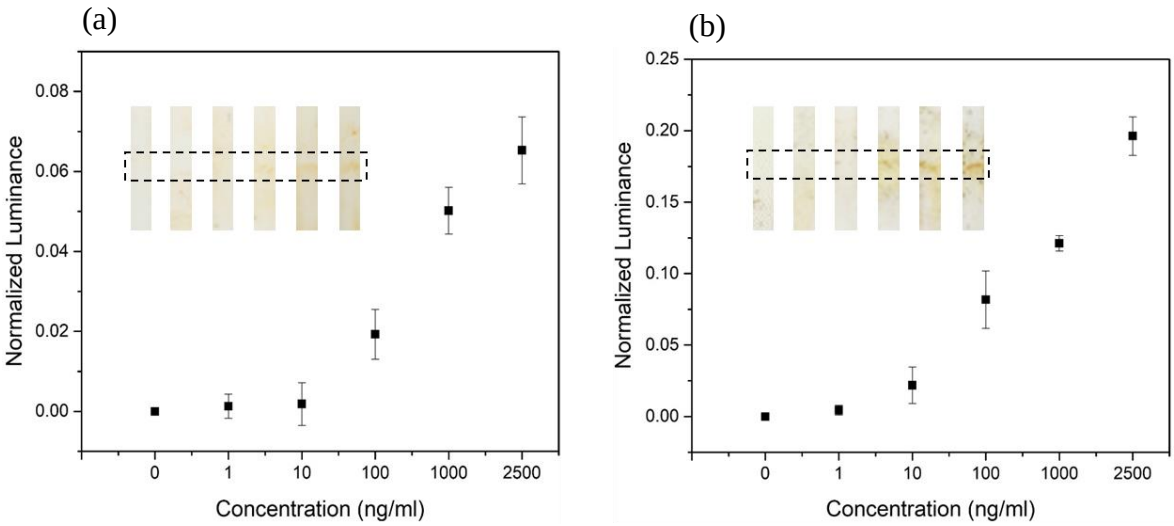

Fig 7.1: Quantification of colour intensities via measurement of normalized luminance of test bands for IGF-1 assay with (a) MB (Strategy 1) and (b) GMB (Strategy 2). Inset images: photographs of LFA strips showing the test bands after assay. From left to right: 0 ng/ml, 1 ng/ml, 10 ng/ml, 100 ng/ml, 1000 ng/ml, 2500 ng/ml. Normalized relative luminance was measured with respect to control LFA strip, which corresponded to 0 ng/ml.

Fig 7.1(a-b) show the calibration curves for IGF-1 concentrations between 0 and 2500 ng/ml, plotted for both assays. These curves were plotted using the normalized relative luminance values obtained via image analysis using ImageJ software. The luminance readouts for various IGF-1 concentrations correlate well with the visual observations. The concentration dependent responses illustrated in the calibration curves indicate that the proposed approach can be used for quantification of analyte concentrations. The relative luminance values are higher in case of strategy 2 (Fig 7.1(b)), indicating that the bands are of higher visual contrasts. Furthermore, the trend seen in the calibration curves supports the efficacy of the proposed assay. Since currently the VDL obtained in the proposed assays are higher than the WADA requirement for a viable IGF-1 assay (LOQ $\leq$ 50 ng/ml), further optimizations are needed. It is also important to note that the correlation curve in Fig 7.1(b) shows that even 10 ng/ml IGF-1 concentration has a readable normalized luminance signal, signifying that the LOQ values suggested by WADA can still be achieved by the proposed assay by using instruments such as smartphones for image analysis.

7.3.2 IL-8 LFA Performance

7.3.2.1 Affimer-Analyte Binding Characteristics

ELISA was performed on the IL-8 model system according to the protocol described in section 3.7.6. The capture biotinylated anti-IL-8 affirmer and recognition anti-IL-8 affirmer concentrations were kept constant, while varying the IL-8 concentrations to obtain a concentration dependent response plot by acquiring absorbance at 450 nm upon completion of the ELISA protocol. The absorbance values were then normalized prior plotting.

The plot in Fig 7.2 shows a linear trend till a concentration of 50 ng/ml, which means that as the analyte concentration increases, the signal readout increases. Beyond this, the curve starts saturating, implying no more IL-8 is captured by the affimers coated on the well plate. The trend seen in the ELISA result validates the affimer-antigen binding and the viability of this model system for use in LFA.

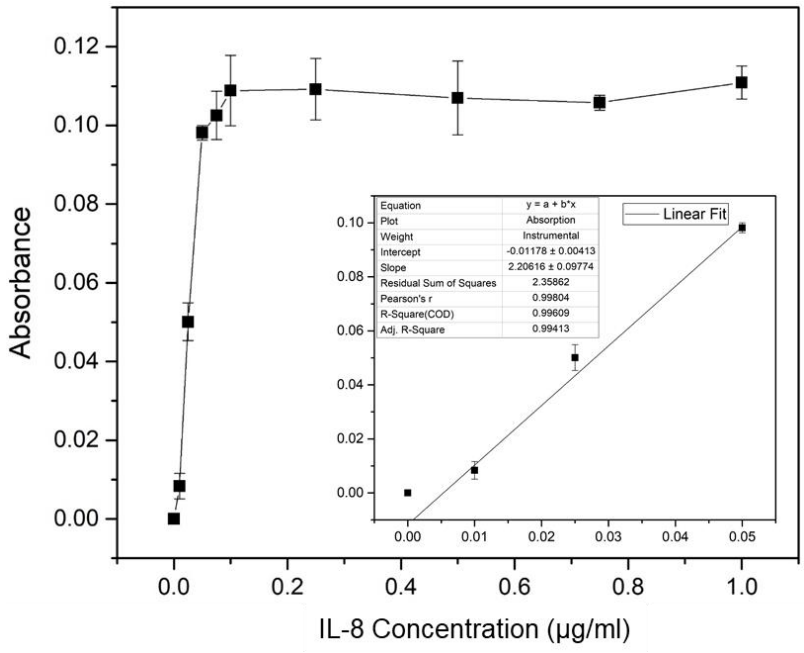

Fig 7.2: ELISA plot showing concentration dependent response of IL-8. Inset shows the linear fit for plot between 0 and 50 ng/ml.

7.3.2.2 Bradford Characterization of Affimer-MB Conjugation

The MB-affirmer conjugation efficiency was studied by Bradford analysis of the affirmer supernatant post its incubation with carboxyl activated MBs and its extraction from the reaction vial, Fig 7.3(a-b). Figure 7.3(b) shows the affimer concentration in the reaction vial before and after the incubation with MBs, which has been calculated using the equation of standard Bradford plot obtained in Fig 7.3(a). Similar to antibody conjugation, the amount of affimers conjugated to MB is predominantly controlled by the availability of free carboxyl groups on the surface and is inversely proportional to the amount of affimers left in the supernatant. Upon subtracting the number of affimers in the supernatant post-incubation from the pre-incubation solution of antibodies, it is observed that ~16 µg of affimers could be conjugated per 125 µg of MB (~5 µl of stock solution). The supernatants collected after the first three washes, post resuspension of storage buffer in the reaction vial, were also analysed. The negligible absorbance values obtained in this case showed that no non-specifically attached affimers were present in the vial.

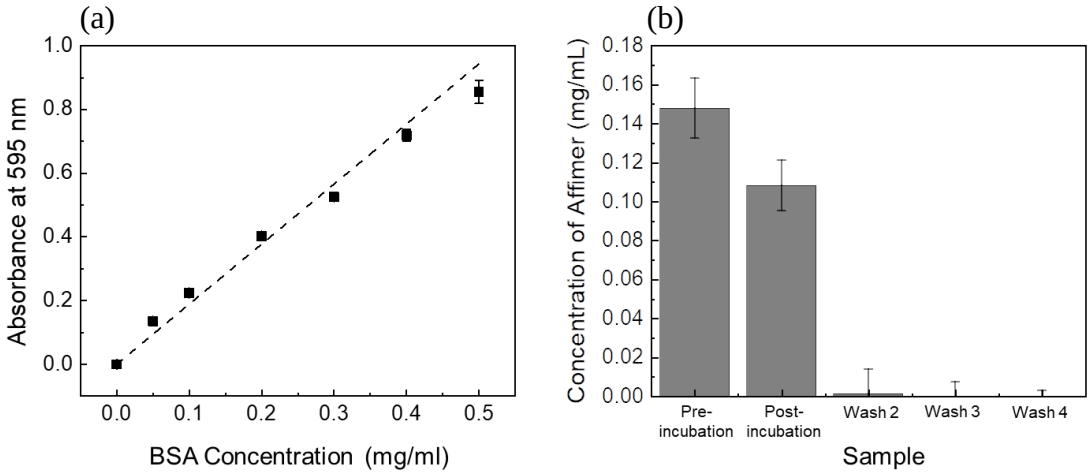

Fig 7.3: (a) Bradford standard plot for calculation of affimer concentration; and (b) Bar graph showing pre-incubation affimer concentration in reaction vial and post-incubation affimer concentration left in supernatant after MB extraction. The supernatants after the first 3 washes have also been analyzed to ensure no non-specifically attached affimers were present in the reaction vial.

7.3.2.3 Preliminary Results for IL-8 Assay

The IL-8 assay was performed using the layout described in Fig 3.4 of chapter 3, using MB reporters. As seen in Fig 7.4, six concentrations of IL-8 were assayed to test the validity of the LFA. It can be observed that the test band intensity improved as the concentration increased, with visible bands appearing at concentration ≥1 ng/ml, which was considered to be the VDL (inset images in Fig 7.4). At the control strip, corresponding to 0 ng/ml, no band appears, implying no non-specific binding of analyte on the test line. The test line was composed of Neutravidin-biotinylated anti-IL-8 affirmer complex. Immobilising small molecules such as affimers on LFA is challenging as they can seep into the NC membrane and thus have low accessibility to the target analyte. [12] This results in limited interaction between the affirmer and IL-8 and thus, yielding a low sensitivity. Therefore, IL-8 affimer molecules (~14 kDa) were conjugated to a Neutravidin (~60 kDa) to increase the size of the complex being immobilized on the test line. The larger size facilitate the retainment of IL-8 affirmers on LFA surface, which provides better accessibility for the affirmer to interact with IL-8. The appearance of test bands proves that this strategy works, however

to improve the band intensity, the immobilisation process needs further optimizations, predominantly with respect to the Neutravidin-biotinylated Affimer capture complex synthesis and the protocol for immobilization of this complex onto the test line.

The visual signals have been quantified using relative normalized luminance values obtained by ImageJ software. The visual observation is correlated with the calibration curve, which shows an increasing trend with increasing IL-8 concentration levels. Using the correlation curve, a readable signal readout at 0.1 ng/ml could also be achieved, showing that the sensitivity of this assay is comparable to the physiological concentrations in athletes with inflammations post muscle damage or excessive stress. [13, 14] Furthermore, the trend seen visually as well as in the calibration curves supports the efficacy of a proposed affimer based LFA system for assaying sports markers.

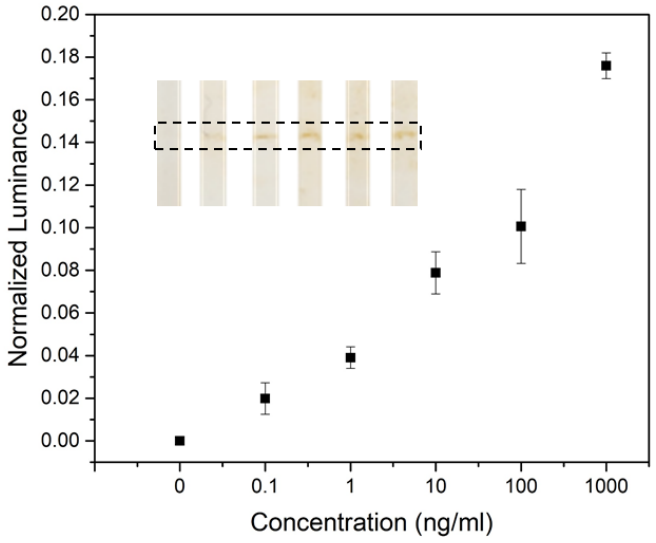

Fig 7.4: Quantification of colour intensities via measurement of normalized luminance of test bands for IL-8 assay with an affimer based system. Inset images: photographs of LFA strips showing the test bands after assay. From left to right (IL-8 concentration in ng/ml): 0, 0.1, 1, 10, 100 and 1000. Normalized relative luminance was measured with respect to control LFA strip, which corresponded to 0 ng/ml.

7.4 Conclusion

In this chapter, two sports markers have been successfully assayed using the LFA layouts proposed in chapter 5 and 6. IGF-1, a prohibited performance enhancing substance, was assayed using an antibody-based approach, using both MB and GMB reporter systems. The LFA fabrication and sample preparation was similar to that of Troponin LFAs, described in the previous chapters. The proposed layouts (strategy 1 and 2) yielded sensitive VDLs of 1 µg/ml with MBs and 0.1 µg /ml with GMBs respectively. The GMB approach incorporated a signal amplification step utilizing a nucleation agent, which helps formation of large Au clusters at the test line. This additional step added an extra 10 min to the overall assay time, yet provided a 10 fold VDL improvement. The proposed layout provides a VDL, which is comparable to the WADA specified LOQ of a viable IGF-1 assay. The VDL can be further improved by optimising the assay parameters such as Ab-MB conjugation, Ab immobilisation on the test line, etc.

The second set of results pertain to a novel affimer based LFA system for detection of IL-8, which is an inflammatory marker. Affimers are small proteins, which can specifically bind to target analyte molecules with affinity comparable to antibodies. However, the stability of affimers outperforms antibodies and therefore has the potential to replace antibodies completely in LFAs. The proposed layout consisted of an MB-affirmer based sandwich LFA. The MB-affirmer conjugation characteristics were comparable to antibody systems tested in the previous chapters. The affirmer-analyte binding characteristics were studied using ELISA. The test line on the LFA strip was composed using a capture complex comprising Neutravidin-biotinylated anti-IL-8 affirmer to improve the accessibility of the affimers to analyte molecules. The assay resulted in a VDL of 1 ng/ml which is comparable to physiological concentrations of injured athletes, thus establishing the validity of an affimer based LFA system, which, to the best of our knowledge, would be the first of its kind. However, to increase the sensitivity of the assay, further optimizations are required to improve the contrast of the test bands.

References

1. Zhang, D., et al., *Quantitative and ultrasensitive detection of multiplex cardiac biomarkers in lateral flow assay with core-shell SERS nanotags.* Biosensors and Bioelectronics, 2018. **106**: p. 204-211.

2. WADA. *WADA Technical Document – TD2014DL*. 2014 [cited 2020 20th May]; Available from: https://www.wada-ama.org/sites/default/files/resources/files/WADA-TD2014DL-v1-Decision-Limits-for-the-Quantification-of-Threshold-Substances-EN.pdf.

3. WADA. *WADA Technical Document – TD2014EPO*. 2014 [cited 2020 20th May]; Available from: https://www.wada-ama.org/sites/default/files/resources/files/WADA-TD2014EPO-v1-Harmonization-of-Analysis-and-Reporting-of-ESAs-by-Electrophoretic-Techniques-EN.pdf.

4. WADA. *WADA Prohibited List 2020*. 2020 [cited 2020 18th May]; Available from: https://www.wada-ama.org/sites/default/files/wada_2020_english_prohibited_list_0.pdf.

5. *Somatropin (Human Growth Hormone): Production & Function*. [cited 2020 23rd May]; Available from: https://schoolworkhelper.net/somatropin-human-growth-hormone-production-function/.

6. Gagnon, P., *Purification tools for monoclonal antibodies*. Vol. 196. 1996: Validated Biosystems, Incorporated.

7. Chames, P., et al., *Therapeutic antibodies: successes, limitations and hopes for the future.* British Journal Of Pharmacology, 2009. **157**(2): p. 220-233.

8. Xu, H., et al., *Aptamer-Functionalized Gold Nanoparticles as Probes in a Dry-Reagent Strip Biosensor for Protein Analysis.* Analytical Chemistry, 2009. **81**(2): p. 669-675.

9. Yonekita, T., et al., *Development of a novel multiplex lateral flow assay using an antimicrobial peptide for the detection of Shiga toxin-producing Escherichia coli.* Journal Of Microbiological Methods, 2013. **93**(3): p. 251-256.

10. Blažková, M., et al., *Development of a nucleic acid lateral flow immunoassay for simultaneous detection of Listeria spp. and Listeriamonocytogenes in food.* European Food Research and Technology, 2009. **229**(6): p. 867.

11. Fisher, T. *Avidin-Biotin Interaction*. 2020 [cited 2020 1st July]; Available from: shorturl.at/jIMN2.

12. Chen, A. and S. Yang, *Replacing antibodies with aptamers in lateral flow immunoassay.* Biosensors And Bioelectronics, 2015. **71**: p. 230-242.

13. Shin, Y.-O., et al., *Comparison of Interleukin-8 Levels in Long-Distance Runners and Healthy Sedentary Non-Athletic Control Subjects.* Korean Journal of Physiology & Pharmacology, 2007. **11**(6): p. 263-268.

14. Zhang, J. and C. Bai, *Elevated serum interleukin-8 level as a preferable biomarker for identifying uncontrolled asthma and glucocorticosteroid responsiveness.* Tanaffos, 2017. **16**(4): p. 260.

Chapter 8

Conclusion and Future Outlook

In this chapter, a brief summary of the thesis has been presented, including the major outcomes. Hypotheses raised for this research are clarified based on the results presented in this thesis. At the end of the chapter, the future work/directions to improve performance of the proposed assays and the possible modifications that could be incorporated for their commercial adaptability have also been discussed.

8.1 Research Summary

This thesis focusses on developing and optimising strategies to make LFAs more reliable for on-site testing of biomarkers related to sports doping. LFA technology possesses tremendous potential due to a myriad of benefits it can provide over traditional lab-based tests. Their low cost, limited sample volume requirement and user friendliness, allow for LFAs to be used as efficient screening devices, augmenting the existing sophisticated lab tests. This can help the governing bodies such as WADA make the current anti-doping programmes more efficient and robust by introducing a widespread testing regime. However, challenges associated with testing in complex matrices such as blood, urine etc., have limited the widespread adoption of LFAs. The interferences from the components of these matrices such as proteins, salts, cells, etc., can affect the sensitivity of LFAs. Since elaborate sample pre-treatment or signal amplification steps increase the complexity of any assay and may not be possible to perform on-site, there is an immediate need to explore alternative ways to simplify these methods for improving LFA sensitivity. In this thesis a few such strategies have been explored to improve the sensitivity and robustness of LFA devices.

Chapter 4 laid the foundation of the LFA studies conducted in this thesis. In this chapter, the rationale for choosing different membranes for the various functional zones was experimentally proven using their flow behaviour pre- and post- blocking with BSA. Good protein binding ability and the high degree of flow control provided by NC membranes (NC 135 grade) implied that they were the best choice for the test zone, whereas, good water absorption provided by cellulose membranes allowed for better wicking and hence was the best choice for an absorption pad. Glass fibre with a high hydrophilicity and porosity enabled efficient channelization of sample solution. This chapter also characterized the MB reporters, which were used as colorimetric labels for naked eye visualization of analytes. Apart from serving as reporters, MBs could be spatially controlled using an external magnetic field for extracting target analytes from a solution. Finally, the antibody-antigen binding characteristics of the proposed model systems: cTnICT and IGF-1, were validated by ELISA.

Chapter 5 discussed an approach to incorporate extraction and assaying of a model target protein (cTnICT) on an LFA strip. The LFA layout comprised of an external magnet that assisted in capturing of anti-TnI antibody conjugated magnetic bead complexes. Upon optimization of magnetic strength applied to capture these complexes at the sample deposition area, VDLs of 1 ng/ml and 10 ng/ml in buffer and 10x plasma, respectively, were obtained prior signal enhancement, which meets the requirement for clinical assaying of cTnICT. A Protein-A modified MB based approach for signal amplification was also demonstrated, which provided at least 10-fold improvement to the test line intensity. The proposed methodology did not require tedious sample pre-treatment protocols and hence possesses the potential for on-site applications.

Chapter 6 discussed another strategy to improve LFA sensitivity by studying a GMB reporter based approach for extraction and assaying of cTnICT in complex matrices. The GMB reporter was synthesised by conjugating MB and AuNP via a linker molecule. This synthesis protocol was found to be more facile than any of the typically reported protocols such as co-precipitation. The GMB reporters enabled a facile nucleation based signal amplification strategy, whereby a nucleation solution could trigger formation of gold clusters on the test line, thus improving its contrast. The assay was demonstrated in both PBS and plasma, with a VDL of 0.1 ng/ml for both matrices with an assay time of 20 min, upon signal amplification. This signal amplification approach was effective, facile, and rapid and did not involve any sophisticated steps.

In Chapter 7, two main sets of results, related to two important sports markers IGF-1 and IL-8, have been discussed. IGF-1, a WADA prohibited substance, was successfully assayed in plasma using the LFA layouts proposed in chapter 5 and 6. The proposed layouts yielded sensitive VDLs of 1 µg/ml, with the layout described in chapter 5 using MBs, and 100 ng/ml, with the layout described in chapter 6 using GMBs. Although the proposed layout provides a VDL comparable to the WADA specified LOQ of a viable IGF-1 assay (≤ 50 ng/ml), further optimisations, such as those related to Ab-MB conjugation, Ab immobilisation on the test line etc., are needed to improve the LODs. The second set of results involves a novel affimer based LFA system for the detection of inflammatory

marker, IL-8. The comparable sensitivity and selectivity and much higher stability of affimers as compared to antibodies provides an alternative recognition unit for LFA fabrication. The proposed layout consisted of an MB-affirmer based sandwich LFA and the parameters such as MB-affirmer conjugation was found comparable to antibody-based assays. Since direct immobilisation of small molecules such as affimers onto NC membranes is challenging, the test line in the proposed layout was composed of a capture complex comprising Neutravidin-biotinylated anti-IL-8 affirmer. This improved accessibility of the immobilised affimers to the incoming analyte molecules during an assay. The preliminary results showed a concentration dependent response of the test line intensity, thus establishing the validity of an affimer based LFA system. Test bands could be observed at IL-8 concentrations $\geq$ 1 ng/ml, which was the VDL of the assay. However, further optimizations are required to improve the LFA responses and enhance the sensitivity of the assay further.

In conclusion, the proposed LFA layouts showed several promising results, with VDLs that are clinically relevant and competitive to existing colorimetric assays for similar model systems. Thus, both the hypotheses stated in section 1.2 of this thesis have been successfully proved. Furthermore, the generic approach of the proposed methodologies could allow translation to detect several other relevant biomolecules of interest, in a wide range of sample matrices. The proposed LFA layouts allowed for facile sample pre-treatment, were cost effective, user friendly and rapid, allowing convenient usage on-site, even without trained personnel or expensive instrumentation. However, there is still scope for improvement of the VDLs achieved by optimising parameters such as test line immobilisation, improving efficiency of MB-biomolecule conjugation etc. The LFA studies in this thesis have been summarized in Table 8.1.

Table 8.1: Summarized list of proposed strategies in this thesis

Strategy	Analyte	Reporter	VDL	Assay Time	Ease of Use
Incorporation of Sample Pre-treatment	TnICT	MB	1 ng/ml in PBS; 10 ng/ml in Plasma	15 min	●●●
Nucleation based Signal Amplification	TnICT	GMB	0.1 ng/ml in PBS and Plasma	20 min	●●○
Incorporation of Sample Pre-treatment	IGF-1	MB	1 µg/ml in Plasma	15 min	●●●
Nucleation based Signal Amplification	IGF-1	GMB	100 ng/ml in Plasma	25 min	●●○
Affimer based LFA	IL-8	MB	1 ng/ml in PBS	15 min	●●●

To summarize, this thesis explored a few strategies to improve LFA performance: incorporation of sample pretreatment into LFA strip, using a composite reporter for analyte extraction, assaying and signal amplification, and using affimers instead of antibodies for a more robust assay. The novelty of the first two strategies are associated to the new layouts which were studied and reported for the first time, whereas the third strategy used a novel and robust biomolecule for capturing and detecting analytes. The efficacy of these strategies was demonstrated by assaying three different model systems: TnICT, IGF-1 and IL-8. These strategies not only allowed for detection of physiological ranges of analytes from complex matrices in a short time span, but also highlighted the tremendous potential of LFAs for future studies.

8.2 Future Outlook

Although the proposed LFA layouts are promising and can yield clinically relevant levels of detection, they still need improvement to compete with some of the commercially available LFAs.[1, 2] One of the most effective ways to improve sensitivity is by improving the test band intensity. Currently, in all the proposed LFA layouts in this thesis, the test line is deposited manually. However, automating this process by using an LFA dispenser can allow for uniform deposition of recognition molecules and therefore resulting in a sharper band. In the recent years, there has been significant advent in automation of LFA

fabrication. For example, commercially available LFA fabrication units, such as that from Ginolis, can dispense solutions, cut uniform strips and even perform quality checks.[3] Such sophisticated fabrication processes not only improve LFA responses but also ensure high throughput production.

The next important step in the research presented in this thesis is clinical validation of the devices. The sample preparation for all the studies in this thesis involve manual spiking of buffer and plasma solutions. However, a blind cohort study including samples from patients/athletes need to be conducted to validate the overall performance of the devices. There are several challenges associated with "real" samples, the most important being the limited sample volumes. Hence, a robust sample preparation protocol needs to be developed so that there is minimal sample wastage. The LFA dimensions may also be altered to optimize parameters such as sample volume requirement for an assay. However, the latter strategy would require different set of optimisation experiments.

Multiplexing of LFA devices is another aspect that can be explored. As explained in section 2.1.2 of chapter 2, the banned substances are categorized into classes. The substances in each class have similar functioning and may even have structural similarity at molecular level. Therefore, identifying one molecule may not be sufficient for doping control. Even in the current anti-doping strategy, tests are conducted to look for multiple substances across classes, which may also include some form of unidentified analogues. Therefore, there is a need for multiplex detection of analytes on LFA devices for effective screening of athletes on-site. Multiplexed detection on LFAs has been reported widely but it is still challenging.[4-6] The main challenges involving multiplexed LFAs are cross reactivity of analytes on different test lines and a limitation in the number of test lines that can be fabricated on one strip. Recently, there have been studies on multi-channel or array type assemblies, which involve several LFA strips combined with a single sample deposition area.[6, 7] This strategy provides a promising multiplexed LFA platform. However, further studies are needed to implement such a system for sports related biomarkers.

Another direction that LFA research can pursue is by studying novel layouts for efficient sample pre-treatment. For instance, in one of the on-going studies in our group, the concepts of magnetophoresis are being implemented on paper for channelizing matrix components away from test bands. Fig 8.1 shows one such layout tested. In this study, a magnetic tape was utilized to activate the arms of the NC membranes. The arm with magnetic tape below allowed the magnetic beads with captured target analytes to flow into them, whereas the other arm without the tape allowed the matrix components to flow through. This could minimise the matrix components interacting with the test line deposited on the activated arm. However, further studies are needed to make the channelling more efficient and minimise the physical adsorption of magnetic beads onto the NC membrane.

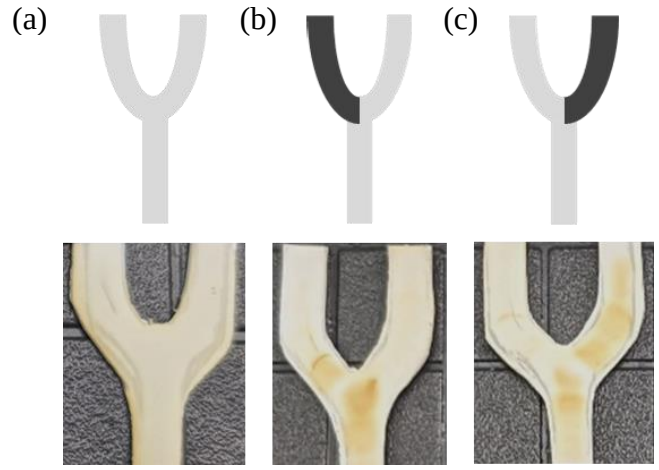

Fig 8.1: Channeling MBs on NC membranes using magnetic tape. (a) Represents a control strip without any magnetic tape underneath; (b) and (c) represent strips with magnetic tape under the left arm (left arm activated) and right arm (right arm activated), respectively. The top row shows schematic of each layout, the bottom row shows images of NC strips upon flowing of MB solution.

Apart from improving the existing LFA layouts for more sensitive detection, use of smart phone technology for more sensitive signal readout is another direction that can help LFAs to be more reliable and user friendly. Recently there have been reports of using smart phones to read various types of signals such as fluorescence [8], luminescence [9], colorimetric [10], SPR, [11] etc. LFA signal readouts have also been studied using this technology. For example, Lee et al. detected micronutrient vitamin D, a nutrition marker,

using an AuNP based colorimetric competitive immunoassay performed on a test strip consisting of a 25-hydroxyvitamin D coated detection zone.[12] The colorimetric signal, amplified using a silver solution, was captured and analysed using a smart phone application, yielding an LOD of 10 nM, which was comparable to commercial ELISA kits. Smart phones have become ubiquitous and an important part of our lives. Hence, they can be utilized for fabrication of sensitive LFAs, especially for on-site applications.

References

1. Christenson, R.H., et al., *Comparison of 13 commercially available cardiac troponin assays in a multicenter North American study.* The Journal of Applied Laboratory Medicine, 2017. **1**(5): p. 544-561.

2. Healthineers, S. *Cardiac Troponin for Earlier Diagnosis of Myocardial Infarctions*. 2020 [cited 2020 14th July]; Available from: https://www.siemens-healthineers.com/en-sg/laboratory-diagnostics/assays-by-diseases-conditions/cardiac-assays/cardiac-troponin-assays.

3. Ginolis. *Ginolis launches the lateral flow assembly (LFA) manufacturing product*. 2014 [cited 2020 1st of July]; Available from: shorturl.at/dezE0.

4. Song, S., et al., *Multiplex lateral flow immunoassay for mycotoxin determination.* Analytical Chemistry, 2014. **86**(10): p. 4995-5001.

5. Yonekita, T., et al., *Development of a novel multiplex lateral flow assay using an antimicrobial peptide for the detection of Shiga toxin-producing Escherichia coli.* Journal of Microbiological Methods, 2013. **93**(3): p. 251-256.

6. Fenton, E.M., et al., *Multiplex lateral-flow test strips fabricated by two-dimensional shaping.* ACS Applied Materials & Interfaces, 2009. **1**(1): p. 124-129.

7. Zhao, Y., et al., *Rapid multiplex detection of 10 foodborne pathogens with an up-converting phosphor technology-based 10-channel lateral flow assay.* Scientific Reports, 2016. **6**(1): p. 1-8.

8. Rajendran, V.K., P. Bakthavathsalam, and B.M.J. Ali, *Smartphone based bacterial detection using biofunctionalized fluorescent nanoparticles.* Microchimica Acta, 2014. **181**(15-16): p. 1815-1821.

9. Kim, H., et al., *Smartphone-based low light detection for bioluminescence application.* Scientific Reports, 2017. **7**(1): p. 1-11.

10. Vashist, S.K., et al., *Graphene-based rapid and highly-sensitive immunoassay for C-reactive protein using a smartphone-based colorimetric reader*. Biosensors and Bioelectronics, 2015. **66**: p. 169-176.

11. Liu, Y., et al., *Surface plasmon resonance biosensor based on smart phone platforms.* Scientific Reports, 2015. **5**: p. 12864.

12. Lee, S., et al., *A smartphone platform for the quantification of vitamin D levels.* Lab on a Chip, 2014. **14**(8): p. 1437-1442.